UNIVERSITÀ
DEGLI STUDI
DI PADOVA

Sede Amministrativa: Università degli Studi di Padova
Dipartimento di MEDICINA MOLECOLARE

CORSO DI DOTTORATO DI RICERCA IN: MEDICINA MOLECOLARE
CURRICOLO: BIOMEDICINA
CICLO: 30

COMPARATIVE ANALYSIS OF ZIKA VIRUS AND OTHER FLAVIVIRUS INFECTION IN HUMAN NEURAL CELLS

Coordinatore: Ch.mo Prof. Stefano Piccolo
Supervisore: Ch.ma Prof.ssa Luisa Barzon
Co-Supervisore: Dott.ssa Marta Trevisan

Dottoranda: Giovanna Desole

CONTENTS

ABSTRACT

Background: Zika virus (ZIKV), West Nile virus (WNV) and dengue virus (DENV) are mosquito-borne flaviviruses that generally cause mild or asymptomatic disease in humans. However, ZIKV infection has been associated with fetal microcephaly and Guillain-Barrè syndrome in adults; WNV infection may evolve to severe neuroinvasive disease in the elderly and immunocompromised subjects; DENV may rarely cause neurological complications in infected individuals. In addition, another emerging mosquito-borne flavivirus, Usutu virus (USUV), which may cause fatal neuroinvasive disease in different bird species, has been recently shown to infect humans but its pathogenicity is unknown.

Aim of the study: In the context of the recent outbreak of ZIKV in the Americas and the increasing evidences of an association between ZIKV infection and the occurrence of fetal microcephaly, aim of this study was to investigate the effect of ZIKV infection in human neural cells in comparison with other flavivirus infections. To this aim, ZIKV infectivity, replication kinetics, cytopathic effect (CPE), and induction of innate antiviral responses were investigated in human induced pluripotent stem cells (hiPSCs), hiPSCs-derived neural stem cells (NSCs) and neurons and compared with other flaviviruses, i.e., WNV, DENV and USUV.

Methods: NSCs and neurons were differentiated from hiPSCs. hiPSCs, NSCs, and neurons were infected with isolates of ZIKV Asian lineage (KU853013), WNV lineage 2 (KF179640), DENV serotype 2, and USUV Europe lineage 1 (AY453411). Time course experiments were performed to evaluate viral load by qRT-PCR and TCID50, expression of host genes involved in antiviral innate immunity by qRT-PCR, expression of cell differentiation markers by IF and qRT-PCR, cell viability and cell death by flow cytometry. The impact of ZIKV on embryogenesis and neurogenesis was evaluated by infection of hiPSCs and NSCs during neural differentiation and embryo body formation.

Results: ZIKV infected and replicated efficiently in NSCs, neurons and hiPSCs. Infection led to typical CPE and cell death by apoptosis. ZIKV infection of hiPSCs, NSCs, and neurons induced the expression of innate immune response genes, especially the cellular pattern recognition receptor (PRR) IFH1 gene (MDA5), IFN-induced protein with tetratricopeptide repeats 1 (IFIT1) and 2 (IFIT2). Infected embryoid bodies were massively destroyed by ZIKV infection and infected hiPSCs and NSCs died before ending the neural differentiation process. ZIKV replication efficiency in NSCs was significantly higher that that of DENV-2 and USUV, but lower than that of WNV. In particular, WNV replicated more efficiently, induced more cell death and higher levels of antiviral gene expression than ZIKV in NSCs, neurons and hiPSCs. The induction of innate immune

response genes in NSCs after infection with ZIKV and DENV-2 infection was milder than after infection with WNV and USUV, in agreement with the adaptation of these viruses to the human host and their ability to shut down the antiviral response.

Conclusion: ZIKV infects and replicates efficiently in NSCs and induces cell death abrogating neural development, although less efficiently than WNV. Because of the similarities between flaviviruses in their interactions with host neural cells, it is conceivable that infection of other human cells, such as those involved in the extablishment of the blood-placenta barrier, are crucial for ZIKV-induced damage of the fetal brain.

1. INTRODUCTION

1.1 Introduction to vector-borne viruses

Arboviruses (acronym for arthropod-borne viruses) include viruses that require hematophagous arthropod vectors, such as mosquitoes and ticks, for transmission between vertebrate hosts [1]. To be transmitted, vector-borne viruses must replicate in the body of the arthropod vector. Different vertebrates, including birds, rodents, bats, horses, or human and non-human primates, may serve as amplyfing hosts [2] (Fig. 1.1).

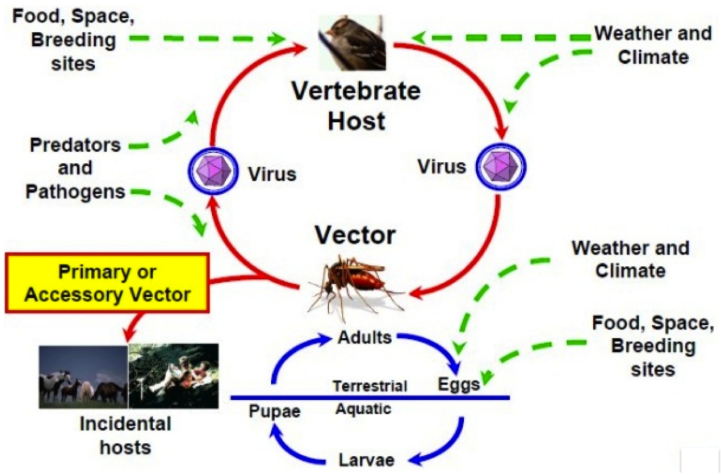

Fig. 1.1: Arbovirus transmission cycle

Biological transmission can be vertical with thE passage of the virus from an infected female vector to female or male offspring. Horizontal transmission can be venereal from a vertically infected male to a female vector, as well as oral from a female vector to a vertebrate host via saliva during blood co-feeding.

Vector-borne viruses are included in different taxonomic families, the majority belonging to the *Flaviviridae*, *Bunyaviridae* and *Togaviridae* families [2,3]. Among them, four major viral genera are responsible of the majority arboviral disease: Flavivirus (e. g., yellow fever, Japanese encephalitis, West Nile, Zika and dengue viruses), Alphavirus (e. g., chikungunya virus and equine encephalitis viruses), Orthobunyavirus (e. g., California encephalitis and LaCrosse viruses) and Phlebovirus (e. g. Rift Valley fever and sandfly fever viruses) [4].

Vector-borne viruses have a worldwide distribution, but they were first isolated in tropical areas in Sub-Saharian Africa, South America and in some Asian countries. In the past decades, due to several factors such as climatic changes, urbanization, globalization, intercontinantal travel and trade, the geographic distribution and the frequency of the epidemic outbreaks of vector-borne viral

infections have expanded across the world [3] and they account for significant global public health problems.

1.2 Flaviviruses

1.2.1 Introduction to Flaviviruses

The family *Flaviviridae,* term originated from the word "flavus" meaning yellow in latin for the hallmark jaundice in victims caused by the infection with yellow fever virus (YFV), is composed of four virus genera: Flavivirus, Pestivirus, Hepacivirus and Pegivirus [5].

A generally accepted hypothesis suggests that flaviviruses derived from a common ancestor within the last 100 000 years [6] with the split between mosquito- and tick-borne flaviviruses around 40 000 years ago [7].

The genus Flavivirus consists of more than 70 virus species, many of them are the most clinically important arboviruses world-wide. These include YFV, through which the genus and family derive their name, Japanese encephalities virus (JEV), West Nile virus (WNV), dengue virus (DENV), Zika virus (ZIKV), tick-born encephalities virus (TBEV) [8] and several other viruses responsible for extensive morbidity and mortality in humans [9].

The viruses can be grouped by their pathogenicity, geographical area, antigenic complex and subcomplexes into clusters, clades and species, according to molecular phylogenetics [10].

They have a similar organization of the genome and mechanisms of replication, but there are differences in their host ranges and transmissibilities. In this regard, Flaviviruses can be divided into four large ecological clusters: mosquito-borne group (MBFV) that are commonly, but not exclusively, vectored by either *Aedes* or *Culex* mosquitoes, the tick-borne group (TBFV), the insect-specific flaviviruses only (ISFV) which are isolated from insects and the unknown vector viruses (NKFV) associated with either bats or rodents [11] (Fig. 1.2).

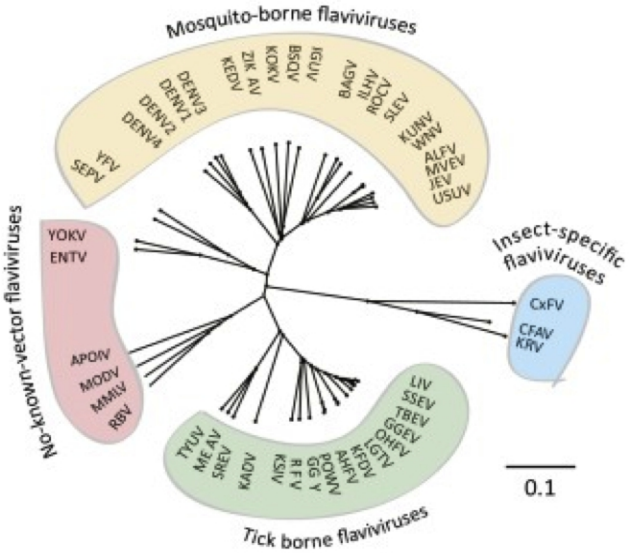

Fig. 1.2: Schematic representation of the distance tree of the four ecological groups of Flavivirus. (Villordo et al. 2016).

While tick-borne flaviviruses present a monophyletic group consisting of a single “serocomplex”, the mosquito-borne viruses include the JE serocomplex, YFV and members of the four DENV serotypes, among many other [6].

Mosquito-borne viruses infect a variety of animal species and humans. They can be further subdivided into *Culex* and *Aedes* clades, which differ in their vertebrate host range and pathogenesis mechanisms. *Culex*-clade viruses are transmitted by *Culex* spp. mosquitoes (JE serocomplex), usually have bird reservoirs and are neurotropic. *Aedes*-clade viruses are transmitted by *Aedes* spp. mosquitoes, have primate reservoirs, are not neurotropic and are mainly associated with hemorragic diseases [6,12,13]. Notably, the recent discovery that ZIKV, transmitted by *Aedes aegypti* mosquito spp., is responsible for neurological disease in fetuses stimulated a re-evaluation of the possible role of the closely related DENV and YFV on the development of neurological diseases [6].

1.2.2 Genome of Flaviviruses

Cryoelectron microscopy and image reconstruction techniques established that mature flavivirus virions are spherical and icosahedral with about 40 nm in diameter [14].

They have a non-segmented, single-stranded, positive-sense RNA genome of about 10 to 12 kb, which is directly translated into viral proteins [11]. The genome is complexed with multiple copies of the capsid C protein (C), which is surrounded by a lipid bilayer containing the envelope (E) protein and the membrane (M) protein. Mature virions contain the M protein produced by the cleavage of the membrane precursor protein (prM) by a furin-like protease located in the *trans*-Golgi to form the M protein [15]. The E protein represents the major virion surface protein and is involved in viral entry, in particular in host cell binding and membrane fusion [15,16]. It is also the also the main antigenic protein of the virus [17] (Fig. 1.3).

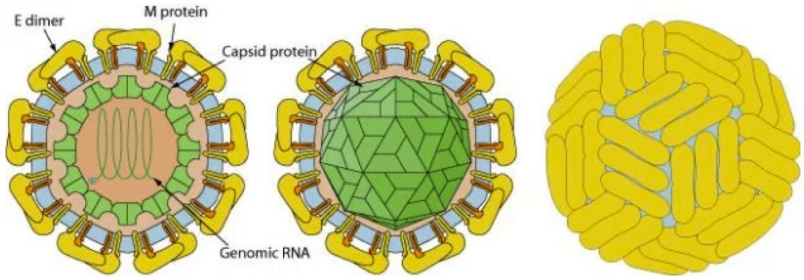

Fig. 1.3 : schematic representation of Flavivirus structure, showing E and M glycoproteins, icosahedral nucleocapsid and genomic positive-stranded RNA.

All members in the Flavivirus genus share certain characteristics of their genome.

The positive-sense genome of flaviviruses is like an mRNA molecule within infected cells. It has a single open reading frame (ORF) flanked by 5'- and 3'- untranslated regions (UTRs), the 5'- end terminates with a type 1 cap, the 3'- end is not polyadenylated and terminates in a conserved CU_{OH} [15]. The 5' UTRs are tipically 100 nucleotides in lenght, while the 3' UTRs are between 400 and 700 nucleotides and only in exceptional cases they can be over 900 nucleotides [18].

In all flavivirus genomes, only two RNA elements are conserved: these are the Y shape stem-loop A structure (SLA) at the 5' end and the small hairpin 3' stem-loop (sHP-3'SL) at the 3' end of the viral genome. These structures are essential for viral RNA synthesis[19].

The RNA genome encodes for a single polyprotein, subsequently translated into mature proteins by cellular and viral protease [20]. Mature proteins comprise three structural proteins contained in the viral particles, namely prM, C and E, and seven non-structural (NS) proteins NS1, NS2a, NS2b, NS3, NS4a, NS4b and NS5 [21], which enable proper replication and assembly of the virions in infected cells [22] (Fig. 1.4). NS3 and NS5 proteins have known enzymatic activities. Specifically, NS3 has trypsin-like serine protease and nucleic acid helicase activities in its N-terminal protease and C-terminal helicase domains, respectively [15]. NS5 has RNA capping function in the methyltransferase and guanylyltransferase sites of the N-terminal domain, and a RNA-dependent RNA-polymerase activity in the C-terminus [23].

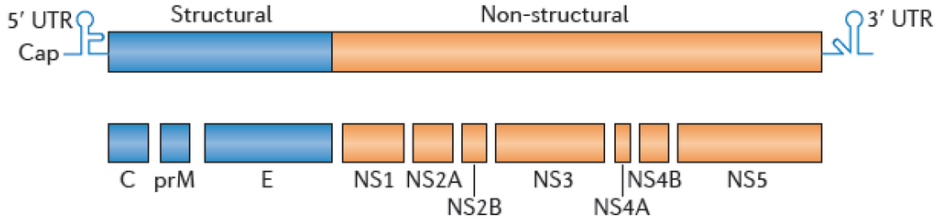

Fig. 1.4 : Flavivirus genome organization. The single open reading frame encoding for a polyprotein which is translated into three structural proteins C, prM and E and seven non structural proteins (NS). (Beck et al. 2016)

1.2.3 Flavivirus replication cycle

Infectious cycle starts with the attachment of the Flavivirus particle to the surface of target cells mediated by the E protein via specific receptors and entry cofactors [24] (Fig. 1.5**).** The viral particle can enter within the infected cell by diverse mechanisms[25-29]. The acidic pH in the endosomal compartment triggers the fusion of the lipid envelope of the viral particle with the membrane of the host cell mediated by conformational rearrangements of the E protein, leading to

the release of the nucleocapsid and viral RNA into the cytoplasm. Viral RNA is translated into a polyprotein that is processed the viral serine proteases and by host proteases to generate structural and non-structural viral proteins.

Specifically, in the lumen of the rough ER, the C protein is budded with the associated genomic RNA to form the nucleocapsid [24]. Next, E and prM proteins envelope the nucleocapsid forming an immature virus particle that translocates into the Golgi [30]. Maturation of viral particles occurs in the trans-Golgi network where prM to M are cleaved by cellular furin-like protease and conformational rearrangements of E occur [19,31]. The mature particles exit from the host cell by exocytosis[32].

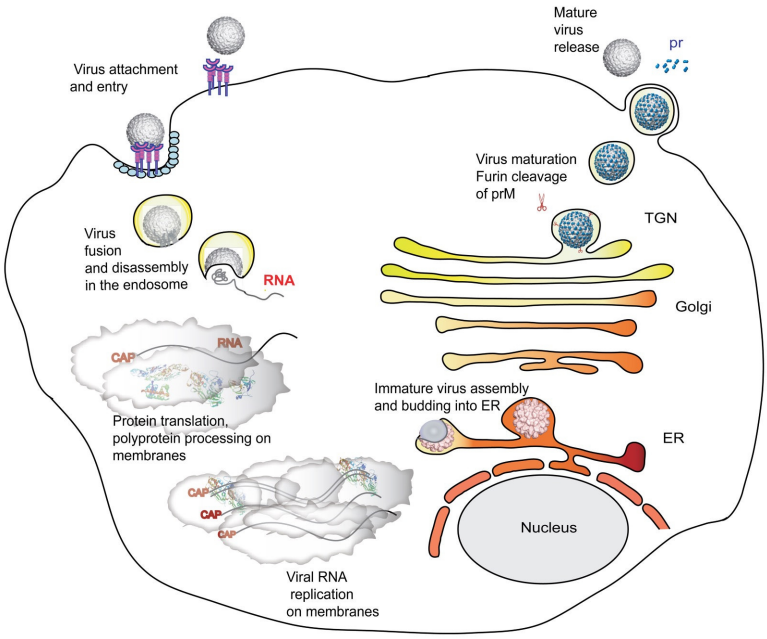

Fig. 1.5 : Flavivirus replication cycle. Sampath, A. et al. 2009.

1.3 Neuropathogenesis of Flavivirus infections

Neurotropic virus infections are associated morbidity and mortality all over the world. Neurotropic viruses can alter the homeostasis, induce neurological dysfunction and result in serious inflammatory disease with a consequent irreversible disruption of the architecture of the CNS, frequently leaving the patient with a poor or fatal prognosis.

The Flavivirus genus of the family *Flaviviridae* represents a group of important human pathogens, many of which are able to induce a range of specific CNS diseases. Neurotropic Flaviviruses comprise West Nile virus (WNV), Japanese encephalities virus (JEV), tick-borne encephalitis virus (TBEV) and the newly emerging Zika virus (ZIKV). All these viruses share the ability to gain entry

to the CNS, infect neural cells and establish acute or persistent infections. They cause a spectrum of clinical syndromes ranging from mild fever to hemorrhagic and encephalitic manifestations [22]. While the neurotropic Flaviviruses WNV and JEV are associated to post-natal encephalitis and rarely they are responsible for congenital brain malformations such as microcephaly, contrary to ZIKV[33-35]. In fact, ZIKV rarely cause meningitis or encephalitis in adults, but it is responsible for congenital malformations, especially microcephaly and fetal death [36]. Recently, ZIKV has been also associated with severe diseases in adults, including Guillän Barrè syndrome [37,38].

The molecular bases of neuroinvasion and neurovirulence are still a mystery for most neurotropic Flaviviruses.

One route for viral entry into the CNS is through the CNS endothelium. Several viruses, including WNV [39], have been reported to directly infect human brain microvascular endothelial cell lines *in vitro*, promoting increased production of chemokines (such as CC-chemokine ligand 2 (CCL2) and CCL5, altered expression of tight junctions proteins [39] and an inceased expression of the vascular cell adhesion molecule 1 (VCAM1) [39]. All these alterations increase the vascular permeability, so the virus can entry and spread in the CNS.

Another important route is through retrograde axonal transport; numerous viruses hijack the axonal transport system for intracellular movement or by hematogenous entry [40,41].

Other routes to reach the CNS is either via a “Trojan horse” mechanism in which infected leukocytes carry pathogens from the blood across the blood brain barrier or by passive diffusion, although neither of these strategies has been supported by direct proof [41].

Importantly an intact immune system is vital to prevent neuroinvasion by WNV and JEV, as demonstrated by fatality of WNV infection of immunocompetent humans [42], or in animal models of JEV [43].

Very rare cases of ZIKV-induced meningoencephalitis in adults are described, but an increase in peripheral nervous system syndromes incidence [44], specifically Guillän Barrè syndrome have been detected [37]. Moreover, ZIKV is able to invade the developing brain of fetuses [33] injuring neural progenitor cells, while other neurotropic Flaviviruses such as JEV and WNV are not associated with congenital malformations [38]. One possible reason is that JEV or WNV are not able to cross the placental barrier in pregnant mothers before reaching the brain of the fetus. Notably, JEV can do this in a mouse model of infection [35], while this does not seem to happen with WNV in pregnant women [34]. On the other hand, ZIKV can cross the placenta and can infect placental stromal macrophages [45], called Hofbauer cells, as well as early trophoblast cells [46].

The molecular determinants for Flaviviruses neuropathogenicity are still not well elucidated. They seem to be spread across the whole viral genome as aminoacids substitutions wihin structural and

not-structural viral proteins, but their functions is not clear [41,47]. Substitution in the E envelope glycoprotein result in altering cellular uptake; in fact, this structural protein is the major virion surface protein and it is involved in host cell binding and entry of flaviviruses [48]. Its structure is different between flaviviruses. For example, DENV is glicosylated at Asn67 on the E protein, which is important for the interaction with DC-SIGN receptor [49], while ZIKV lacks this glycosylation site but is glycosylated at Asn154. The E protein of DENV is also glycosylated at the same site (Asn153) and this modification is important for virion release [50]. Similarly, the glycosylation of WNV E protein enhances virus neurovirulence [51]. The region surrounding this glycosylated site varies among Flaviviruses and represents an important determinant for antibody specificity.

Not all individuals infected with a neurotropic Flavivirus develop neuropathogenesis, suggesting an important role for host factors controlling the antiviral immune response.

1.4 ZIKA VIRUS (ZIKV)

1.4.1 Phylogeny

The phylogenetic analysis, based on the genome sequences of representative Flavivirus members, showed that ZIKV clusters with the four serotypes of DENV at a higher hierarchical level [15] (Fig. 1.6), with approximately 43% amino acid identity across the viral polyprotein and in the ectodomain E [38].

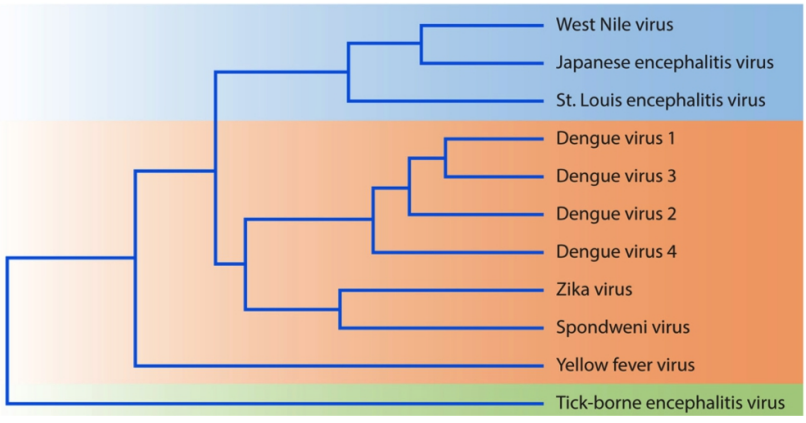

Fig. 1.6 : Phylogenetic tree illustrating the genetic relationships between Flaviviruses that are human pathogens. The dendogram was constructed using the amino acid sequence of the complete polyprotein.

ZIKV is classified into the Spondweni serogroup, genus Flavivirus, including ZIKV and Spondweni virus, this relationship results in an individual ZIKV cluster in the phylogenetic tree [52].The full genome of ZIKV (the ZIKV MR 766 prototype strain) was sequenced for the first time in 2007 [53], while the full sequences of other ZIKV strains from Brazil, Cambodia, the Central African Republic, French Polynesia, Guatemala, Malaysa, Nigeria, Puerto Rico, Senegal, Thailand and Yap state reported in GenBank (http://www.ncbi.nlm.nih.gov/GenBank/) were sequenced during the recent epidemics [54-57].

Nowadays, ZIKV isolates can be classified into two major lineages corresponding to the African lineage and the Asian lineage (comprising the American starins), both emerged from East Africa during the late 1800s or early 1900s and with an 89% sequence homology [57] (Fig. 1.7). Phylogenetic studies showed that ZIKV strains circulating in French Polynesia during the 2013-2014 outbreak and those isolated in the Americas since 2015 belong to the Asian lineage and share 99% sequence identity [58].

A neglected ZIKV lineage is probably present in Africa, designated African II, and represents a sister group to both African and Asian lineages [59,60].

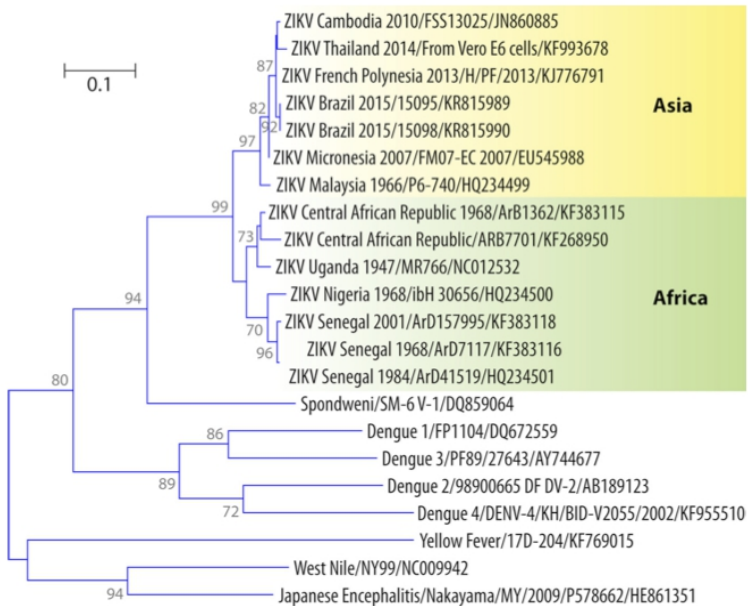

Fig. 1.7 : Phylogenetic tree of ZIKV illustrating African and Asian lineages.

1.4.2 Routes of transmission

1.4.2.1 Vector-borne transmission

Like other flaviviruses, ZIKV is transmitted by mosquitoes, primarily of the *Aedes* genus. Several *Aedes* spp. have been implicated in ZIKV transmission, such as *Ae. aegypti*, *Ae. africanus*, *Ae. hensilli*, *Ae. albopictus*, *Ae. vitatus, Ae. hirsutus, Ae. unilineatus, Ae. metallicus, Ae. apicoergenteus, Ae. opok, Ae. dalzieli, Ae. luteocephalus, Ae. Tayliri* [61-65].

Monkeys probably serve as reservoir hosts for ZIKV in the sylvatic transmission cycle [64,66], while humans are the amplifying hosts in the urban transmission cycle and the epidemics are caused and sustained by the urban cycles of transmission between humans and mosquitoes.

ZIKV was isolated for the first time from *Ae. africanus* in 1948 [67] and the first isolate of ZIKV from a mosquito other than *Ae. africanus* was obtained from *Ae. aegypti* in Malysia in 1966 [68]. *Ae. hensilli*, the most abundant mosquito specie in Yap island, was conceivably the main vector for ZIKV transmission during the outbreak that occurred in 2007 [69]; laboratory experiments showed the ability of *Ae. hensilli* to transmit ZIKV [70]. *Ae. aegypti* and *Ae. polynesiensis*, the most common local mosquito species, were probably involved in ZIKV transmission in French Polynesia [71]. *Ae. aegypti* and possibly also *Ae. albopictus* are the vectors responsible for transmission in Brazil and in other countries in South and Central America [72,73].

ZIKV replicates in the mosquito's midgut epithelial cells and then its salivary gland cells. After 5-10 days, ZIKV can be found in the mosquito's saliva which can then infect humans. If the mosquito's saliva is inoculated into human skin, the virus infects epidermal keratinocytes, skin fibroblasts and Langherans cells [74].

1.4.2.2 Non vector-borne transmission

Unlike many Flaviviruses, ZIKV can be transmitted from human to human through different routes, including sexual transmission, vertical transmission, blood transfusion and organ donation [38].

Though being spread by mosquitoes, sexual transmission of ZIKV has been documented [75]. Sexual transmission of ZIKV is supported by the evidence of ZIKV infection in women and men acquired from their infected partners by unprotected vaginal, oral, or anal intercourse [76]. ZIKV RNA persists for a long-time in semen of infected men [76,77,78], with reports showing detection of ZIKV RNA in semen sample for up 6 months after symptom onset [79,80].

Similarly, ZIKV RNA has been detected in the female genital tract beyond viremia up to 3 weeks after the onset of illness [81-83].

ZIKV RNA can be detected also in other body fluids: viral RNA and infectious virus have been detected in urine and saliva even after clearance of the virus from blood [84-87] and this can be consistent with viral replication in urogenital and oral tissues.

Remarkably, vertical transmission of ZIKV from mother to fetus has become a major public health problem because, ZIKV infection during the first trimester of pregnancy may lead to fetal microcephaly and other brain anomalies [88].

Transplacental transmission has been extensively documented by detection of the virus in the amniotic fluid, in the placenta after miscarriage and in brain tissues of microcephalic fetuses [89].

While other viruses, such as cytomegalovirus or rubella virus are able to cross the placenta and cause microcephaly, this ability has never been associated before with flaviviruses [90,91]. Specifically, although perinatal transmission has already been reported for DENV [92,93] and WNV [94], a very low rate of DENV-induced microcephaly have been reported so far and no clear evidence of association between WNV infection and microcephaly have been observed [34,95].

Two cases of perinatal transmission of ZIKV were reported during the outbreak in French Polynesia in 2013 from pregnant women who got infected a few days before delivery [96].

ZIKV RNA was detected in the breast milk of three symptomatic mothers [96,97]. This route of transmission has been documented for other flaviviruses [98,99].

Like other flaviviruses, ZIKV can potentially be transmitted through blood transfusion and several affected countries have developed strategies to screen blood donors [100]. The virus was detected in 3% of asymptomatic blood donors in French Polynesia [101], and cases of ZIKV transmission through blood transfusions have been reported in Brazil [102,103].

1.4.3 Epidemiology

The very first known case of ZIKV fever was in a sentinel Rhesus monkey stationed on a tree platform in the Zika Forest in Uganda in 1947 [64], while the first human cases were reported in Nigeria in 1954 [104]. A few outbreaks have been reported in tropical Africa and in some areas in Southeast Asia [105]. In 1977–1978, ZIKV infection was described as a cause of fever in Indonesia [106]. Before 2007, there were only 13 reported natural infections with ZIKV, all with a mild, self-limited febrile illness [107].

1.4.3.1 Yap Islands outbreak, 2007

The first major outbreak, with 185 confirmed cases, was reported in 2007 in the Yap Islands of the Federated States of Micronesia. The most common symptoms were rash, fever, arthralgia, and conjunctivitis, and no deaths were reported. While the way of introduction of the virus on Yap Island remains uncertain, it is likely to have happened through introduction of infected mosquitoes or a human infected with a strain related to those in Southeast Asia [69] . This was also the first time Zika fever had been reported outside Africa and Asia [108].

1.4.3.2 2013-2014 Oceania outbreaks

In October 2013, there was an outbreak of Zika fever in French Polynesia, the first outbreak of several Zika outbreaks across Oceania[109]. During this outbreak, for the first time, an increased incidence of Guillain-Barré syndrome and other severe neurological complications, including cases of fetal microcephaly, were observed [110]. Then, the virus spread to other islands in the Pacific Region, with outbreaks recorded in 2014 in New Caledonia, Cook Islands, and Vanuatu [109]. It is thought that the 2013–2014 outbreak involved introduction of a ZIKV strain from Southeast Asia, independent from the Yap island outbreak [111].

1.4.3.3 2015-2016 epidemic

Since its first appearance in the Western hemisphere in February 2014, ZIKV has rapidly spread throughout South and Central Americas. In May 2015, the virus was detected in an HIV-infected patient from Rio de Janeiro, Brazil, who had no travel history and presented with rash, myalgia, and conjunctivitis [112]. In June 2015, another case of ZIKV infection was reported in an Italian traveler who returned from Brazil in March 2015 and had symptoms of diffuse rash, fever, and conjunctivitis [113]. In May 2015, Brazil officially reported its first 16 cases of the illness and, following the outbreak of Zika fever in North-eastern Brazil, physicians observed a very large surge of reports of infants born with microcephaly, with 20 times the number of expected cases. Subsequently, ZIKV rapidly spread from Brazil to other countries of South and Central America, such as Colombia, which was also highly affected by ZIKV disease [114]. Phylogenetic analysis of partial and full ZIKV genome sequences showed relatedness with ZIKV strain isolated in French Polynesia, suggesting that the virus was introduced from the Pacific Islands [110,115]. Several cases of imported ZIKV infection have been recorded in Europe, North America, and Asia, including infections in pregnant women. In addition, autochthonous ZIKV infections due to possible sexual transmission were recorded in the USA and Europe [116]. In February 2016, the World Health Organization (WHO) declared the outbreak a Public Health Emergency of International Concern as evidence grew that ZIKV is a cause of birth defects and neurological

problems [117]. In April 2016, WHO stated there was a scientific consensus, based on preliminary evidence, that ZIKV is a cause of microcephaly in infants and Guillain-Barré syndrome in adults. Studies of the current and prior outbreaks found Zika infection during pregnancy to be associated with early pregnancy loss and other pregnancy anomalies [118].

1.4.4 Clinical manifestations

Infection with ZIKV is often asymptomatic, but in 20% of cases it can cause an influenza-like viral illness similar in the early stages to that caused by other arboviruses, such as DENV and chikungunya virus (CHIKV)[119]. Common symptoms are fever accompanied macular or papular rash, arthritis or arthralgia, non-purulent conjunctivitis, myalgia, headache, retro-orbital pain, edema and vomiting [120]. The period of incubation is not yet known, probably it is up to 10 days from the mosquito inoculation [69,121]. Generally, symptoms last less than seven days [122] and the disease is usually mild enough that people do not have to go to the hospital [117]. (Fig. 1.8)

1.4.4.1 Neurologic complications in adults

A temporal and geographic relationship was observed between Guillan-Barrè syndrome (GBS) and ZIKV outbreak in French Polynesia, an increase in the number of patients with GBS was reported [123]. GBS is a rapid-onset muscle weakness caused by the immune system damaging the peripheral nervous system and which can progress to paralysis [37]. Other arboviruses, such as WNV [124], DENV [125] and JEV [126] have been associated with GBS.

A case-control study on 42 GBS patients diagnosed after a ZIKV outbreak in French Polynesia between October 2013 and April 2014 demonstrated a strong association between GBS and previous ZIKV infection. All GBS patients had neutralizing antibodies against ZIKV compared to 56% in the control group of patients without GBS. Most patients with GBS experienced a transient illness in a median of 6 days before the onset of neurological symptoms, suggesting a recent ZIKV infection [127].

Other neurological conditions have been associated with ZIKV infection, such as acute meningoencephalitis [44] and acute myelitis [128], with detection of ZIKV RNA in cerebrospinal fluid (CSF). (Fig. 1.8)

1.4.4.2 Neurological complications in newborns

The infection may also be vertically transmitted and can cause multiple problems, most notably microcephaly in the fetus, a condition in which the brain does not develop properly resulting in a

smaller than normal head [88]. The association between ZIKV infection and microcephaly was supported by a retrospective analysis of the outbreak in French Polynesia in 2013-14, which demonstrated an incidence of microcephaly of 0.95% in women infected in the first trimester, while the baseline prevalence was 0.02% [129]. In 2014-2015, a two-fold increase of cases of congenital cerebral malformations and a 31- fold increase of brainstem dysfunction were also observed in French Polynesia. Microcephaly was clearly associated with ZIKV infection because of the detection of viral RNA or infectious ZIKV in the amniotic fluid of some fetuses [110]. The association of ZIKV infection with microcephaly and other neurological defects was also supported by several case reports and case series of laboratory-confirmed ZIKV infection during pregnancy, including a fetus with microcephaly recovered after elective termination at 32 weeks of gestation, with almost complete agyria, hydrocephalus, and microcephaly, with ZIKV RNA and viral particles detected at high titer in the brain but not in other tissues [89]. Decreased fetal head circumference and abnormal intracranial anatomy with enlarged ventricles and short corpus callosum were reported in a case of ZIKV infection that occurred during pregnancy at the 11th week of gestation; post-mortem examination showed apoptosis and calcification in intermediately differentiated neurons of the neocortex; high ZIKV RNA load was demonstrated in brain tissue, placenta, and fetal membranes, while lower amounts of viral RNA were detected in fetal muscle, liver, and lung. Notably, the mother had prolonged viremia both at 16 weeks and at 21 weeks of gestation, but not after delivery, thus suggesting that the persistent viremia was a consequence of viral replication in the fetus or placenta [130]. The reported microcephaly cases may represent only the severe end of the disease spectrum [131]. Ocular findings in infants with presumed ZIKV-associated microcephaly have been also described. Approximately 30% of children with suspected ZIKV infection in utero had evidence of significant retinal and optic nerve abnormalities, the most common of which were focal pigment mottling of the retina and chorioretinal atrophy[132]. Other severe anomalies in infants born from women infected with the virus were reported, such as hydrops fetalis, a condition in which the fetus is characterized by an accumulation of fluid in at least two fetal compartments [133]. (Fig. 1.8)

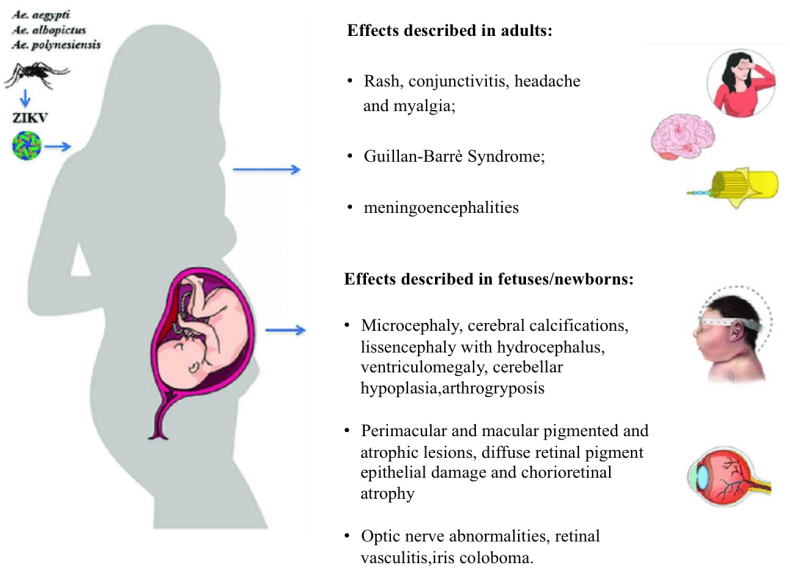

Fig. 1.8 : Clinical manifestations of ZIKV infection in adults and fetuses or newborns.

1.4.5 Models of ZIKV infection

Even before the first suspected cases of neurological disorders associated with ZIKV, some studies reported the neurotropism of ZIKV strains isolated in Uganda [134-135]. They described the presence of neuropathological changes, such as the severe neuronal degeneration or reactive astrocytosis in the hippocampus of newborn and adult mice inoculated with ZIKV.

Recently, after the outbreak of ZIKV in South and Central America, the scientific world started to investigate the vulnerability of neural cells to ZIKV infection.

1.4.5.1 *In vitro* model of ZIKV infection in Central Nervous System

In order to find the connection between ZIKV exposure and neurological defects or diseases, human induced pluripotent stem cells (hiPSCs) were employed to study the neurovirulence of ZIKV after differentiation in different types of human neural stem cells (NSCs), neural progenitor cells (NPCs) and their progeny as in cerebral organoids [33,136,137,138]. Also, viral neurotropism was analyzed in human organotypic fetal brain slices [139,140], human NPCs derived from fetal brain [140-142] and immortalized cell lines.

The ZIKV MR766 strain (African lineage from Uganda) was used to infect hiPSC-derived forebrain-specific NPCs grown in monolayer cultures. Infection led to cell-cycle dysregualtion and increase of apoptosis and affected signaling pathways, including downregulation of cell cycle genes

and upregulation of apoptosis genes. At variance, hiPSCs and immature neurons exhibited lower permissiveness to ZIKV infection [33]. Following this first report, other studies demonstrated similar results of ZIKV infection and its pathological effects in hiPSC- and fetal brain tissue-derived neural progenitors grown in monolayer and 3D neurosphere cultures. Garcez *et al*. [137] observed that both ZIKV MR766 strain and DENV-2 16681 strain infected hNSCs, but only ZIKV increased cell death in NSCs, impaired the formation of neurospheres and reduced the growth rate of human brain organoids.

In further studies, brain organoids appeared an interesting platform for analysis of ZIKV-induced neural damage [138,143-146]. In fact, iPSCs-derived brain organoids can reproduce the endogenous human brain development with similar structural organization and molecular signatures [147-150]. Brain organoids allowed to investigate the consequences of ZIKV infection on cortical layer tickness, cell-type specificity in the complex tissue and human-specific and developmental stage – specific features. Quian and colleagues [145] showed that in a forebrain-specific human brain organoid model, transient exposure to ZIKV MR766 resulted in preferential infection of radial glial cells, although the virus could be detected to a lesser extent in immature neurons, intermediate progenitor cells and astrocytes. Infected early stage organoids showed decreased proliferation and increased cell death, enlarged ventricules and thinner ventricular zone and neuronal layer, which are the hallmarks of microcephaly [89,151].

Another important study exploited brain organoids with a mixture of cell types of different brain regions [148] to compare the impact of different viruses and viral strains. Results showed that DENV [137] and YFV [138] were not implicated in microcephaly development and they did not affect the size of brain organoids. The Brazilian ZIKV strain reduced neuronal layer tickness in human cerebral organoids more than the African strain. Interestingly, brain organoids derived from non-human primates iPSC (chimpanzee) were not susceptible to the Brazilian ZIKV strain, suggesting a potetial strain- and species-specific impact of ZIKV [138].

It is worthy to underline that the first studies were performed using the prototype ZIKV strain MR766 of African origin and the basic results were confirmed with recent clinic isolates of Asian origin, such as the Cambodian strain FSS13025 [152a] and strains isolated from Brazil [138], Mexico [153] and Puerto Rico [154]. At the moment, the ability of different ZIKV strains to cause human neurological abnormalities remains unclear. Quantitative differences in NPC proliferation, cell death and gene expression have been detected in cellular models [152,138]. Moreover, it is important to consider any strain-specific phenotypes in experimental models in the context of the passage histories of the strain. For example, the prototype MR766 strain has gained adaptive

properties due to the extensive passages in suckling mouse brain, while other strains from the recent outbreak in the Americas have been passaged a few times in the laboratory.

1.4.5.2 Mechanisms of ZIKV entry in human cells and host antiviral response

In vitro studies demonstrated that ZIKV enters and infects target cells using adhesion factors such as DC-SIGN and phosphatidylserine binding receptors [138,155]. AXL receptor was described as the candidate receptor for the entry in human skin fibroblasts [156], radial glia cells [157], astrocytes [139,158] and microglia [158] in the developing human brain; blood-brain barrier endothelial cells [159] and trophoblast progenitors in placenta [160], which correlates with the high efficiency of infection in these cell types.

Despite the high expression level of AXL in NSCs and NPCs [138, 140, 157-159], AXL does not seem to be an exclusive entry receptor for ZIKV in NPCs and cerebral organoids, since it is reported that ZIKV can still infect AXL-deficient human NPCs in monolayer or organoid cultures [158]. Whether TAM receptors, including the family members AXL, act as entry receptors remain controversial even for the other flaviviruses WNV and DENV. TAM receptors are required for WNV and DENV [161] attachment and entry; however TAM receptors do not seem to be necessary for the entry of these viruses, although viral replication was less efficient because TAM receptor binding downregulates type I interferon responses [162]. More recently, an *in vivo* study of flavivirus pathogenesis in TAM-receptor deficient animals showed an increased WNV infection of cells in the brain associated with alterations of blood-brain barrier permeability [163].

ZIKV infection increases expression of the innate immune receptor Toll-like 3 (TLR3) in human fibroblasts leading to type I and II interferon (IFN) responses [156]. ZIKV, also, is sensed by TLR3 in iPSC-derived human brain organoids and neurospheres [146]. ZIKV induces an innate immune response in human fetal brain microglia [164] and other cell types. Moreover, in human skin fibroblasts [156] and lung epithelial A549 cells [165] ZIKV induced expression of the transcription factor IRF7 and other interferon-stimulated genes.

Other studies, however, reported that ZIKV infection did not induce a type I interferon response and cytokine secretion in NPCs and THP-1 human monocytic cells [142], while downregulation of several immune response genes was detected in ZIKV-infected human microglia cell line [166].

Activation of apoptosis through caspase 3 was frequently observed in ZIKV-infected neural progenitors *in vitro* and in animal models of infection [140,138,145,146,152,167-170].

1.4.5.3 *In vivo* models of ZIKV infection in the central nervous system

ZIKV can block type I IFN receptor signalling in primate and human cells, but not in mouse cells [171]. Most of recent studies relied on mice deficient for type I (A129 mice) or type I/II interferon receptors (AG129) to avoid encountering an innate immune response that would prevent robust infection in juvenile and adult models. Aliota and colleagues [172] reported that subcutaneous injection of a French Polynesian strain of ZIKV in AG129 mice caused lethal infection characterized by early viremia, high viral loads in several organs, illness and brain degeneration. Acute neutrophilic encephalopathy developed in AG129 mice after intraperitoneal inoculation of ZIKV MR766; in this model of infection, mice were euthanized at 14 days post-inoculation [173]. Julander et al. [174] showed that subcutaneous infection of AG129 mice using a Malaysian strain of ZIKV caused encephalities, inflammatory lesions in the cerebellum and myelitis, with death within 21 days after infection.

Similar results were observed in A129 mice infected with an African strain (MP1751), a Cambodian strain (FSS13025) [175] or a French Polynesian strain (H/PF/2013) [176] of ZIKV.

Infection of A129 mice showed similar results. Rossi and colleagues [175] found that AG129 mice developed more severe neurological symptoms than A129 mice after infection with a Cambodian strain of ZIKV, so it seems that type II interferon signaling affects some aspects of the disease.

Two studies used triple knockout mice deficient for IRF3, IRF5, IRF7. The first study [176] reported that triple knockout mice were more susceptible to the intravenous injection of French Polynesian strain of ZIKV than A129 mice, and, also, this viral strain was more pathogenic to A129 mice compared to the African strain. The second study [177] demonstrated the neurotropism of ZIKV for NPCs and immature neurons in adult brain.

Immunocompetent mouse strains (CD1, C57BL/6 and 129Sv/Ev mice) were resistant to subcutaneous or intraperitoneal inoculation of ZIKV and did not developed disease [175,176,178]. Disease occurred only when mice were infected during the neonatal period [176,179]. Fernandes and colleagues [179] found that newborn swiss mice infected with ZIKV (brasilian strain SPH 2015) through intracerebral route exhibited a more severe brain injury than the animals inoculated through the subcutaneous route.

Intracerebral inoculation of ZIKV MR766 was performed in C57BL/6 mice at postnatal day 7 and 21. In 7-day-old infected mice, the number of proliferating cells in the ventricular zone decreased and neuronal apoptosis was observed, while mice infected at postnatal day 21 had severe paralysis, but a less prominent neuronal apoptosis [180].

Three studies reported the effects of ZIKV infection after direct injection into the embryonic lateral ventricles or early postnatal brain [181].The analyses revealed death of immature and mature

neurons, reduction of NPC proliferation and differentation resulting in a thinner cortical layer; also, the virus was mainly located in the ventricular zone and striatum of newborn mice.

Mouse models of sexual and vertical transmission were employed to understand the ability of ZIKV to cross the placental barrier and the developing or developed blood-brain barrier (BBB). Miner et al. [182] crossed A129 female mice with wild-type (WT) males and infected pregnant mice with ZIKV (H/PF/2013 strain) through subcutaneous routes on embryonic day 6.5. High levels of viral RNA were detected in the placenta, as well as placenta abnormalities and fetal demise. Fetuses showed intra-uterine growth restriction and apoptotic cells in the brain.

In vivo models allowed to demonstrate that the brain and testes are the main sites of ZIKV replication in young A129 and AG129 mice [175,176]. Testicular damage was evident in A129 mice after intraperitoneal inoculation of ZIKV (Asian strain SMGC-1) and in wild-type (WT) mice after intratesticular injection [183].

Replication of ZIKV (Cambodian strain FSS13025) in the vaginal tract of WT mice after vaginal inoculation was reported by Yockey's group, suggesting the possibility of viral transmission through sexual contact. In this study, A129 mice developed paralysis and died within 9 days, while WT mice did not develop the disease. In addition, intravaginal infection lead to intra-uterine growth restriction of the fetus if infection occured in the early phase of pregnancy.

1.5 WEST NILE VIRUS (WNV)

1.5.1 Molecular classification and phylogeny

The first classifications of WNV were based on cross-neutralization reactions and revealed that WNV belongs to the JE serocomplex, including other neurovirulent viruses such as Murray Valley encephalitis virus (MVEV), St. Louis encephalitis virus (SLEV) and Usutu virus (USUV)[184]. Even though WNV has a single serotype, it has a considerable genetic variability [185].

Phylogenetic classification of WNV remains dynamic, with the large increase in genome sequence and surveillance data available in recent years. Present analyses support that WNV aligns into at least seven different lineages (Fig. 1.9) [186], on the basis of nucleic acid homology, with the major lineages diverging by 25%-30% nucleotide differences [187,188].

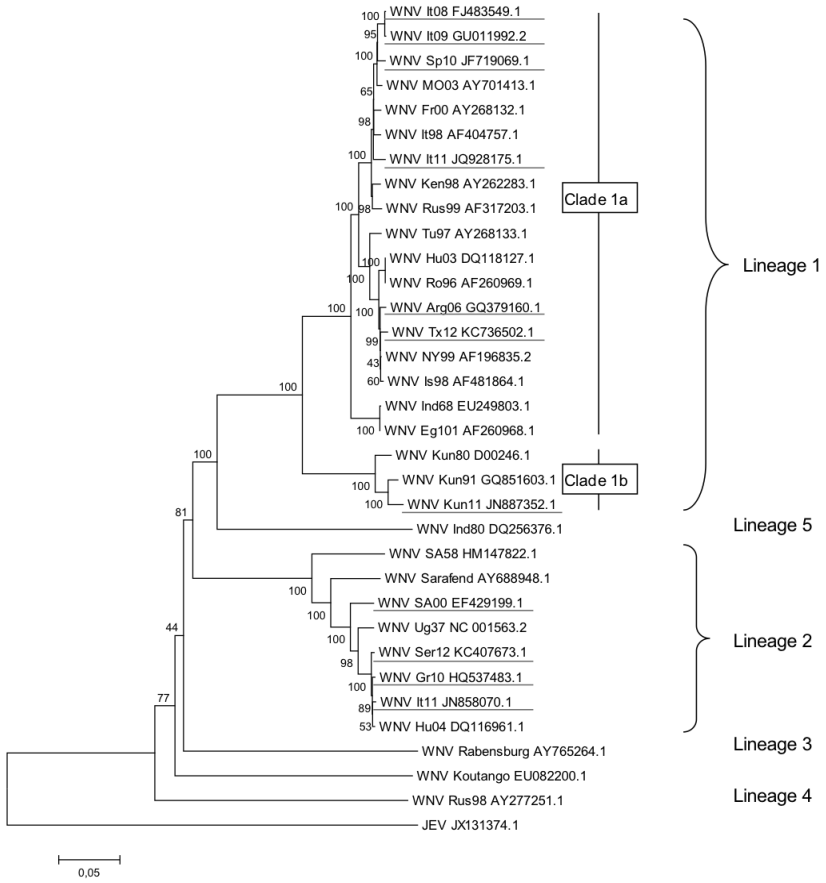

Fig. 1.9 : Phylogenetic classification of WNV using genetic alignement of complete genomic sequences

WNV strains that cause disease in humans and horses belong to the major lineages 1 and 2 [189,190], while other lineages have been sporadically detected in mosquitoes and birds but not associated with human disease [191].

Lineage 1, the largest and the most widespread, contains WNV strains isolates from Europe, Africa, Australia, Asia, North and Central America, Middle East and Oceania (Kunjin strains) [186]. Lineage 1 can be subdivided into three different clades: 1a, 1b, and 1c. Clade 1a is the most widely distributed and contains strains from the Americas (including the NY99 strain), Europe, Africa, the Middle East and Israel. Until recently, clade 1a comprises most of the isolates associated with outbreaks of human encephalities, including the ongoing epidemic in North America [192].

Lineage 2 WNV, until the mid-2000s, was predominantly limited to sub-Saharan Africa and Madagascar, where it has been a cause of mild febrile illness in humans, rarely progressing to severe disease and typically not associated with outbreaks [193]. However, in 2004 and 2005, WNV strains belonging to lineage 2 were first identified in wild birds in Hungary, with subsequent rapid spread to central Europe [194,195]. Since 2004, WNV lineage 2 has been observed in central and Eastern Europe. In 2010 it caused outbreaks in Romania and Greece and in 2011 it was detected for

the first time in Italy [196]. These lineage 2 viruses have been implicated in avian, equine, and human cases of neuroinvasive disease with associated deaths, including cases reported in Russia, Hungary, Italy, and Greece [187, 188,197,198].

The phylogenic classification does not consistently correlate with the geographical distribution of WNV, which may be attributed to the broad dissemination of the virus by migrating bird species [199].

1.5.2 Epidemiology

The epidemiology of WNV is continuously changing. WNV was first isolated in December 1937 from the blood of a 37 year-old febrile woman in the West Nile district in the Northern Province of Uganda, currently the Ardua district, during an epidemiological study defining the endemic zone of YFV [200].

Since that time, the virus was not observed again until the 1950s, when there were some sporadic reports of WNV circulation in Albania, Bulgaria, Belarus, Ukraine and Moldavia [201] and the first WNV epidemics occurred in Israel and Egypt [202,203]. Neuroinvasive cases (West Nile neuroinvasive disease, WNND) were recorded in 1957 and 1962 [204]. More recent outbreaks were reported in South Africa in 1974, when WNV caused approximately 10 000 human fever cases [205]. Since that time, only sporadic outbreaks with low clinical incidence occurred and WNV was rarely seen and was considered of only minor importance to public health, but in the mid-1990s, the epidemiology of WNV apparently changed. Epizootics and epidemics of severe neurologic disease in horses, birds and humans began to occur with increasing frequency [206-209]. The first cases of WNV in its lethal encephalitic form were reported in Algeria in 1994 with a total of 50 cases of human infections including 20 WNND and one death [210]. In 1996, the first large-scale epidemic took place in Bucarest, Romania, where WNV emerged as major cause of arboviral encephalitis. This outbreak was characterized by a high number of neuroinvasive cases with 393 recognized human cases of encephalitis and 17 deaths recorded in people over 50 years of age [211]. After 1996, outbreaks of West Nile encephalitis in people and horses were reported with increasing frequency in the Mediterranean basin [212], Russia [206] and Australia [213]. WNV activity, with or without recorded human or horses clinical cases, have been lately reported in Algeria, Marocco, Egypt, Israel, Romania, Russia, Poland, Czech Republic, Hungary, Croatia, Serbia, France, Portugal, Spain, and Italy, which overall have accounted for hundreds of cases and dozen of deaths [214]. Since 2008, in Europe there has been an increased WNV activity in Hungary (2008-2009) [215], Italy (2008-2009) [216], and Greece, including the emergence of WNV lineage 2, with a

rapid rise in the number of cases of neuroinvasive disease in animals and humans [217].

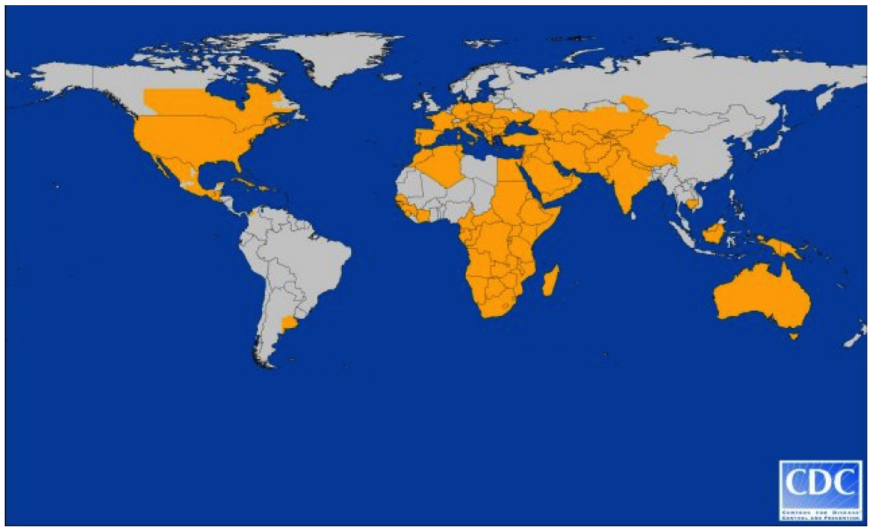

Fig. 1.10 : Global distribution of WNV (US Central for Disease Control and Prevention, CDC)

In 1999, WNV caused an outbreak in New York City marking its first appearance in the Americas. Subsequently, WNV has spread rapidly throughout the Western Hemisphere, including the USA, Caribbean, Mexico, Canada and as far south as Argentina and Brazil [218]. In North America, the virus has caused thausands of cases of meningitis, encephalitis, and poliomyelitis, resulting in significant morbidity and mortality.

1.5.2.1 Epidemiology of WNV in Italy

Notwithstanding the evidence of the presence of WNV in Italy at least since 1998, with the equine outbreak in Tuscany region [219], human disease due to WNV infection was not documented for a decade, until the first human case of WNV neuroinvasive disease was diagnosed in 2008 [220]. The first human cases of WNND and WNF were detected in the Po river area in northeeastern Italy (Emilia-Romagna [216] and Veneto [221] regions) in September-October 2008, following the alert from the veterinary surveillance that reported equine cases of WNND in the same areas [222]. Phylogenetic analyses demonstrated that the WNV strains responsible for the Italian outbreaks in 2008-2009 belonged to lineage 1 [223]. In 2009, WNV circulation was reported in larger area near the Po river that involved Veneto, Emilia-Romagna and Lombardy regions, with occurence of several human cases(214,224). During 2010, there was a decrease of WNV activity as a result of

effective vector control measures applied in the areas of WNV circulation surrounding the Po river [225]. In 2012, largest human outbreak ever recorded in Italy occurred in Northeastern Italy, with 25 confirmed cases of WNND, 17 of WNF and 14 positive blood donors [226]. Human cases of WNV neuroinvasive infections in 2011 and 2012 registered in Veneto and Friuli-Venezia-Giulia Regions were caused by a new lineage 1 strain [216] (Fig. 1.11) [227].

In Italy, the onset of WNV disease in humans ranged from late July to late October, with peaks of cases reported in late August and early September. In patients with WNND, the fatality rate was approximately 10% and death occurred mainly in elderly and immunocompromised patients [198].

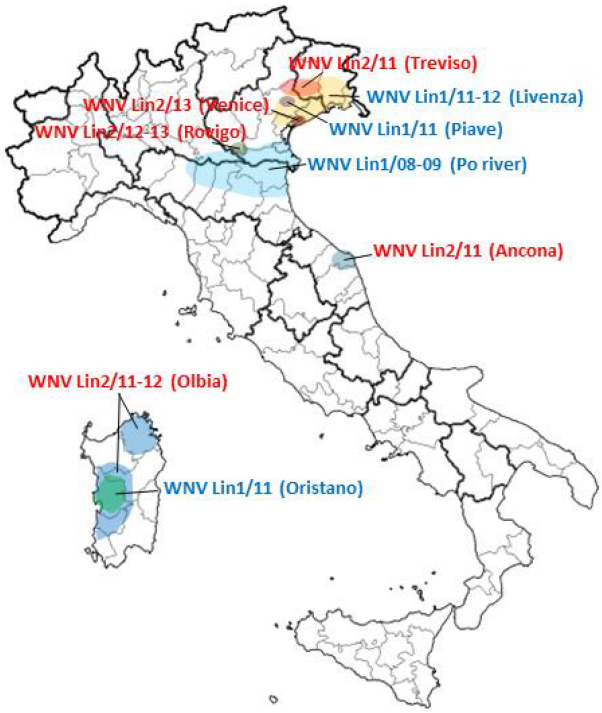

Fig. 1.11: epidemiology of WNV in Italy

1.5.3 Routes of transmission

WNV is maintained in nature in an enzootic transmission cycle between avian hosts and ornithophilic mosquito vectors. Mosquitoes become infected by feeding on infected birds [190].

WNV can be incidentally transmitted to mammals, including horses and humans [228], which are incidental or "dead-end" hosts for WNV, as the low viremia is usually insufficient to infect a feeding naïve mosquito and maintaining the transmission cycle [229]. Although human cases occur primary after mosquito inoculation, infections after blood transfusion, organ transplantation, and intrauterine transmission have been reported [64].

1.5.3.1 Vector-borne transmission

The ability of different mosquito species to acquire and transmit WNV is highly variable [230]. At least over 60 species of mosquitoes from 11 different genera have been described as competent vectors. Mosquitoes of the *Culex* genus are the predominant vectors in the enzotic cycle, although the particular species of *Culex* varies according to geographic locations [231].

In North America, *Cx. pipiens*, *Cx. restuans*, *Cx. quinquefasciatus*, *Cx. salinarus*, *Cx. tarsalis*, and *Cx. nigripalpus* have been described as the most efficient competent vectors; although other species such as *Aedes albopictus*, may also play role in viral transmission as bridging vectors that can transmit the virus to mammals [232]. In Europe, the virus has been isolated from more than 40 different species, being again those of the *Culex* species the main vectors [233].

1.5.3.2 Non vector borne transmission

Even though the main mode of WNV transmission to vertebrate hosts is *via* infected mosquito bite, it has been documented that alternative less common modes of non-vector-borne transmission in humans also exist: through solid organ transplantation from an infected donor to healthy recipient; through the placenta from an infected mother to her fetus (vertical transmission), and through transfusion of infected blood and blood products [190]. The first case of virus transmission through transfusion of red blood cells, platelets and fresh-frozen plasma was reported in 2002 [234] which drove implementation of screening of blood units with NAT test in 2003 and subsequent years.

In addition, in 2002, WNV transmission was reported through solid organ transplantation from an organ donor, probably infected through blood transfusion, to four transplant recipient [235].

In the same year, the first case of transplacental WNV transmission was reported: a WNV-infected woman delivered at term a live infant that was positive for WNV-specific IgM and neutralizing antibodies with severe cerebral abnormalities (white matter loss, focal cerebral destruction) [236].

In 2002, another case of probable non-vector-borne transmission of WNV through breast milk was reported, but since there was no further confirmed cases of transmission [64,237,238].

Sexual transmission of WNV has not been documented, but recently a report described the development of WNV meningoencephalitis in a middle aged woman within two weeks of unprotected vaginal intercourse with her infected husband. The husband had flu-like illness and rash the day after the sexual contact and there was no reported mosquito bite exposure [239].

1.5.4 Pathogenesis

Understanding the full range of WNV pathogenesis in humans has been difficult, mainly due to the

difference in virulence between WNV strains and the high prevalence of asymptomatic or sub-clinical infections.

The vast majority of our current knowledge regarding WNV pathogenesis resulted from animal models (mostly rodent) infected under controlled conditions with a known amount of needle-inoculated virus. On the basis of these studies, three distinct phases of WNV pathogenesis have been identified:

1. an early phase, with initial infection and spread;
2. a visceral-organ dissemination phase, characterized by peripheral viral amplification;
3. a central nervous system (CNS) phase, characterized by neuroinvasion.

These phases may not accurately reflect the course of a natural infection in humans, but this sequence is thought to recapitulate the stages of pathogenesis in humans, following infection by a mosquito [240].

Briefly, following a subcutaneous bite of an infected mosquito, WNV replicates in keratinocytes [241] and skin-resident dermal dendritic cells (DCs) and Langherans cells. Infected DCs migrate to the regional draining lymph node and seed the virus within this node [242]. Replication within the draining lymph node leads to viremia and subsequent infection of peripheral organs, including spleen, heart, liver and kidneys. Between 6 and 8 days after infection, WNV is cleared from peripheral organs and infectious virus is detected within the brain and spinal cord, in part owing to the virus crossing the blood-brain barrier, where it is responsible for inflammation of the brain and the spinal cord [240].

The specific target cells for WNV infection in the spleen and other peripheral tissues are not well defined, but are thought to be substes of DCs, macrophages and possibly neutrophils [243,244].

1.5.5 Clinical manifestations

It is generally estimated that the majority (75 to 80%) of WNV infections in humans are asymptomatic. Of those who develop symptoms, approximately 20% of the infected people develop an acute, systemic febrile illness, termed WN fever (WNF), and less than 1% develop neurologic illness, which is primarily attributed to the neuroinvasive disease (WNND), with viral infection of the CNS.

1.5.5.1 West Nile fever (WNF)

West Nile fever is the predominant clinical syndrome seen in most WNV-infected persons that develop symptoms.

Following an incubation period of approximately 2-14 days, infected persons typically show sudden onset of fever (usually >39°C), headache, fatigue, myalgia, rash, often accompanied by

gastrointestinal complaints, including nausea and vomiting that may lead to dehydration [245].
Most patients experience complete recovery [246]; however some otherwise healthy persons may continue to experience a prolonged fatigue, headaches, and difficulties concentrating for days or weeks following infection [247].

1.5.5.2 West Nile neuroinvasive disease (WNND)

Severe WNND is associated with neurological involvement that varies from meningitis and/or encephalities to poliomyelitis-like condition with acute paralysis [248].
Aseptic meningitis (West Nile meningitis, WNM) is similar to that of other viral meningitides. It involves infection of the meninges and makes up the largest percentage of the neuroinvasive disease in younger age groups.
Encephalitis (West Nile encephalitis, WNE) involves viral infection of the brain parenchyma itself and is more typically manifested in older persons, particularly over the age of 55 years [249], or immunocompromised individuals. It ranges in severity from a mild self-limited confusional state to severe encephalopaty, coma, and death.
Acute poliomyelitis-like syndrome (West Nile poliomyelitis, WNP) results from viral infection of the anterior horn cells of the spinal cord, leading to acute flaccid limb weakness [245].
Importantly, other forms of acute flaccid paralysis (AFP) associated with West Nile virus infection include Guillan-Barrè syndrome (GBS) and other demyelinating neuropathies [124].

1.5.6 Neuroinvasion

WNV is both neuroinvasive and neurotropic and invasion of the CNS tissues constitutes the third phase, where the virus targets and replicates in neuronal cell subsets. To establish infection in neurons of the brain, WNV first must cross the BBB, a highly regulated interface between the blood and the brain composed of four main cellular components: endothelial cells and their basement membrane (composed of collagen IV, laminin, proteoglycans, and glycoproteins), astrocytes, microglial cells and pericytes (PCs) [250]. Endothelial cell models have been developed to study the mechanism of WNV translocation across BBB *in vitro*. These models demonstrated the transcellular transport of virions across the infected endothelial cells and an increased permeability of the BBB, which can facilitate paracellular entry of WNV into the brain parenchyma [41]. In any case, the mechanisms by which the virus gains entry into the CNS remains poorly understood.
The mechanism by which WNV cross the BBB may depend on the infection route and the pathogenicity of the WNV strain. Several models have been proposed for WNV entry into CNS:

- crossing of the BBB likely occurs through a hematogenous route: according to literature, increased viral burden in the serum correlates with greater and more rapid WNV entry into the

CNS [251] and for this reason the hypothesis of hematogenous dissemination of WNV into the CNS has been a common focus of investigation;

- viral entry *via* passive diffusion of cell-free virions as result of blood-brain barrier (BBB) breakdown: The hypothesis of viral entry into CNS across a more permeable BBB due to intravascular levels of pro-inflammatory cytokine, which are produced during peripheral immune response. This cytokine response can mediate increased vascular permeability, but may also allow WNV to cross the BBB and infect neurons [252]. In particular, WNV infection in peripheral tissues induces TLR3-mediated secretion of pro-inflammatory cytokines, including IL1β, IL-6, IL8 and TNF-α, which may disrupt the BBB. Among these, secreted TNF-α modulates BBB permeability by altering endothelial cell tight junctions, which may allow WNV to cross the BBB and infect neurons [253]. The flux of WNV into CNS can be also enhanced through degradation of the tight junction proteins of the BBB extracellular matrix by activation of matrix metalloproteinases;

- The 'Trojan Horse' mechanism, *via* infected inflammatory cells: WNV is transported by infected immune cells (e.g., neutrophils or CD4+ or CD8+ T cells) across paracellular junctions between endothelial cells into the brain parenchyma [254]. The 'Trojan Horse' hypothesis has been proposed in many reviews [255-258];

- WNV may penetrate into the CNS through a transneural route and two neuroanatomical areas have been hypothesized to be involved in this mechanism: from the peripheral somatic nerves or from the olfactory nerves into the CNS [259]. In this regard, reports underline the susceptibility of peripheral neurons to infection by WNV [260];

- Infection or passive transport through choroid plexus epithelial cells that have been documented in animal models [261] or direct infection of brain microvascular endothelial cells [262].

Considering *in vivo* and *in vitro* data, the route of WNV neuroinvasion may be much more complex than one distinct path from the peripheral site of inoculation to the CNS and WNV may enter the brain though a combination of mechanisms. Also, the ability of WNV to invade the CNS may depend on the route of transmission and the pathogenicity of the WNV strain [41,263].

1.5.7 Tropism

The skin cells that are targeted *in vivo* by WNV are unknown; however, it is believed that WNV

infects Langerhan cells (LCs), resident dendritic cells (DCs) and keratinocytes [241]. Importantly, LCs are *in vivo* cell targets also for DENV [264] and DCs are susceptible to WNV infection *in vitro* [265].

WNV replication is tipically restricted to the skin, draining lymph nodes, spleen, and CNS in humans and in wild-type mouse models [240,241].

Regarding the neurotropism, studies in humans and mice have demonstrated that neurons are the primary cells targeted by WNV [266]. In humans, WNV is most often detected in neurons in the cerebral cortex, thalamus, brainstem, basal ganglia, cerebellar Purkinje cells, and spinal cord (mainly anterior horn), and, in some cases, infection has been detected in the olfactory bulb and hippocampus. WNV has been detected in the same regions of the brain of experimentally infected mice as in humans, indicating a similar tropism of WNV in humans and animal models [267]. Moreover, WNV-positive brain microvascular endothelial cells and astrocytes have been detected in birds and humans, respectively, suggesting that these cells may serve as secondary targets *in vivo* [268,269]. Astrocytes and endothelial cells form with neurons the neurovascular unit (NVU), which regulates blood flow, the integrity of the BBB, and neuronal activity [266]. *In vitro* studies demonstrated that pathogenic strains of WNV replicate within all NVU cell types, though replication in astrocytes was the most restricted [39,270]. Moreover, although with several differences, neurons and astrocytes were found to support productive WNV infection, whereas microglial cells were poorly permissive to viral growth [271].

Examination of WNV replication within neurons, endothelial cells and astrocytes demonstrated that high and low neuropathogenic strains of WNV replicate with similar kinetics and to equivalent levels in brain microvascular endothelial cells and neurons. However, astrocytes exhibited lower susceptibility to the low neuropathogenic strain compared to the high neuropathogenic strain, suggesting a possible role for this cell type in limiting WNV replication within the CNS [270].

1.5.8 Innate immune response

The innate immune system acts as the first line of defense against invading viral pathogens and it is critically important for contrlling WNV infection [272]. Innate immune response is mediated by specialized cellular proteins termed pattern-recognition receptors (PRRs). PRRs are expressed by a variety of cells which are responsible for sensing the presence of pathogens invasion through evolutionary conserved viral components, known as pathogen-associated molecular patterns (PAMPs) that are broadly shared by different microorganisms and essential to the infectivity of the pathogen. Currently, three classes of PPRs have been shown to be involved in the recognition of PAMPs, namely: retinoic acid-inducible gene I (RIG-I)-like receptors (RLRs), Toll-like receptors (TLRs), and nucleotide oligomerization domani (NOD)-like receptors (NLRs). Among these

receptors types, RLRs and TLRs detect pathogen structures in immune cells and activate intracellular signalling cascades that lead to production of type I interferons (IFNs), proinflammatory cytokines and stimulate the expression of antiviral genes.

WNV-host interaction within the innate immune signalling network and the antiviral effector genes that control WNV infection were identified by several groups in the scientific world. (Fig. 1.12) [256].

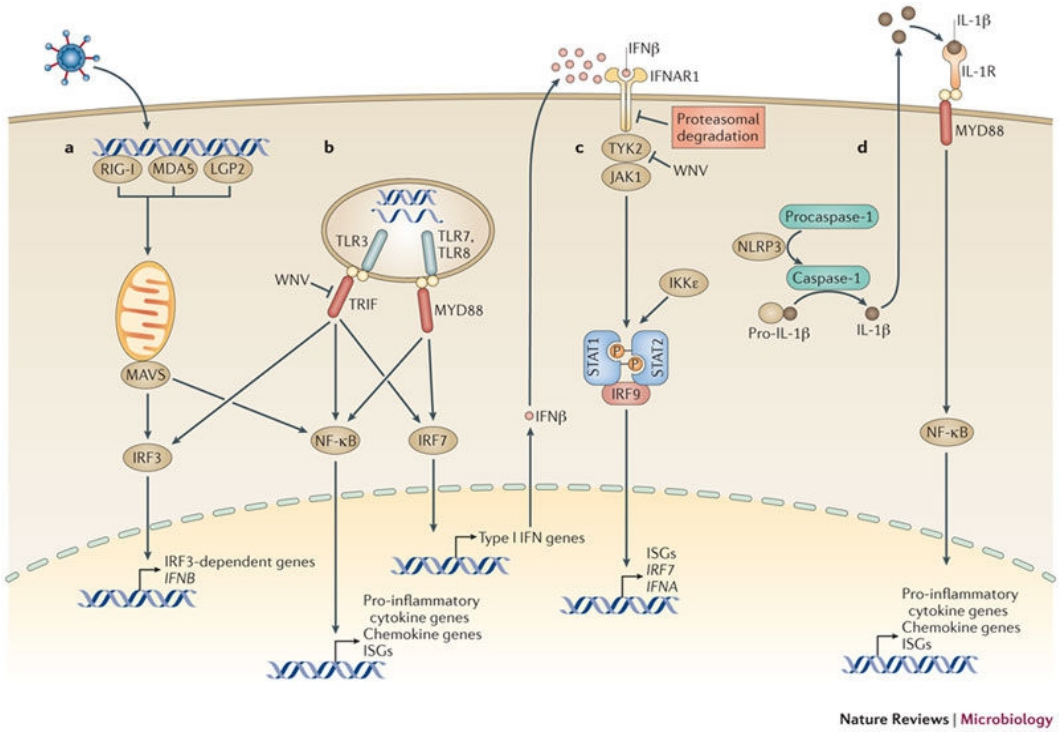

Fig. 1.12 : Cell intrinsic innate immune response to West Nile virus infection

The RIG-I like receptors are cytosolic proteins consisting of three members: RIG-I (also known as DDX58), melanoma differentation-associated antigen 5 (MDA5) and laboratory of genetics and physiology-2 (LGP2) [273]. They are critical sensor of viral RNA in the cytoplasm and they are expressed basally in nearly all cell types in the body [274]. They recognize PAMPs and activate downstream effectors which drive the transcription of IFNβ, IFNα, proinflammatory cytokines, and interferon-stimulated genes (ISGs) [275]. Fredericksen and colleagues reported the activation of RIG-I and MDA5 in primary mouse cells infected with WNV *ex vivo* [276], suggesting that WNV presents viral PAMPs that can trigger RIG-I and MDA5 signalling.

In addition to RLRs, TLRs are important for recognizing WNV infection. They are transmembrane proteins suitable for detecting distinct viral PAMPs outside the cells, in cytoplasmic vacuoles after phagocytosis or endocytosis [277]. More than ten TLR proteins exist in mammals; among these receptors, TLR2 and TLR4, which are located in the plasma membrane, are involved in the

recognition of viral envelope proteins on the cell surface. TLRs 3, 7, 8 and 9 reside on cytoplasmic vescicles such as endosomes and ER and recognize microbial nucleotides [277]. TLRs activate a signaling pathway that leads to the production of type I IFNs and pro-inflammatory cytokines [278]. TLR3 and TLR7/8 are important in regulating immunity to WNV, but unlike the RLRs, they fuction in a cell- and tissue-specific manner. TLR3 signalling in cortical neurons, but not in macrophages or DCs, promotes type I IFN production [279]. TLR7/8 signalling is important for triggering type I IFN and proinflammatory cytokine production within neurons, macrophages and keratinocytes, but not DCs [280].

NOD-like receptors are essential for the fomation of the inflammasome complex, which promotes viral clearance through secretion of pro-inflammatory cytokines of the IL-1β family. Activation of the NLRP3 inflammasome and subsequent secretion of IL-1β family pro-inflammatory cytokines are involved in cell protection against WNV [281]. Increased levels of IL-1β are observed in humans during the course of WNV disease and mice lacking IL-1β signalling are more susceptible to WNV infection [281].

Both RLR and TLR signalling activate IRF transcription factors, in particular IRF3 and IRF7, which are essential for regulating type I IFN response following viral infections [240,282,283].

1.6 DENGUE VIRUS

1.6.1 Classification and epidemiology

Dengue virus is the most important arbovirus known to affect the mankind and represents a significant public health problem, in particular in the developing world.

Neutralization assay data distinguished four antigenically closely related DENV serotypes termed DENV-1, DENV-2, DENV-3, and DENV-4 [284,285], which share approximately 65% of their genome [286]. This classification was based on sequencing of the E gene within each serotype [287]. (Fig. 1.13) .

Recently, dengue virus serotype 5 (DENV-5) was identified [288]; the discover was based on an atypical virus isolated in 2007 from a patient in Borneo. This virus is phylogenetically distinct and elicits a different antibody response from that initiated by DENV serotypes 1-4; also, the virus seems to circulate among non human primates [289].

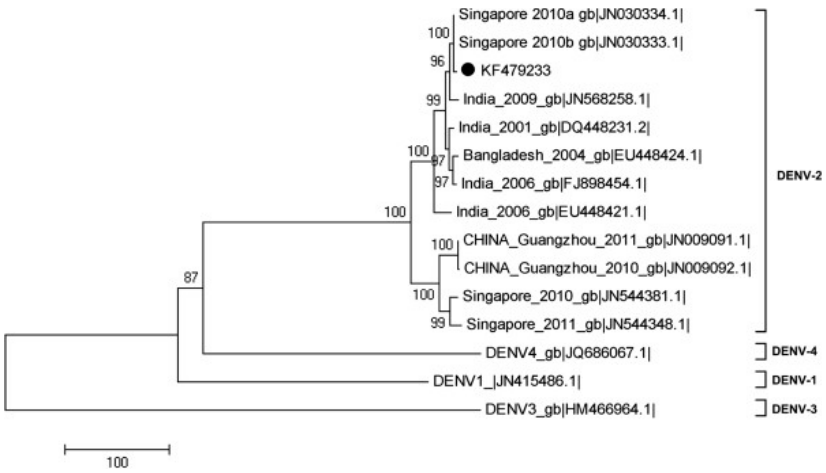

Fig. 1.13: Phylogenetic tree based on dengue virus E gene: DENV-1, DENV-2, DENV-3, and DENV-4.

DENV-1 and DENV-2 were isolated during World War II in the Pacific [296], while DENV-3 and DENV-4 were isolated in the 1950s during epidemics in the Philippines and Thailand [290].

Currently, more than 100 countries, in the World Health Organzation (WHO) regions of Africa, South-East Asia, the Americas, the Eastern Mediterranean and the Western Pacific are endemic with DENV [291]. In 2014, Japan reported its first outbreak of the disease in 70 years [292].

It is estimated that 400 million infections occur each year and there are 3,6 billion people at risk of getting infected [293].

The first well-characterized clinical description of dengue disease was noted in 1780 during the outbreak in Philadelphia [294]. Subsequently, DENV spread during the 18th and 19th centuries in areas of Asia and Africa [295] and after World war II, many Asian countries became hyperendemic with DENV infection [296].

In recent decades, dengue incidence in South America and the Carribean has increased significantly. In addition, the high movement of people through travel provides continuing exposure to DENV infection in North America and Europe [297].

The map below (Fig. 1.4) [298] illustrates dengue risk areas worldwide

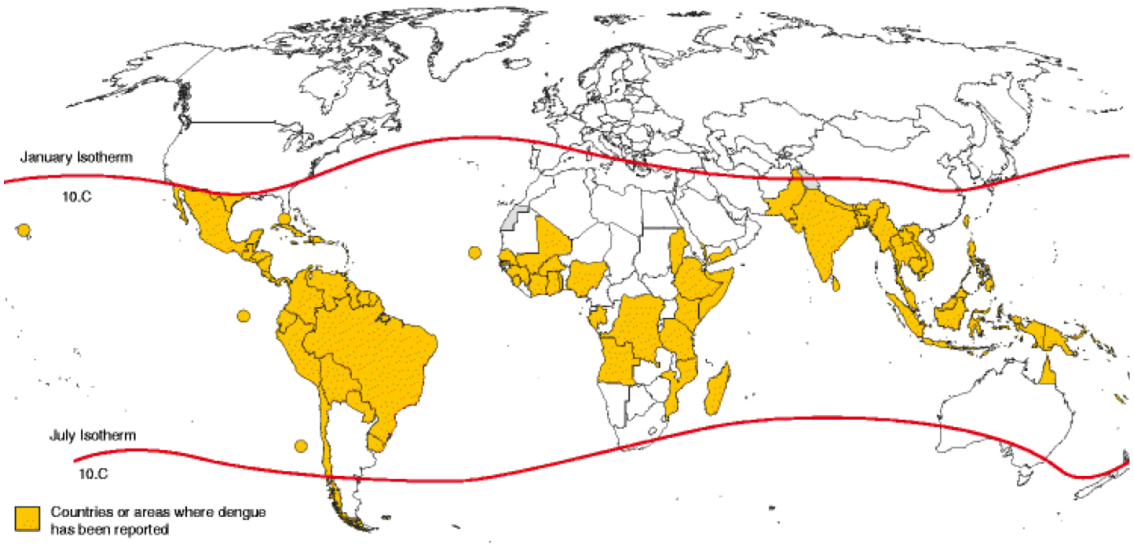

1.6.2 Dengue virus transmission

The primary vector of DENV transmission is represented by *Aedes aegypti,* while Aedes *albopictus* acts as a secondary vector [295, 299]. DENV is acquired by *Aedes spp.* when they bite humans or primates infected with DENV, so these species can transmit DENV through biting another host. The preference for human blood exhibited by *Aedes spp*. increases the possibility of disease transmission [300].

1.6.2.1 *Aedes aegypti* species

Aedes aegypti originated from Sub Saharan Africa; it is known as the principle vector of DENV. The official common name for *Aedes aegypti* is "yellow fever mosquito" as this species was previously known as the vector of YFV. Besides DENV and YFV, this species can also transmit CHIKV [301]. *Aedes aegypti* inhabits tropical and subtropical climates, with the geographic range spanning all continents except Antarctica [302]. *Aedes albopictus*, also known as the "Asian tiger mosquito", it is the secondary vector of DENV transmission. It was identified as a vector of DENV in 1931 [303].

1.6.2.2 *Aedes albopictus* species

Currently, *Aedes albopictus* can be found in temperate regions in its area of origin (Asia), Europe, America, Africa and a number of locations in the Pacific and Indian Oceans [304-306]. The widespread distribution of *Aedes albopictus* is likely because it inhabits a more temperate enviroment than the tropical *Aedes aegypti* [307]; this may lead to an increased risk of DENV transmission as it brings a greater number of dengue-suscetible persons in contact with vectors. Other factors such as uncontrolled urbanisation and global warming also affect the density, larval

development rate, and survival of adult *Aedes albopictus*, increasing the vector capacity and DENV transmission [308].

In experimental conditions it was demonstrated that DENV can be transmitted by other *Aedes* species, including *Ae. polynesiensis, Ae. scutellaris* and *Ae. Japonicas* [309,310]. *Ae. polynesiensis* is implicated in the natural transmission of DENV, but the contribution of these mosquitoes to overall transmissionhad not been quantified, but probably negligible [311].

1.6.3 Clinical manifestations of dengue virus

DENV infection causes wide range of clinical symptoms from asymptomatic to mild febrile illness, to classical dengue fever, to severe manifestations such as dengue haemorrhagic fever (DHF) and dengue shock syndrome (DSS) [312].

Classical dengue fever consists of an acute febrile illness characterized by fever, headache, myalgias, arthralgias, nausea, vomiting and rash. It has an incubation period of 4-7 days and a convalescence of several weeks.

The severe form of dengue (DHF and DSS) are vascular leak syndromes characterized by an increased vascular permeability, leakage, hypovolemia, shock and death if not corrected.

Probably, it is caused by a phenomenon known antibody-dependent enhancement (ADE), which occurs in a secondary dengue infection and it consists of an immunological cascade beginning with the infection of cells of the monocytic lineage, with a subsequent production of cytokines and other chemical mediators [313].

1.6.3.1 Neurological complications

Less commonly, other severe disease manifestations can occur, for example organ failure and neurological disease similar to viral encephalitis [314].

During the recent years, an increase of neurological complications after DENV infections were reported [315-317]. In general neurological dengue is characterized by a wide variety of CNS manifestations including non-specific alterations of consciousness, seizures, headache and meningeal signs; in analogy with WNV and JEV, paralytic or Parkinsonian symptoms may appear.

1.6.3.2 Neuropathogenesis

Much of the knowledge on the neuropathogenesis of dengue derived from animal models aimed at studying hemorrhagic disease. In these models, DENV induced neurological syndromes, so they were exploited to understand viral neuropathogenic mechanisms [318]. DENV probably enters the CNS through a cytokine-mediated breakdown of the BBB or a Trojan-horse mechanism [319-320].
DENV showed tropism for neurons of the anterior horns, hippocampus, cerebral cortex and olfactory bulb *in vivo* and induced apoptosis in human and murine neurons both *in vivo* and *in vitro* [321-323].

1.6.4 Innate immune response

Dengue virus induces the activation of innate immunity in infected cells.Interferon-dependent innate immune response is necessary for protection against DENV infection. Type I IFNs (IFN-α/β) are produced within an hour after infection and induce antiviral activity. *In vitro* studies revealed that DENV infection stimulates interferon secretion [324] and pretreatment with inteferon is able to control DENV infection [325]. *In vivo* studies demonstrated that these IFNs are highly activated in uncomplicated cases, yet they are less effective in severe disease [326].
Type II interferon (IFN-γ) is mainly produced by T cells and NK cells. The IFN-γ receptors are highly expressed on monocytes, macrophages and endothelial cells. IFN- γ production by DENV-specific T lymphocytes has been revealed *in vitro* [327]. Importantly, the effect of IFN- γ on DENV infection *in vitro* remains obscure since both stimulatory and inhibitory consequences have been reported. A massive production of cytokines (TNF-α, IL1β, etc) is stimulated by T cells activation and infected keratinocytes, DCs, and endothelial cells can release cytokines [328,329].

1.6.5 *In vitro* MODEL OF INFECTION

A large variety of cell lines have been studied *in vitro* for their relative permissiveness for DENV infection, including endothelial cells, fibroblasts, myeloid-derived cells, and lymphocytes [330]. However, *in vivo*, few human cell types can support DENV replication.
Since DENV is delivered to its host through mosquito bite to the skin, keratinocytes [331] and human Langherans dendritic cells (DCs) represent a relevant target for DENV infection. Many studies showed that these cells are permissive to DENV [332-338]. In addition, apoptotic DCs and keratynocites are present in skin explant after transcutaneus infection [331].

Monocytes/macrophages [339] and lymphocytes [340] in humans and murine models support DENV replication and are considered the major sites of DENV replication *in vivo*.
Other cells of non–hematopoietic lineages including endothelial cells, hepatocytes [341], Kupffer cells, neurons and microglia are also permissive to DENV infection. The permissiveness of endothelial cells to DENV can contribute to the pathogenesis of the disease by increasing viremia and cytokine secretion [329,342,343].

1.6.6 *In vivo* MODELS OF INFECTION

Like ZIKV, DENV is not able to block type I IFN receptor signalling in mouse cells. Many studies reported that laboratory mouse strains support DENV infection and replication, but do not develop disease and viral titer in tissues is low. Thus, mouse models are not suitable to study cells permissive for DENV infection. [344,345] demonstrated that mouse adaptation of DENV strains resulted in loss of human pahogenic properties, so the use of wild type mouse models did not reflect the nature. At the moment, the A/J mouse strain represents the most promising model of immunocompetent mouse [346]. The knockout AG129 mouse strain also shows increased susceptibility to DENV infection, suggesting the involvement of IFNs in dengue pathogenesis in humans [347] .
Non-human primates are the animal species besides humans that are naturally infected and can be experimentally infected by the parenteral route. They are acceptable animal models to study virological and immunological aspects in DENV infections [348-349]. Furthermore, a study [350] reported the recapitulation of human dengue hemorrhagic fever in Rhesus monkey through viral intravenous administration.

1.7 Usutu Virus (USUV)

1.7.1 Transmission, epidemiology and clinical presentations

USUV belongs to the JE serocomplex, like WNV, and its transmission involves ornithophilic mosquitoes as vectors and birds as the main amplifying hosts [351], while mammals represent incidental or “dead-end” hosts. Although USUV has been found in nine mosquito species, *Culex pipiens* is considered to be the most common vector [351]. USUV has been detected in 62 bird species in African and European countries among which some wild migratory species are considered responsible for USUV introduction into Europe from Africa (e.g. *Falco tinnunculus*), and others for USUV dissemination through Europe (e.g. *Pica pica*, *Passer domesticus*, *Gallus*

gallus and *Turdus merula*) [352]. Birds may show symptoms ranging from mild to severe, such as encephalitis, myocardial degeneration, and necrosis of liver and spleen [353]. Neurological signs, such as incoordination and inability to fly are associated with brainstem and cortical neuron necrosis [353]. Moreover, USUV infection has been proved in different mammalian species, especially bats, horses, dogs and red deer [352].

USUV was first isolated in 1959 from a pool of *Culex neavei* mosquitoes collected in Ndumu, South Africa [354]. In the following years, USUV was reported in several mosquito species in other African countries including Uganda, Senegal, Central African Republic (RCA) and Tunisia (2014) [351,352]. In the past, USUV was not considered as a potential threat for humans because the virus had never been associated with severe or fatal diseases. In Europe, USUV emerged in 1996 causing high number of bird deaths, as demonstrated by the retrospective analysis of archived tissue samples from dead Eurasian Blackbirds in Tuscany, Italy [355].

During summer 2016, a large USUV epizootic was reported in Belgium, Germany, France and for the first time in the Netherlands [356]. Moreover, USUV infection has been demonstrated serologically in birds in England, Poland and Greece, and in a horse in Serbia [352].

USUV frequently co-circulates with WNV in many European countries, not only geographically but also in terms of host and vector species [357].

Up to now, few cases of USUV infections in humans have been registered in Africa and Europe. Infected patients may be asymptomatic or present a wide range of symptoms [352]. The first case of USUV infection in humans was reported in RCA in 1981 (which is also the first virus isolate from humans), and the second case in Burkina Faso in 2004. They presented mild symptoms including fever, rash and jaundice [358].

From 2008 to 2016, USUV-specific antibodies have been detected in healthy blood donors among Italy, Germany and Serbia, with seroprevalence ranging from 0,02% to 1,1% [352]. Between July and August 2017, seven out of 12,047 blood donations from eastern Austria reacted positive at WNV NAT, and six of these resulted to be USUV infections [359]; moreover, retrospective analyses of four blood donors diagnosed as WNV-infected in 2016 showed that one was USUV-infected [359].

1.7.2 Phylogeny

USUV strains are classified into African and European groups, according to the geographical origin of isolation, and each group is in turn sub-classified into several lineages. The African group involves three lineages (Africa 1 to 3), while the European group involves five lineages (Europe 1 to 5) [356]. Comparative analysis between USUV genomes revealed specific amino acidic mutations related to geographical source of isolation and hosts [352]. In particular, two specific

mutations (in E and NS5 proteins) in Bologna/09 strain (representing the first human isolate from an immunocompromised patient with neuroinvasive disease) have been hypothesized to be associated with altered tropism for human neural cells and neuroinvasive capacity [360]. Moreover, the Bologna/09 strain substitutions are common to DENV, JEV, WNV and MVEV flaviviruses that also threaten human health [351]. When comparing USUV with other JE serocomplex viruses, the closest relative is MVEV that exhibits 73% and 82% identity at the nucleotide and amino acid levels, respectively, while WNV exhibit 68% identity with USUV at the nucleotide level and 75% at amino acid level.

1.7.3 Tropism, pathogenesis and innate immune response in non-neural cells

USUV host range, pathogenesis and triggered innate immune response are largely unknown.
In 2013, Scagnolari *et al.* demonstrated that USUV was able to infect a variety of human cell lines completing the replication cycle in Hep-2 and Vero cells within 48 h [361]. In addition, in 2015, Cacciotti *et al.* published data showing the capacity of USUV and WNV lineage 1 and 2 to grow in immature monocyte-derived dendritic cells (DCs); however, USUV replication peak began earlier than that of WNV and USUV viral titer was significantly lower than that recorded for WNV [362]. In 2016, K.L. Barr *et al.* found that both USUV and ZIKV replicated well in cells from multiple animal species [363].
In 2013, Scagnolari *et al.* showed that pre-treatment of Vero and Hep-2 cells with IFNs type I and III significantly inhibited USUV replication, but the inhibitory effects considerably dropped if IFN was added after viral infection had been initiated [361]. In particular, the potential of IFN lambda 1-3 to inhibit USUV replication was lower than that of type I IFNs in Hep-2 cells [361]. Furthermore, USUV weakly induced types I and III IFNs in Hep-2 cells only after 24 and 48 h p.i., even though IFN alpha subtypes were less induced than other subtypes at both time points [361]. In 2015, Cacciotti *et al.* published an interesting study where IFN activity in USUV-infected immature and mature DCs was found to be greater than that induced by both WNV lineage 1 and 2, suggesting that USUV may be not as efficient as WNV to counteract cellular early antiviral immune response [362]. This hypothesis was supported by the detection of high levels of IFN alpha subtypes only in USUV-infected mature DCs [362]. Furthermore, ISG15 pathway underwent a significantly higher activation in USUV- infected DCs than WNV, and USUV yield reduction through IFN administration was higher than that recorded for WNVs [362]. All in all, besides the ability of USUV to trigger IFN production and specific ISGs more efficiently than WNV, it seems to be also more sensitive to types I and III IFNs than WNV.

1.7.4 Neurotropism, neuropathogenesis and innate immune response: preliminary studies

1.7.4.1 *In vivo* models

USUV was demonstrated to be neuroinvasive in suckling mice [364]. Hence, after USUV infection of 1-week-old suckling mice by intraperitoneal inoculation, clinical signs, e.g. depression, disorientation, paraplegia, paralysis and coma were observed [364]. There was widespread neuronal apoptosis, especially in the brainstem but also in white matter (cerebellum, medulla and spinal cord), frequently accompanied by multifocal demyelination [364]. Differently from other flaviviruses, neuroinvasion occurred only in animals that were not older than 1 week at the time of injection [364]. In contrast, adult mice survived to USUV infection, independently of the infecting dose inoculated [365]. However, mice deficient in the alpha/beta interferon receptor (IFNAR (−/−) mice) were highly susceptible to USUV infection and were shown to represent a potential model for the study of host-virus interactions and for lethal challenge DNA vaccine testing [366].

1.7.4.2 *In vitro* models

A n *in vitro* study on USUV (Vienna2001-blackbird, 939/01 strain) neural tropism and neural damage demonstrated that USUV efficiently infects several neural cells, i.e. murine neurons, astrocytes and microglia, thus suggesting a broad neurotropism for USUV in the murine CNS, possibly associated with neuronal toxicity [367]. Notably, USUV could replicate in human astrocytes more efficiently than ZIKV, it reduced cell proliferation and elicited a strong anti-viral response. Moreover, iPSC-derived human neural stem cells (NSCs) were to be highly permissive to USUV infection and underwent caspase-dependent apoptosis. Here below, the experimental evidences of this study are described deeper into details [367].

• **Murine CNS cells\J**

After infection with USUV of slices of hippocampus obtained from mouse brains, a strong pan-flavivirus staining was observed in astrocytes, microglial cells and neurons. The presence of USUV antigens was also demonstrated in infected primary hippocampal neurons, in both soma and axons, and viral titer confirmed efficient replication. At late time-points post-infection, neuronal damage (refringent cell bodies and neurite destruction) was observed. Moreover, after infection of spinal glial cells, containing ~80% astrocytes and ~20% microglial cells, USUV antigens were observed and very efficient replication assessed by titration.

• **Primary human astrocytes\J**

After infection of astrocytes with USUV and ZIKV, USUV-infected condition showed sparser

cellular population than non-infected and ZIKV-infected conditions. Interestingly, USUV-infected astrocytes showed a decrease in proliferation. Moreover, pan-flavivirus staining was found in 48% of cells infected by USUV and 41% by ZIKV, with endoplasmic reticulum localization, a characteristic site for flavivirus replication. As regards the growth kinetics of the two viruses, USUV reached a plateau in replication between 24 h and 96 h p.i. and it was followed by a drop in viral titer, whereas ZIKV viral titer was significantly lower than USUV and the plateau started earlier and lasted longer. The results of pre-incubation of astrocytes with either anti- AXL or anti-DC-SIGN antibodies before infection, confirmed that blocking AXL decreased ZIKV replication to a higher extent compared to blocking DC-SIGN, and demonstrated that USUV replication was not affected by blocking either proteins. A PCR array of 84 genes involved in several antiviral pathways, such as the IFN response and the cellular PRR, showed that 33 genes were significantly upregulated (more than two-fold) by USUV in astrocytes. Several cytokines, chemokines and PRR genes were found upregulated upon both USUV and ZIKV infection, but in a stronger way following USUV than ZIKV infection, up to 100 times for *CCL5* and *CXCL10* chemokines and for *IFN-B*. Other genes, such as *TLR9* PRR, *CCL3*, *CD40* and *CTSB* chemokines and *FOS* and *IRF7* transcription factors, were specifically upregulated in USUV-infected astrocytes.

• **Human iPSCs-derived NSCs\l**

Pan-flavivirus antibody staining was detected in human iPSCs-derived NSCs two days after infection with USUV and ZIKV at MOI of 2; specifically, in 77% of USUV- infected cells and only in 21% of ZIKV-infected cells. USUV titer was significantly higher than ZIKV titer. Apoptotic death was observed in USUV-infected NSCs 4 days p.i., characterized by round-up morphology and condensed nuclei, ~80% trypan blue- positive cells, and activated-caspase 3. Furthermore, USUV-associated cellular death was strongly decreased by treating NSCs with the anti-apoptotic agent Z-VAD (pan- caspase inhibitor) prior to USUV infection.

1.8 Induced pluripotent stem cells

Induced pluripotent stem cells (iPSCs) are a type of pluripotent stem cell that can be generated directly from adult cells. They resemble embryonic stem cells(ESCs) [368], so they are able to self-renew and to make cells from all three basic body layers (pluripotency).

The breakthrough of iPSCs showed that the introduction of four specific transcription factors could convert adult cells into pluripotent stem cells [369]. iPSCs derived by introducing Oct-4, SOX2, Myc, and KLF4, as set of pluripotency-associated genes (reprogramming factors), into a given cell

type.

Oct-4 (octamer-binding transcription factor 4) also known as POU5F1 (POU domain, class 5, transcription factor 1) is a homeodomain transcription factor of POU family. This protein is critically involved in the self-renewal of undifferentiated embryonic stem cells [370]. Oct4 expression is associated with an undifferentiated phenotype [371] and its knockdown promotes differentiation [372].

SOX2 (SRY (sex determing region Y)-box 2) is a transcription factor essential for maintaining self-renewal of undifferentiated ESCs . SOX2 binds to DNA cooperatively with Oct4 at non-palindromic sequences to activate the transcription of key pluripotency factors [373].

KLF4 (Kruppel-like factor 4) is a member of the KLF family of transcription factors and regulates proliferation, differentiation, apoptosis and somatic cell reprogramming [374].

Myc is a regulator gene coding for a multifunctional, nuclear phosphoprotein acting as transcription factor and playing a role in cell cycle progression, apoptosis and stem cell self-renewal.

1.8.1 Reprogramming techniques

First attempts to generate induced pluripotent stem cells relied on the use of integrating viruses, as retroviral vectors [369] and constitutive lentiviral vectors [368]. Retroviral vectors showed an efficiency of reprogramming of about 0,01% in human fibroblasts, whereas lentiviral vectors had approximately 0,1% efficiency [368,369], but lentiviruses do not shut down their expression when the pluripotent state is achieved. The development of reprogramming techniques led to the use of inducible lentiviruses, that could be silenced once the pluripotency was achieved [375-377]. However, these methods have been criticized for the permanent integration into the genome, that can result in alteration of gene function [378] and reactivation of viral transgenes, implicated in tumorigenesis [379]. Other approaches have been developed to avoid this problem, employing non-integrative vectors as adenoviruses, that transiently express the reprogramming factors, even if with very low efficiency (0,0006%) and so not practical for iPSC generation [379], or “zero footprint” Sendai-virus based vectors, with higher efficiencies [380]. The first method that evolved without the use of viral vectors was employing expression plasmids, that don’t integrate into the genome and don’t require viruses in any part of the reprogramming process [381,382]. Other viral-free methods that showed to make reprogramming possible are recombinant proteins [383,384], and modified RNAs [385].

1.8.2 Applications

As hiPSCs are capable of self-renewal and differentiation, they represent a suitable tool both for generating “disease in a dish” models to study the mechanisms of pathogenesis, and for obtaining

different cell types required for drug development. Indeed, hiPSCs can be differentiated into a variety of cell types, including neurons, cardiomyocytes, hepatocytes, keratinocytes, and hematopoietic cells [386]. There are different strategies to initiate hiPSC differentiation based on the delivery of key factors regulating the events of cell differentiation during embryonic development: one way to differentiate them is to generate embryoid bodies (EBs), i.e. three-dimensional (3D) aggregates of pluripotent stem cellsrecapitulating the stages of embryological development [387]; other approaches include growth on particular feeder layers [388] or on extracellular matrix (ECM) proteins [389].

1.8.2.1 Drug discovery

An important role offered by the use of hiPSCs-based technology is their application in drug discovery or toxicity prediction. This approach allows to avoid the use of animals or animal cells to test efficacy and toxicity of drugs, bypassing the limits due to their inability to recapitulate the exact human physiology. Since hiPSCs represent a theoretically unlimited source of cells which can be turned into any type of somatic cells, large libraries can be generated to predict toxicology and therapeutic responses of newly discovered drugs in high- and low-throughput drug testing. This represent an advantage since *in vitro* primary cultures obtained from patients can only grow for few passages before becoming senescent [386].

1.8.2.2 Regenerative medicine

A potential application of hiPSCs in the next future could be in the field of regenerative medicine. In this case an injured or damaged tissue will be replaced with a new one generated from patient-specific hiPSCs. This approach will overcome the problems due to immunorejection or scarce availability of donors, often encountered in transplantational medicine. In the case of patients with monogenic diseases, patient-specific hiPSCs might be first corrected by homologous recombination, and then differentiated into specific cell types involved in the disease, and transplanted into the body of the patient from which the cells were first isolated. The correction can be carried out by genome editing techniques employing zinc finger nucleases (ZFNs), transcription activators-like effector nucleases (TALENs), and clustered regularly interspaced short palindromic repeats (CRISPR)/CRISPR-associated (Cas) nucleases, as systems for the introduction of specific insertions or deletions.

1. 8. 2. 3 Disease modeling

hiPSCs have been applied to the modeling of a variety of human diseases, such as degenerative disorders and infectious diseases [390]. For studying degenerative disorders, adequate controls are

of course required to distinguish disease-specific phenotypes from inter-individual or technical variabilities related to hiPSCs generation. Again, controls for monogenic disease models may be obtained by rescuing the mutated gene by targeted gene correction, achieved through homologous recombination using nucleases [391]. These techniques can also be used to introduce specific mutations in hiPSCs to generate disease-specific genotypes [392].The complex host-pathogen interaction typical of infectious diseases can be studied with the aid and the advantages of hiPSCs. In fact, human *in vitro* model system of such diseases can be unavailable due to tissue inaccessibility and challenges in primary culture growth [393] while animal model-based systems might contain a mixture of cell types that can be resistant to infection, or, upon infection, present a phenotype differing from that of humans. Infectious agents could be, moreover, strictly species-specific or can grow only in a limited set of human cell types [392]. hiPSCs can, therefore, be employed as an *in vitro* model to study virus-host interactions, such as those of ZIKV, investigating infectivity, tropism, replication, and inflammatory responses in stem cells, neural progenitors and neurons systems.

1.9 Modelling susceptibility to infectious disease

There is a clear evidence that some individuals respond differently to infectious agents compared to others. Epidemiological studies have highlighted the role of host genetic factors as determinants of the spectrum of clinical phenotypes. Since the early 1940s, twin studies have demonstrated that infectious diseases such as TB, leprosy, malaria and pneumonia have a heritable component to them [9,394-396] making the basis for further studies to identify the specific genes involved [397]. Recently, unbiased whole-genome approaches have revealed robust associations between genetic markers and susceptibility to disease.

Flaviviruses can cause severe clinical manifestations only in a small percentage of infected individuals. At the moment, the reasons have not been completely elucidated, but host-dependent genetic factors might be important.

1.9.1 Human genetic traits associated with the risk of severe WNV infection

It is notable that of those infected with WNV only 1 in 150 infected individuals develops meningitis or encephalitis [398]. The most common host risk factor identified for severe illness is age. For the elderly, the risk is most likely related to a compromised immune system or pre-existing medical conditions, such as autoimmune diseases, diabetes and obesity that increase accessibility of infection to the CNS [397]. The existence of rare, extreme outcomes to WNV infection has stimulated the interest in host genetic risk factor [256,399].

Currently, a limited number of host genetic factors have been linked with susceptibility to WNV

infection. Studies in mouse (genus *Mus*) models have shown that susceptibility to WNV correlates with the occurance of a point mutation responsible for the truncation of the 2'-5'-oligoadenylate synthetase (2'-5'-OAS) L1 isoform, suggesting the relevance of the enzyme in WNV restriction in target tissues [400]. OAS is a member of the IFN-regulated gene family, and the OAS gene cluster consists of three genes, *OAS1, OAS2* and *OAS3* which encode various forms of the 2',5'-oligoadenylate synthase, a protein that activates latent RNase L, resulting in viral RNA degradation and inhibition of viral replication. In human studies of WNV infection, 23 single nucleotide polymorphisms (SNPs) in the *OAS* genes were identified at a higher frequency in symptomatic individuals. In another study, an allele of OAS1 ('A' allele at SNP rs10774671) that enhanced mRNA splicing was more common in WNV-infected individuals than in uninfected controls [401].

A 32-base-pair deletion in the gene encoding the chemokine receptor CCR5 (producting a truncated form of the protein that eliminates its surface expression) has been associated with more severe disease following flavivirus infection [402]. CCR5Δ32 homozygous individuals had an early clinical presentation of the disease and a higher frequency of systemic disease with lymphadenopathy, neurological deficits and gastrointestinal complications [403].

TLR-3 modulates the immune response by recognition of dsRNA and induces the production of IFN type I and the subsequent induction of the pro-inflammatory cytokine TNF-α. This gene has been studied as a genetic risk factor for WNV infection [404]. Elevated levels of TLR3 result in an elevation of cytokine levels and may contribute to the increased permeability of the BBB that has been observed in elderly individuals, suggesting another possible mechanism for the increased severity of WNV infection. Finally, significant associations between WNV infection and SNPs in IRF3 and MX1 innate immune response and effector genes have been reported [405]. Thus, genetic variations in the interferon (IFN) response pathway appear to correlate with the risk of symptomatic WNV infection in humans; but further investigation is needed to better define how these polymorphisms within the coding region alter protein expression and function during WNV infection.

In vitro model systems to study the host-pathogen interactions are limited because of tissue scarcity and challenges in primary culture. hiPSCs-derived differentiated cells hold immense promise for the development of cell system for the investigation of the genetic basis of infectious disease susceptibility in humans.

So patient-specific iPSCs provide a potentially valuable tool for understanding the genetic basis and the mechanisms of individual susceptibility or resistance to infectious disease.

2. AIM

Susceptibility of the CNS to viral infection is a major determinant to clinical outcome, but little is known about the molecular factors involved in this vulnerability. Neurotropic viruses use different mechanisms to infect and spread among neural cells, to establish acute or persistent infection, and to cause neural cell injury.

An understanding of viral infection in neural cells and cellular response to viral infection might be useful to identify shared and virus-specific mechanisms of neural injury and to identify potential molecular targets for therapy.

Zika virus (ZIKV) has recently drawn attention due to the major 2015-16 outbreaks. The virus can be transmitted vertically from the mother to her fetus and infection during the first trimester of pregnancy may lead to fetal microcephaly and other brain anomalies [88].

West Nile virus (WNV), a well-known neurotropic *Flavivirus,* can cause severe disease in a minority of infected humans, mostly immunocompromised and elderly individuals.

Recently, there has been an increasing number of reported cases of neuroinvasive diseases caused by viruses, such as dengue virus (DENV) which usually are associated to hemorragic disease.

The emerging Usutu virus (USUV) may cause lethal neuroinvasie disease in a variety of bird species. Cases of asymptomatic human infection have been reported and a few cases of infection in humans affected by meningoencephalitis. Its pathogenicity for humans is unknown.

Advances in human induced pluripotent stem cell (hiPSC) technology have paved the way of disease modeling *in vitro*, which can be used to study infectious disease pathogenesis, such as ZIKV, WNV, DENV or USUV disease.

Aim of this study was to investigate the infectivity, tropism, and replication kinetics of ZIKV, in comparison with WNV, DENV and USUV in hiPSCs, hiPSCs-derived neural stem cells (NSCs) and neurons, and the effect of infection on host innate antiviral responses. The comparative analysis between ZIKV and other flaviviruses should provide the opportunity to identify virus-specific features of the neural-tropism mechanisms and damage involved in human disease. To accomplish this task, protocols to differentiate hiPSCs into neural stem cells (NSCs) and neurons were optimized; these cells were used to characterize virus-host interactions; NSCs and neurons were generated from patient-specific iPSCs and used to model individual susceptibility to neuroinvasive viral infection.

3. MATERIALS AND METHODS

3.1 Cell lines

3.1.1 Vero cells

African green monkey kidney (Vero) cells were maintained at 37°C in Dulbecco's modified Eagle medium (DMEM, Thermo Fisher Scientific, USA) supplemented with 10% Fetal Bovine Serum (FBS, Thermo Fisher Scientific, USA).

3.1.2 Peripheral blood mononuclear cells (PBMCs)

Blood mononuclear cells (BMCs) are circulating cells such as monocytes, macrophages and lymphocytes, characterized by having a round nucleus. Due to the fact that they are derived from blood, they are cultured in suspension with expansion medium (EM, see table 3.3) in order to select erythroblasts population. To gain an *in vitro* neural model, blood from a healthy individual was obtained and processed.

3.1.3 Irradiated MEFs

Mouse embryonic fibroblasts (MEFs, Global Stem, USA) were employed as a feeder layer to grow human Induced pluripotent stem cells (hiPSCs), for their ability to maintain the undifferentiated state of Embryonic Stem cells (ESCs) and iPSCs. They are derived from the CF1 lineage and rendered mitotically inactive via irradiation treatment. To seed MEFs, a frozen vial was rapidly thawed in a water bath at 37°C, centrifuged at 1100 rpm for 5 minutes at room temperature (RT) and resuspended in MEF medium (see table n. 3.1). MEFs were then plated in 6-well plates, at a concentration of approximately $1{,}5x10^5$ cells/well and incubated at 37°C, 5% CO_2. They were ready to use after 24 hours.

3.1.4 human Induced Pluripotent Stem Cells (hiPSCs)

hiPSCs were generated, through Sendai Virus vectors transduction, starting from erythroblasts of a healthy donor (BD-B clone). hiPSCs colonies were grown on MEFs-feeder layer with iPS medium (see paragraph 3.1.3 and Table n. 3.2) or on Geltrex substrate (Thermo Fisher Scientific, USA) with serum-free StemMACS medium (Miltenyi Biotec, Germany) supplemented with 1% Penicillin/Streptomycin (Pen/Strep, Thermo Fisher Scientific, USA) (see paragraph 3.1.4.2).

3.1.4.1 Culture of hiPSCs on MEF feeder

To maintain and expand hiPSCs colonies, cells were cultured with iPS medium (see table n. 3.2), with a daily medium change. To expand colonies, cells were detached from the feeder with an

enzymatic method using collagenase IV (Thermo Fisher Scientific, USA). After a wash with PBS, 1 mg/ml of collagenase IV was added to the cells and incubated at 37°C for 10 minutes, then the enzyme was discarded and 1 ml of iPS medium without basic fibroblast growth factor (b-FGF) was added. Cells were then scraped to detach the clumps from the well; the medium containing the cell suspension was then aspirated and centrifuged at 1100 rpm for 5 minutes at RT to allow the removal of supernatant; clumps were then resuspended in iPS medium with 10 ng/ml of b-FGF and plated at the desired concentration in MEFs pre-coated multiwells plates.

3.1.4.2 Culture of iPSCs clones on Geltrex

Geltrex (Thermo Fisher Scientific, USA) has been employed as an alternative to MEFs when a feeder-free layer was necessary, to avoid MEFs contamination and for differentiation protocols. Geltrex is a soluble form of basement membrane purified from Engelbreth-Holm-Swarm (EHS) mouse tumor cells. The major components of Geltrex Matrix include laminin, collagen IV, entactin and heparin sulfate proteoglycan. It is used to maintain the pluripotent and undifferentiated state of hiPSCs. StemMACS medium (Miltenyi Biotec, Germany) was employed in combination with Geltrex. This medium has the advantage of being serum-free and containing bovine albumin that helps cells in their metabolic and biosynthetic activity, proliferation and survival.

Geltrex is normally kept at -80°C; in order to use it, it was thawed overnight at 4°C, resuspended in DMEM/F12 (concentration 10 µl/ml) and then plated into the multiwell plate; after one hour Geltrex was replaced with StemMACS medium. Depending on the need of hiPSCs growing in single cells or colonies, two enzymatic methods were used. If clumps were needed, colonies were washed with PBS, then 2 U/ml of dispase (Thermo Fisher Scientific, USA) was added and cells were incubated at 37°C for 5 minutes after which dispase was discarded and colonies were detached from the well using a scraper. Cells were then centrifuged at 1100 rpm for 5 minutes at RT, supernatant was eliminated and clumps were resuspended in StemMACS medium and plated at the desired concentration in new wells pre-coated with Geltrex.

If single cells were required, colonies were washed once with PBS and accutase (Thermo Fisher Scientific, USA) was added and incubated for 10 minutes at 37°C; 5 volumes of PBS were then added and cells were pelleted by centrifugation at 1100 rpm for 5 minutes at RT. At this point, StemMACS medium supplemented with 10 µM Rock Inhibitor (Y-27632, Miltenyi Biotec, Germany) was used to resuspend the cells, that could be plated on a well previously coated with Geltrex. From the day after, medium had to be changed daily.

3.1.4.3 Freezing/thawing of hiPSCs clones

To freeze hiPSCs, colonies were detached from MEF cultures using collagenase IV as previously

described, then resuspended in 1 ml of freezing solution, composed by 500 µl of iPS medium without b-FGF and 500 µl of freezing solution containing filtered FBS and 20% of dimethyl sulfoxide (DMSO; Sigma-Aldrich, USA). Cells were aliquoted into cryovials and placed into a cooler at -80°C. After 24 hours, cells could be moved into liquid nitrogen at - 200°C for long time storage.

In order to thaw hiPSCs, cells were recovered from liquid nitrogen and rapidly thawed at 37°C, then resuspended in 9 ml of iPS medium to dilute DMSO, centrifuged for 5 minutes at 1100 rpm at 4°C and resuspended in iPS medium with 10 ng/ml of b- FGF and Rock Inhibitor 10 µM, then plated on MEF coated wells.

3.2 Reprogramming of erythroblasts

3.2.1 Isolation of circulating mononuclear cells

Venous blood was drawn from a healthy donor in 0,129 M trisodium citrate to avoid platelet aggregation. PBMCs were separated from other blood components (plasma, erythrocytes, platelets) using Histopaque -1077, density 1,077 g/ml (Sigma-Aldrich, USA). Whole blood was first mildly centrifuged at 1000 rpm for 10 minutes at RT without brake to separate platelet-rich plasma (PRP) from other blood components.

Blood cells were diluted with PBS and carefully added on the top of the Histopaque-1077 solution, avoiding to mix the phases, then centrifuged 30 minutes at 1800 rpm at RT, without brake, to let red blood cells (RBCs) separate from PBMCs. Buffy coat containing PBMCs was recovered and diluted with further PBS, then centrifuged at 1500 rpm at RT for 10 minutes to recover cells. Two washes were performed with PBS and then cells were resuspended in EM (see table n. 3.3.). Medium was changed every 3 days. After 8-10 days most of the cells were at the erythroblast stage.

3.2.2 Reprogramming with Sendai virus

hiPSCs colonies were obtained by transduction with Sendai Virus-based vectors. Transduction was done using the CytoTune-iPS Sendai Reprogramming Kit (Gibco, Invitrogen, USA), that provided four vectors, each expressing one of the four Yamanaka factors (Oct3/4, Sox2, Klf4 and c-Myc). The vials contained about 100 µl of the reprogramming vectors at a concentration of about $\geq 3\times10^7$ cell infectious units/ml (CIU/ml).

Transduction with Sendai virus vectors was performed after 8 days of PBMCs culture in EM, to have a large population of erythroblasts. Reprogramming protocol published by Yang et al. [406] was applied with some modification.

Erythroblasts were collected and counted. $2x10^5$ cells were transduced with the 4 viral vectors at a

multiplicity of infection (MOI) of 10. After addition of viral vectors, cells were plated in 6-well plate with EM and were spinoculated at 2250 rpm for 90 minutes at RT in order to help transduction, then incubated for 2 hours at 37°C. After that, cells were collected in a 15 ml tube and centrifuged at 1500 rpm for 10 minutes at RT to eliminate the excess of viral vectors. After discarding the supernatant cells were finally resuspended into EM and plated on MEF coated wells. The plate was centrifuged at 500 rpm for 30 minutes at RT in order to enhance cells adhesion. Next, cells were incubated at 37°C, 5% CO_2. Two days after transduction, medium was switched with FBS-iPS medium (see table n. 3.4) with the addition of growth factors as in expansion medium (see table n. 3.3). On the 4th day post transduction (p.t.), medium was switched to FBS-iPS medium without growth factors and on the 6th day p.t., from this to 1:1 FBS-iPS and iPS media. After 8 days, cells were fed only with iPS medium (see table n. 3.2) that was changed daily. When colonies started to emerge, they were picked with a pipette, plated into a MEF-coated 6 well with iPS medium plus b-FGF and Rock Inhibitor 10 μM and expanded. Fig. n. 3.1 summarize the main steps of the reprogramming protocol.

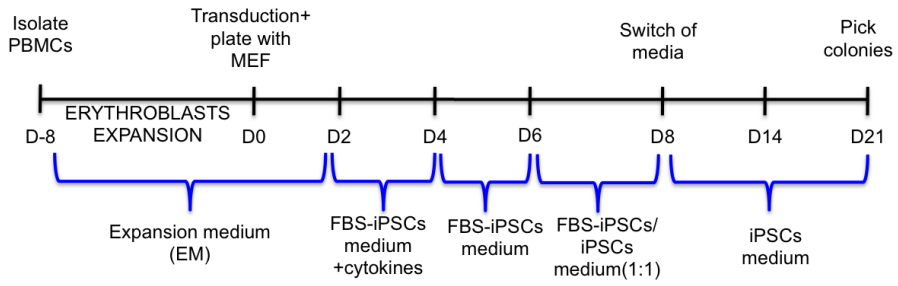

3.3 Media

3.3.1 MEF Medium

MEF medium was used to thaw and seed MEFs.

Table n. 3.1 MEF medium

MEF MEDIUM	
DMEM (Dulbecco's Modified Eagle Medium)	
Filtered FBS (Fetal Bovine Serum, Life Technologies)	10%
GlutaMax 100x (Gibco, invitrogen)	1%
Penicilin/Streptomycin (Life Technologies)	1%

3.3.2 iPS medium

IPS medium was employed to grow colonies on MEF feeders.

Table n. 3.2 iPS medium

iPS MEDIUM	
DMEM/F-12, GlutaMAX supplement (Gibco, invitrogen)	
KnockOut Serum Replacement (Gibco)	20%
Non-Essential Amino Acids (NEAA, Life Technologies)	1%
GlutaMax 100x (Gibco, invitrogen)	1%
Penicilin/Streptomycin (Life Technologies)	1%
β-mercaptoethanol (Sigma-Aldrich)	0.1%
basic-FGF had to be added daily not to lose its activity, in a concentration of 10 ng/ml	

3.3.3 Expansion medium (EM)

EM was used to expand PBMCs towards the erythroblasts lineage.

Table 3.3 EM medium

Expansion Medium	
Iscove Modified Eagle Medium (Euroclone)	
L-Ascorbic Acid (Sigma-Aldrich)	50 ug/ml
Stem Cell Factor (SCF, ORF Genetics)	25 ng/ml
IL-3 (r&D Systems)	10 ng/ml
Erythropoietin (EPO, R&D Systems)	2U/ml
IGF-1 (R&D Systems)	40 ng/ml
Dexamethasone (Sigma-Aldrich)	1uM

3.3.4 FBS-iPS medium

FBS-iPS medium was used in the first days after reprogramming.

Table n. 3.4 FBS-iPS medium

FBS-iPS medium	
DMEM/F-12, GlutaMAX supplement (Gibco, invitrogen)	
Filtered FBS (Fetal Bovine Serum, Life Technologies)	20%
Non-Essential Amino Acids (NEAA, Life Technologies)	1%
GlutaMax 100x (Gibco, invitrogen)	1%
Penicilin/Streptomycin (Life Technologies)	1%
β-mercaptoethanol (Sigma-Aldrich)	0.1%
b-FGF (ORF Genetics)	10 ng/ml
L-Ascorbic Acid (Sigma-Aldrich)	50 ug/ml

3.4 Differentiation of hiPSCs into Neural Stem Cells

Feeder-free-growing hiPSCs at 15-25% of confluency were treated with Neural Induction Medium (Gibco, Life Technologies, USA) and maintained with an every-other-day medium change of 2.5mL/well on 6-well plates, for 7 days. Neural Induction Medium contains Neurobasal Medium (Gibco, Life Technologies, USA), Neural Induction Supplement 50X (Gibco, Life Technologies, USA), and 1% Pen/Strep (Gibco, Life Technologies, USA). On day 7, neural stem cells (NSCs) were ready to be expanded. The neural expansion stage comprised a medium switch, replacing Neural Induction Medium with Neural Expansion Medium, changed daily. Neural Expansion Medium contains 50% Neurobasal medium (Gibco, Life Technologies, USA), 50% Advanced DMEM/F-12 (Gibco, Life Technologies, USA), Neural Induction Supplement 50X (Gibco, Life Technologies, USA), and 1% Pen/Strep (Gibco, Life Technologies, USA).

At 90% confluency, usually on days 4-6 after plating, NSCs were ready to be passaged. After removing Neural Expansion Medium from the wells and washing with 1mL of PBS, cells could be detached in single-cells using 1mL/well of Accutase (Thermo Fisher Scientific, USA). Incubation with Accutase lasted 10 minutes at 37°C and then 5 volumes of PBS were added to dilute the enzyme. Cells were then centrifuged for 5 minutes at 1100 rpm at RT, the supernatant discarded, and the cells resuspended in Neural Expansion Medium with 5μM RI and plated on Geltrex-coated wells. RI was used to avoid apoptosis until passage 4.

3.5 Differentiation of NSCs into neurons

Feeder-free-growing NSCs were detached by Accutase treatment when confluency of 50% was reached. Cell suspension was then plated on a poly- L-ornithine (20ug/ml) and laminin (10ug/ml) (all Sigma-Aldrich, USA) -coated culture plate in Neural Expansion Medium. 24h after the passage, the medium was replaced with Neural Differentiation Medium and it was changed every 3-4 days, substituting half of the medium with fresh one. At day 20, neurons (p.0) were ready to be plated for further experiments. Neural Differentiation Medium consists of Neurobasal Medium (Gibco, Life Technologies, USA) supplemented with 2% B-27 (Gibco, Life Technologies, USA), GlutaMAX 100X 2mM (Gibco, Life Technologies, USA), and 1% Pen/Strep (Gibco, Life Technologies, USA).

Below it is reported a schematic representation (Fig. 3.2) of the neural differentiation protocol of hiPSCs.

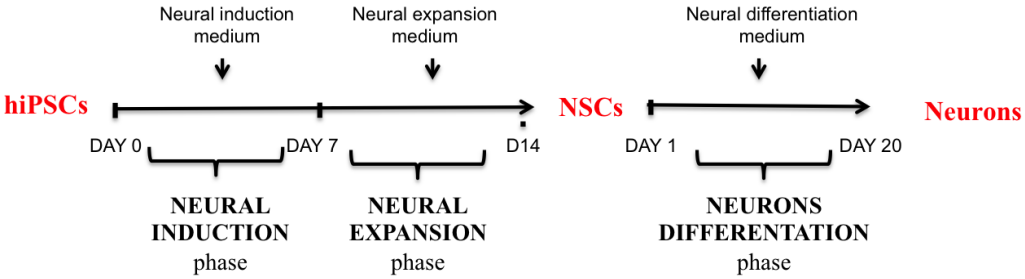

3.6 Alkaline phosphatase test

Alkaline phosphatase has been shown to be upregulated in undifferentiated cells, such as embryonic stem cells, embryonic germ cells and iPSCs. Its detection can be considered an early proof of the stemness of reprogrammed cells, being also faster than antibody-based assays. For this test the Alkaline Phosphatase Live Stain (Thermo Fisher Scientific, USA), was employed. . hiPSCs grown on MEF were washed twice with DMEM/F12. The AP Live Stain was prepared by diluting the 500X stock in DMEM/F12 1:500, and it was added to cells and incubated for 20-30 minutes at RT in the dark. The solution was then discarded and cells were washed twice for 5 minutes with DMEM/F12 to prevent background signals. To observe fluorescence, DMEM/F12 was added and cells were analyzed with a fluorescence microscope with standard FITC filter (Leica). The fluorescence fades away after 60-70 minutes. After the test, medium was changed to iPS medium with b- FGF.

3.7 Analysis of gene expression by RT-PCR and qRT-PCR

3.7.1 RNA extraction, quantification and Reverse transcription

Total RNA was extracted from cell pellets using RNeasy Mini Kit (Qiagen, Netherlands), with silica-membrane spin columns, following the manufacturer's protocol. The final elution volume was 35 µL. RNA quantification was assessed with NanoDrop 1000 spectrophotometer (Thermo Fischer Scientific, USA) that permits to quantify RNA concentration starting from 2 µL of sample.
To eliminate any residue of DNA, a DNase treatment was performed on the samples using TURBO DNA-*free* kit (Ambion, Thermo Fisher Scientific, USA) following the producer's instructions. After the treatment, another quantification of RNA concentration was done with Nanodrop 1000.
Reverse transcription was performed with 1 µg of extracted RNA , using, for each sample, the mix of table n. 3.5. All reagents were from Applied Biosystem.

Reagente	Quantità
Buffer 10X	6 µL
$MgCl_2$ Solution	11 µL
dNTPs	1 µL
Random examers	2 µL
Rnasi inibitor	1 µL
Mulve Reverse Trascriptase	1.25 µL

Table n 3.5.: Reverse Trascription reagent mix

To reach the final volume 60 µL DEPC water was added. To allow the reaction, the thermocycler was set as in table n. 3.6.

25 °C	48 °C	95 °C	4 °C
10 minutes	60 minutes	5 minutes	∞

Table 3.6 : Temperature and times for RT reaction

3.7.2 RT-PCR analysis

RT- PCR was performed to evaluate the expression of the following markers:

- Pluripotency genes: *OCT4, NANOG, DNMT3B,TERT, REX1* and *SOX2*;
- Differentiation genes of the three germ layers : *TUBB, PAX6* (ectoderm), *PECAM, CDH5, GATA2*, *FLK1* (mesoderm), *AFP, GATA4* (endoderm);
- Neural Stem Cells genes: *NESTIN, PAX6, SOX1, SOX2*;
- Neurons genes: *TUBB, MICROTUBULE ASSOCIATED-PROTEIN 2 (MAP-2), NEURON-SPECIFIC ENOLASE (NSE)*;

The reaction mix was prepared in 45 µL with 5 µL of template cDNA (table n. 3.6). All reagents were from Applied Biosystem.

Reagente	Quantità
Buffer 10X	5 µL
dNTPs	4 µL
$MgCl_2$ Solution	3 µL
Primer Fw	1 µL
Primer RW	1 µL
AmpliTaq Gold™ polimerasi	0.25 µL
Milli-Q water	30.8 µL

Table n. 3.6: PCR reagent mix

A RT-PCR reaction was moreover done to verify the expression of the housekeeping gene *ACTIN*. The thermocycler was set with the following parameters:

Stage 1	95 °C for 10 minutes
Stage 2	95 °C for 30 seconds (denaturation phase)
35-40 cycles	XX °C for 30 seconds (annealing phase)
	72 °C for 30 seconds (elongation phase)
Stage 3	72°C for 7 minutes

The annealing temperature (XX) and the number of cycles were different according to the type of primers employed.

RT-PCR products were resolved by electrophoresis on 1,5% agarose gel and then visualized by UV exposition via the GelDoc 2000 (Bio-Rad, CA) device and analyzed with Image Lab 4.1 software.

3.7.3 Real-time quantitative PCR

qPCR analysis was performed using the 7900HT Fast Real-Time PCR System instrument (Applied Biosystem- Life Technologies).

For each reaction, 5 µL of cDNA were used in a total volume of 25 µL! ! with a mix composed of Fast SYBR Green Master Mix (Thermo Fisher Scientific, USA) and the primer pairs (10 µM). Samples were analyzed with primers amplifying *IFIT1, IFIT2, MDA5, RIG-I, TLR3, TLR7, IL-1β, IRF3, IRF7, VIPERIN, IFN-α* and *IFN-β* immune response genes.

To allow the reaction to occur, the thermocycler was set as follows:

Stage 1	50 °C for 2 minutes 95°C for 10 minutes (polymerase activation)
Stage 2 *40 cycles*	95 °C for 15 seconds (denaturation phase) 60 °C for 1 minute (annealing and elongation phase)
Stage 3	Gradient: 60-95 °C for 30 minutes (melting)

All results were normalized to Human Glyceraldehyde-3-phosphate dehydrogenase (GAPDH) and analyzed using $\Delta\Delta Ct$ method [407].

3.8 Indirect Immunofluorescence assays (IIF)

Cells were fixed with 4% paraformaldehyde (PFA; Sigma-Aldrich, USA) in phosphate-buffered saline (PBS, Thermo Fisher Scientific, USA) for 20 minutes at RT. For membrane permeabilization, cells were washed three times with PBS/0.05% Tween 20 (Sigma-Aldrich, USA) and then treated with PBS/0.1% Triton X-100 (Sigma-Aldrich, USA) for 15 minutes at RT. After washing three times with PBS/0.05% Tween 20, they were blocked with 4% Bovine Serum Albumin (BSA, Sigma-Aldrich, USA) in PBS at RT for 1h and incubated at 4°C ON with the primary antibodies diluted in PBS with 4% BSA. Primary antibodies specific for Flavivirus Envelope protein E (1:500, Merck Millipore, USA), PAX6 (1:100, Sigma-Aldrich, USA), Nestin (1:100, Abcam, England), β-Tubulin (1:1000, Abcam), MAP-2 (1:250, Abcam), OCT4 (1:200, Santa Cruz Biotechnology), SSEA3 (1:50, Abcam), SSEA4 (1:50, Abcam), KLF4 (1:50, Santa Cruz Biotechnology), SOX2 (1:50, Merck Millipore) were used. To remove the unbounded antibodies, three washes of PBS/0.05% Tween 20 were performed and the corresponding secondary antibody anti-mouse IgG FITC (Chemicon international, USA) or anti-rabbit IgG Alexa Fluor-546 (Invitrogen, Thermo Fisher Scientific) diluted 1:250 in PBS 1X was added and incubated in the dark at RT for 1h. At the end three washes were performed with PBS/0.05% tween 20 and then cell nuclei were stained with the intercalating 1000x 4',6-diamidino-2-phenylindole (DAPI, Invitrogen, Thermo Fisher Scientific,USA) or DRAQ5 Fluorescent probe solution (Thermo Fisher Scientific, USA).

Cells were visualized under a fluorescent microscope (Leica) with 20x magnification or a confocal microscope (Leica) with 63x magnification.

3.9 Embryoid bodies test

The embryoid bodies (EBs) test is an assay that evaluates the ability of iPSC clones to differentiate into the three germ lineages: ectoderm, mesoderm and endoderm. This is achieved through formation of embryoid bodies, i.e. aggregates of pluripotent stem cells that differentiate randomly towards all lineages.

hiPSC clones growing on MEFs were washed with PBS and detached from the well with collagenase IV as previously described, then they were resuspended with iPS medium without b-FGF to prevent retention of staminality and plated in Ultra Low Attachment Plates (Corning, Corning Incorporated, USA), to let them grow in suspension. The medium was changed every three days; after seven days, EBs were collected with a pipette and moved to a 6-well plate coated with porcine gelatin 0,1% (Merck Millipore, Germany). Briefly, 1 ml per well of porcine gelatin was added to a 6-well plate and let polymerize for 20 minutes at RT; after this incubation, gelatin solution was removed and DMEM 10% FBS (Thermo Fisher Scientific, USA) was added to the well. Medium was changed every three days. After a week, cells were incubated with 0,05% trypsin-EDTA (Gibco, Life Technologies) for 5 minutes at 37°C and diluted with two volumes of DMEM 10% FBS medium. Cells were then centrifuged at 1200 rpm for 5 minutes at RT to eliminate the solution, washed with PBS and centrifuged another time to obtain a pellet. RNA was extracted as previously described and reverse transcribed to cDNA. RT-PCRs allowed to assess expression of the three germ layers markers: Ectoderm, Mesoderm and Endoderm (see paragraph 3.7.2).

3.10 Viral strains and infections

The following flavivirus strains, grown on the permissive Vero cell line, were employed for infection experiments:

- ZIKV: Asian lineage, strain DOM/2016/PD2 (GenBank KU853013), human isolate from the Dominican Republic, 2016 [408], titer 1×10^6 TCID50/mL;
- WNV: lineage 2, strain AUT/2008 (GenBank KF179640), goshwak isolate from Austria, 2008; kindly provided by Prof. N. Nowotny, titer 1.7×10^7 pfu/mL;
- DENV: serotype 2 strain, clinical isolate, kindly provided by M. Niedrig, Robert Koch Institute in Berlin, titer 2×10^5 $TCID_{50}$/mL;
- USUV: lineage Europe 1, strain Vienna 2001 (GenBank AY453411), Eurasian Blackbird isolate 939/01 from Vienna, kindly provided by Prof. N. Nowotny, University of Vienna, titer 5×10^6 TCID50/mL.

For infection experiments, cells were seeded in tissue culture well plates and incubated at 37 °C and 5% CO_2. The next day, growth medium was removed and replaced with infection medium, containing the virus diluted in DMEM with 1% Pen/Strep at the specified MOI. After incubation at 37 °C and 5% CO_2 for 1h and 30 minutes, the infection medium was replaced with growth medium and cells were maintained at 37 °C and 5% CO_2. A lysate from uninfected Vero cells was used as mock control in all infection experiments.

3.10.1 Analysis of virus replication kinetics

The kinetics of virus replication was measured in cell culture supernatants and cell lysates collected at different time points post-infection (p.i.) by using quantitative real-time RT-PCR (qRT-PCR), plaque assay and TCID50 assay.

3.10.1.1 Quantitative real-time RT-PCR (qRT-PCR)

For qRT-PCR analysis, nucleic acid purification from cell supernatants and cell lysates was performed on a Roche MagNA Pure 96 System (Roche Diagnostic, USA), followed by one-step RT-PCR using primers and TaqMan-probe sets specific for ZIKV NS5 [55], WNV NS5 [409], DENV NS5 [410] and USUV NS5 [411] on a 7900HT Fast Real-Time PCR System instrument (Thermo Fisher Scientific, USA).

3.10.1.2 50% Tissue Culture Infective Dose (TCID50)

Supernatants of infected cells were collected at different time points p.i. and serially diluted, ranging from 10^{-1} to 10^{-8}, in DMEM with 1% Pen/Strep, and inoculated on Vero-P cells seeded in 96 well tissue culture plate ($1{,}5x10^4$/well) in triplicate. After an incubation of 1h 30 minutes at 37 °C in 5% CO_2, DMEM with 6% FBS and 1% Pen/Strep was added to each well and the incubation continued for 5 days. Next, crystal violet fixing/staining solution (Sigma-Aldrich, USA) was added to each well and incubated at RT for 30 minutes, the plates were washed two times in tap water by immersion in a large beaker. The plates were allowed to air dry at RT. TCID50 was assessed by presence or absence of the deep purple color in each well. The viral titer was calculated by Sperman-Kärber algorithm.

$$T=10^{1+d(S-0{,}5)+1}\ TCID_{50}/mL$$

Where d represents Log10 of the diluition and S is the sum of wells with CPE for a specific diluition factor.

3.10.1.3 Plaque Forming Assay

Viral titer was expressed as Plaque-Forming Units per mL (PFU/mL). Monolayers of Vero cells was seeded in duplicate in 6 well plates and after 24h they were infected with serial 10-fold dilutions of infected cells supernatants and incubated for 1h 30 minutes at 37°C in 5% CO_2 . The inoculum was removed and MEM 2X containing 4% FBS (all of Thermo Fisher Scientific, USA) and 50% agarose (Lonza, Switzerland) was added to each well and incubated at 37°C. After 72h, MEM 2X containing 4% FBS and 50% agarose with 0.003% Neutral Red Dye (Sigma-Aldrich, USA) was added to each well followed by an incubation at 37°C for 24 h and the plaques were counted.

3.11 Apoptosis assay

The activity of Caspase 3 was measured at 72h and 96h p.i. in mock and infected NSCs plated in 12 wells tissue culture plates ($7x10^4$/well) in quadruplicate. For each virus a MOI of 1 was adopted.
Cells on Geltrex were washed with PBS and detached from the well with Accutase as previously described (see paragraph 3.1.4.2), then they were fixed with 4% PFA (Sigma-Aldrich, USA) in PBS (Thermo Fisher Scientific, USA) for 10 minutes at 37°C and 1 minute on ice. PFA was removed and the cells were permeabilized in 90% methanol for 30 minutes on ice and stored at -20°C ON.
The next day, cells were washed twice with incubation buffer (PBS with BSA 0.05%) and then, incubated 1h at RT with anti-cleaved Caspase-3 primary antibody (Cell Signaling Technology, USA) diluted 1:100 in incubation buffer. After washing three times with incubation buffer, cells were resuspended in PBS for data acquisition with Becton Dickinson LSR II Flow Cytometer (BD Bioscience, USA) and analysis using Flowing software.

3.12 Cell viability assay MTT

Cell survival was evaluated by MTT assay in mock and infected NSCs plated in 96 well tissue culture plate ($8x10^3$ /well). Upon viral infection with a MOI of 1, cell viability was analyzed at 72h and 96h p.i..

Freshly dissolved solution of MTT (5mg/mL, AppliChem) in PBS was added to each well and incubated 4h at 37 °C. Then, a solubilization solution (10% sodium dodecyl sulfate (SDS) and 0.01 M HCl) was added and, after an ON incubation at 37 °C, absorbance was read at 620 nm.
All data of mock and infected samples were normalized to blank corresponding to medium without cells. The ratio between infected sample and mock, after normalization, provided the percentage of cell survival.

3.13 Statistical analysis

Data were presented as mean value ± standard deviation (SD). Statistical analysis was conducted using an unpaired Student's t-test and the statistical significance was defined as $p < 0.05$.

4. RESULTS

4.1 Human induced pluripotent stem sells (hiPSCs) were derived from erythroblasts using Sendai virus vectors approach

Peripheral blood mononuclear cells (PBMCs) were isolated from blood of a healthy donor, expanded and differentiated for 10 days in EM medium in order to obtain the erythroblast population.

For the reprogramming, $2x10^5$ cells were transduced with non-integrating Sendai virus vectors expressing the four Yamanaka factors (Oct4, Sox2, Klf4 and c-Myc) at a MOI of 10. Clones derived from the reprogramming were manually picked, expanded and frozen for back-up purposes. One of these derived hiPSC clones, named BD-B-hiPSCs, was characterized to confirm the pluripotency state and employed for neural differentiation experiments.

4.1.1 Characterization of iPSCs clone confirmed the pluripotency status

The pluripotency features of the derived clone were analyzed by alkaline phosphatase (AP) expression test, RT-PCR and indirect immunofluorescence (IIF) for expression of the pluripotency markers, and embryoid bodies (EBs) assay.

Alkaline phosphatase is a typical marker expressed by undifferentiated cells. Colonies, grown on MEF-feeder layer, were treated with AP Live stain solution (see paragraph 3.6), a fluorescent stain that emits a signal detected by a fluorescence microscope with standard FITC filters. As shown in Figure 4.1, the undifferentiated state of hiPSCs was demonstrated by the expression of the enzyme.

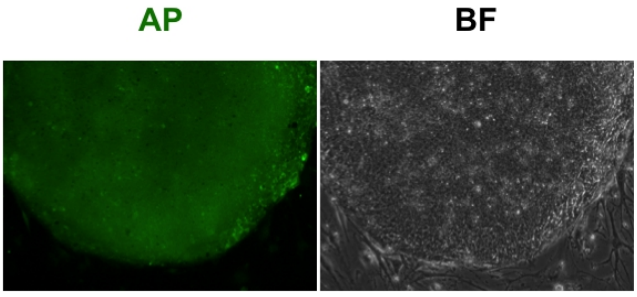

Fig. 4.1: Alkaline phosphatase (AP) analysis performed on BD-B-hiPSC clone . BF: Bright Field; 10X magnification.

To evaluate the expression of pluripotency genes in BD-B-hiPSCs, cells were cultured on Geltrex in StemMACS, to avoid murine contamination derived from MEF feeder-cells. After 7 days in culture, hiPSCs were collected and RNA was extracted, reverse transcribed to cDNA, and amplified by RT-PCR to detect expression of the pluripotency genes *DNMT3B, TERT, NANOG, OCT4, REX1* and *SOX2*, as described in paragraph 3.7.1-3.7.2. Gel electrophoretic analysis showed the expression of all the analyzed markers, confirming the pluripotency of the hiPSCs clone (Fig. 4.2A).
In order to further assess the pluripotency of the clone, hiPSCs were grown on MEF-coated 24-well plates for 5 days and analyzed for pluripotency markers expression by IIF as described in paragraph 3.8. An intense fluorescent signal when observed at a fluorescent microscope, indicating the expression of pluripotency markers OCT4, Nanog, KLF4, SSEA3, SSEA4, TRA-1-60 and SOX2 (Fig. 4.2B).

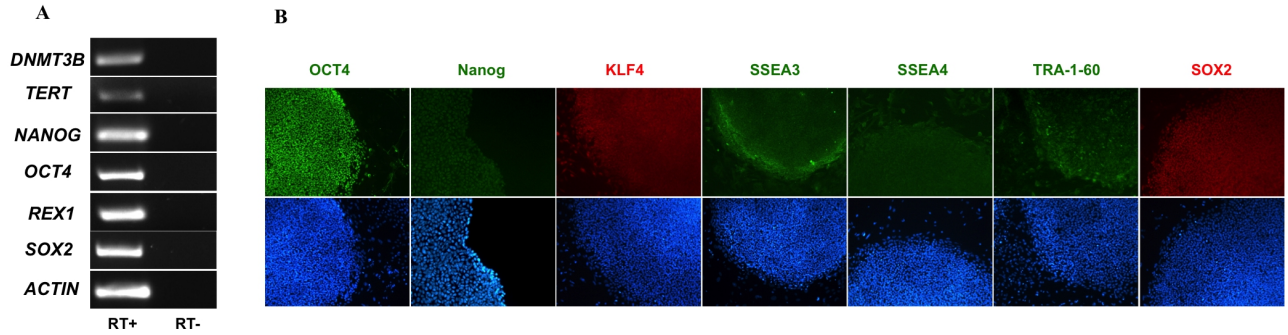

Fig. 4.2 : BD-B- hiPSCs pluripotency markers analysis. (**A**) RT-PCR products derived from amplification of pluripotency genes. (**B**) IIF analysis of pluripotency proteins expression. Nuclei were stained with DAPI.10X magnification.

In order to assess the potential of hiPSCs to differentiate into the derivatives of the three germ layers (ectoderm, mesoderm and endoderm), an embryoid bodies (EBs) test was performed. hiPSCs were grown in suspension in iPS medium (see paragraph 3.9) without b-FGF to allow EBs formation. After 7 days of culture, cells started to aggregate, to increase in dimensions and to assume a spherical shape (Fig. 4.3A). Once formed, the EBs were transferred into 0.1% gelatin pre-coated 6-well plates with MEF medium, to allow their growth in adhesion (Fig. 4.2B). Cells were harvested after 7 days to verify by RT-PCR the expression of differentiation markers belonging to the three germ layers: ectoderm (*TUBB, PAX6*), mesoderm (*KLF1, GATA2, PECAM, CDH5*) and endoderm (*AFP, GATA4*). As shown in Fig. 4.3B, gel electrophoresis analysis revealed the expression of all the analyzed genes, thus further confirming the pluripotency of the characterized hiPSC line.

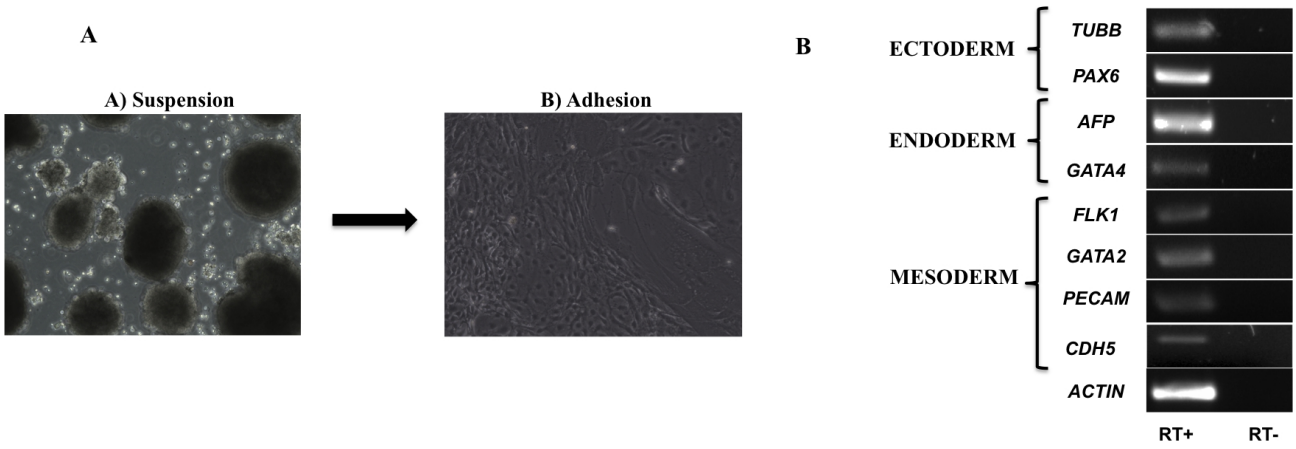

Fig. 4.3 : Embryoid bodies (Ebs) test performed on hiPSCs clone. (**A**) EBs in suspension for the first 7 days (left panel) and EBs after adhesion on gelatin-coated surfaces (right panel) (10x magnification). (**B**) RT-PCR products derived from the amplification of markers belonging to the three germ layers.

4.2 Differentiation process of hiPSCs into neural stem cells (NSCs) and neurons

To generate an *in vitro* model of flavivirus infection of human neural cells, hiPSCs were differentiated into neural cells. The BD-B-hiPSC clone was grown on Geltrex with StemMACs medium and, at 15-25% of confluency, culture medium was switched to Neural Induction Medium (see paragraph 3.4). Approximately 7 days after the medium switch, cells with rounded immature neural morphology (i.e., NSCs) appaired and started to grow in monolayer (Fig. 4.4B). Then, NSCs were further differentiated into immature neurons. To this purpose, NSCs, seeded on poly-L-ornithine and laminin- coated plate, were maintained in Neural Differentiation Medium. As shown in Fig. 4.4C, after 20 days of differentiation cells acquired an elongated shape characteristic of neurons with soma, dendrites and axons.

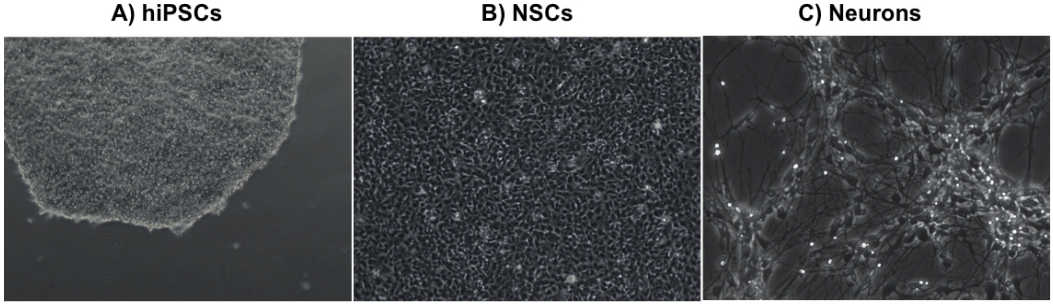

Fig. 4.4: Differentiation of hiPSCs into NSCs and neurons**. A)** hiPSCs cultured in a feeder-free layer. **B)** NSCs obtained from hiPSCs after 7 days of differentiation and **C)** neurons derived from NSCs after 20 days of differentiation.

4.2.1 Characterization of hiPSCs-derived neural cells

NSCs and neurons differentiated from hiPSCs were analyzed for the expression of neural markers by RT-PCR analysis and IIF to confirm NSCs identity. Expression of the neural stem cell genes was evaluated in cells cultured on Geltrex in Neural Expansion Medium. When cells reached sub-confluency, cells were harvested and the RNA was extracted and reverse transcribed to cDNA (see paragraph 3.7.1-3.7.2). cDNA was employed to amplify the NSCs genes *NESTIN, PAX6, SOX1,* and *SOX2*. Furthermore, in order to prove the loss of the pluripotency, expression of the pluripotency marker OCT4 was examined. Gel electrophoresis (Fig. 4.5A) showed positivity for all neural markers, validating NSCs identity. As expected, the stem cell marker gene *OCT4* was not expressed.

NSCs grown on Geltrex-coated 24 well plates in Neural Expansion Medium were also analyzed for neural markers expression by IIF (paragraph 3.8). As shown in Fig. 4.5B, an intense fluorescent signal was observed in NSCs stained for Nestin and PAX6, while the pluripotency marker OCT4 was not detected, proving the loss of the pluripotency.

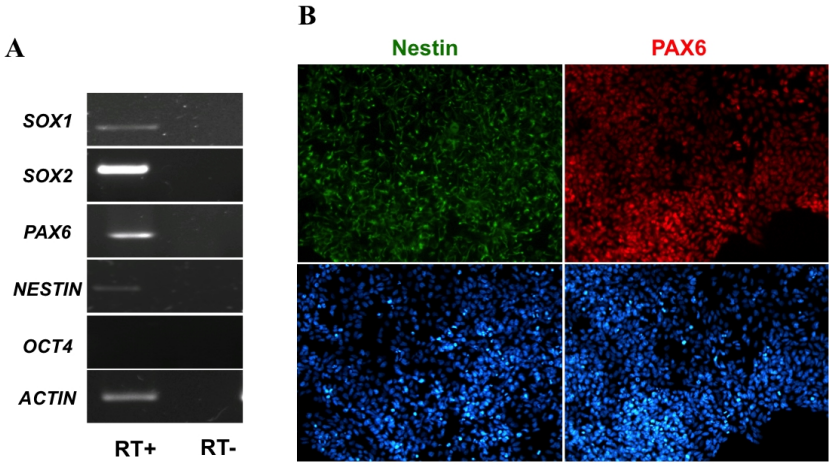

Fig. 4.5: Characterization of hiPSCs-derived NSCs. (**A**) bands on agarose gel obtained from amplification by RT-PCR of NSCs markers and pluripotent marker *OCT4*.(**B**) IIF for NSCs markers expression Nestin and PAX6 on NSCs. Nuclei were stained with DAPI.20X magnification.

4.2.2 Characterization of NSCs-derived immature neurons

In order to confirm the identity of immature neurons, cells were maintained in Neural Differentiation Medium on poly-L-ornithine and laminin-coated 24 well plates (see paragraph 3.5) and expression of neural marker genes was examined through RT-PCR analysis. Expression of neuron-specific genes, i.e. the microtubule protein β-Tubulin (TUBB), Microtubule Associated Protein 2 (MAP-2) and Neuron-Specific Enolase (NSE), was demonstrated in differentiated cells (Fig. 4.6A). As shown in Fig. 4.6B, expression of TUBB and MAP-2 was also confirmed by IIF

(see paragraph 3.8). Neurons stained positive for both markers, while no immunostaining was detected for the pluripotency protein OCT4 (Fig. 4.6B).

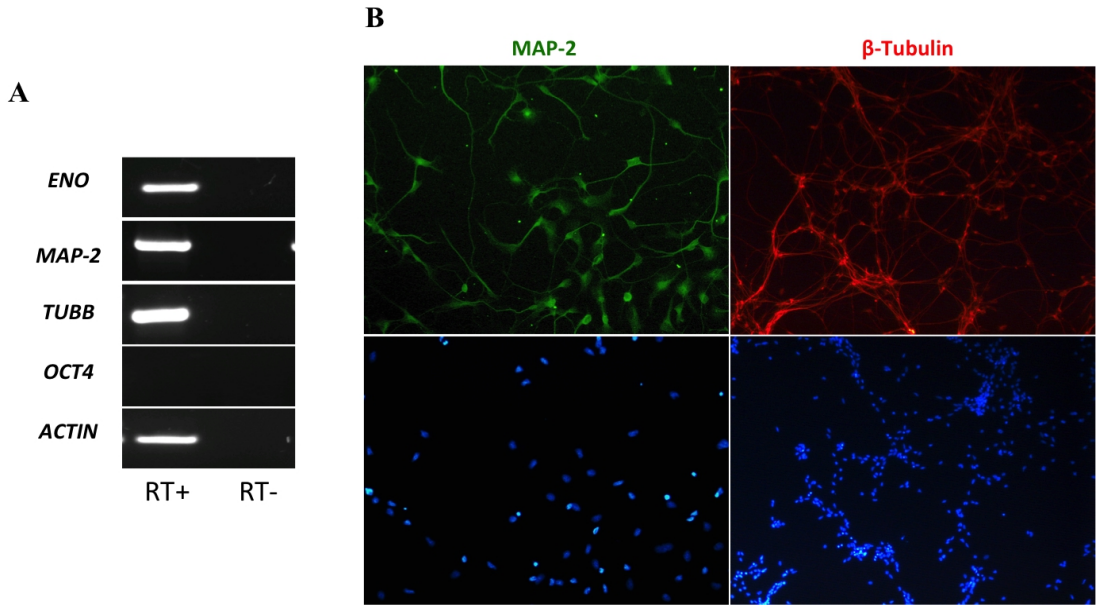

Fig. 4.6 : Characterization of NSCs-derived immature neurons. **(A)** agarose gel electrophoresis of amplification products of neuron markers (*ENO, MAP-2, TUBB*) and the pluripotent marker *OCT4*. (**B**) IIF for the neuron markers MAP-2 and β-Tubulin in hiPSC-derived immature neurons. Nuclei were stained with DAPI. Magnification 20×.

4.3 Viral infection and replication kinetics in hiPSCs, NSCs, and neurons

To evaluate the permissiveness of hiPSCs, hiPSCs-derived NSCs and neurons to ZIKV infection in comparison with other flaviviruses, cells were exposed to ZIKV, WNV, USUV and DENV-2 at the specified moltiplicity of infection (MOI). At different days post infection (dpi), supernatants and/or cell pellets were harvested for subsequent analysis.

4.3.1 ZIKV, WNV, USUV and DENV infect hiPSCs, NSCs, and neurons

HiPSCs, NSCs and neurons were incubated with ZIKV, WNV, USUV and DENV-2 at MOI 1 and the percentage of infected cells was evaluated by immunofluorescence staining with antibodies against viral envelope (E) glycoprotein. Briefly, infected cells were fixed in PFA 4%, permeabilized with Triton X-100, and blocked in BSA. At 72h pi, cells were immunostained with a Panflavivirus antibody targeting Flavivirus E protein. To verify that all cell types retained their identity after

infection, immunostaining against OCT4 for hiPSCs, PAX6 for NSCs and β-Tubulin for neurons was also perfomed. As shown in the panels (Fig. 4.7), positive anti-E immunostaining was detected in NSCs infected with ZIKV, WNV, USUV and DENV-2.

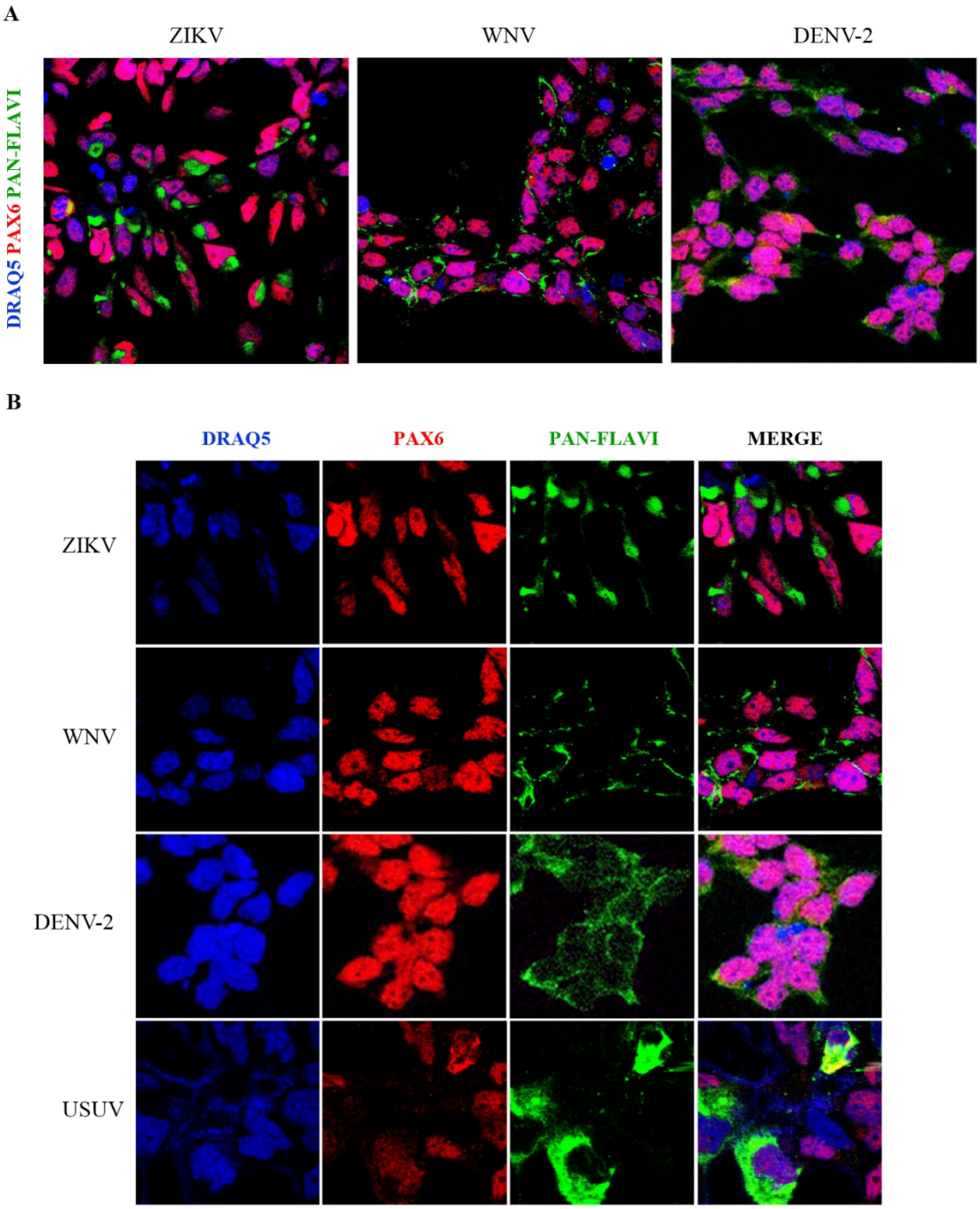

Fig 4.7 Flavivirus infection of NSCs. ZIKV, WNV, DENV-2 and USUV envelope E glycoprotein (goat anti-mouse IgG H&L FITC-conjugated, green) and NSCs marker PAX6 (goat anti-rabbit IgG AlexaFluor546-conjugated, red) stained by IIF in NSCs at 72 hpi with ZIKV, WNV and DENV, and at 96 hpi with USUV (MOI 1). (**A**) ZIKV, WNV and DENV-2 merge at 60× magnification zoomed two times. (**B**) ZIKV, WNV, DENV-2, and USUV details at 60× magnification zoomed four times. Nuclei were stained with DRAQ5 (blue); confocal fluorescence microscope.

An intense fluorescent signal was detected in about 25%, 70%, 40% and 15% of NSCs infected

with ZIKV, WNV, USUV and DENV-2. The immunostaining was observed in proximity of the nucleus, probably in correspondence of the endoplasmic reticulum (ER) and Golgi apparatus, which are the main sites of flavivirus replication. Each virus was associated with a different pattern of intracellular immunostaining, probably correponding to different rearrangements of cell membranes to create an adequate enviroment for viral replication.

Immature neurons derived from NSCs also supported ZIKV and WNV infection, with about 20% and 40% of cells, respectively, showing positive anti-E immunostaining (Fig. 4.8).

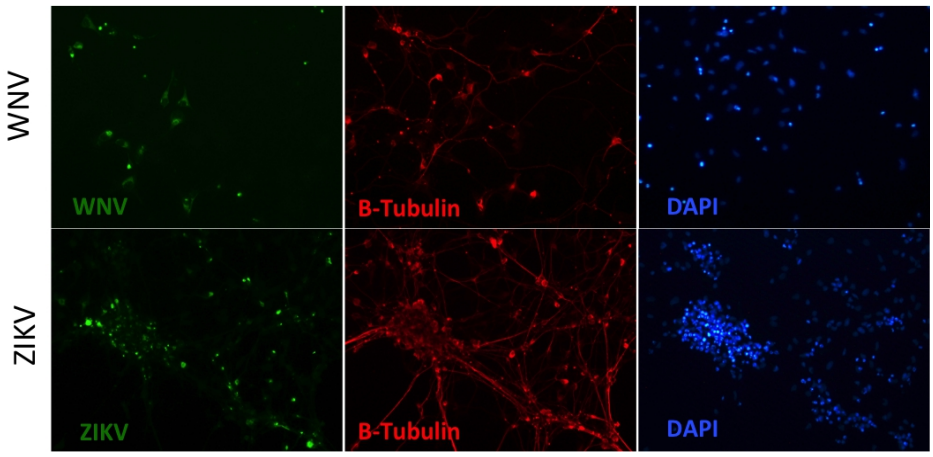

Fig.4.8 : WNV and ZIKV envelope E protein and the neuron marker β-TUBULIN (red) stained by IF in infected neurons. Nuclei were stained with DAPI (blue). Magnification 20×.

Furthermore, hiPSCs were permissive to ZIKV and WNV infection. Also in this cells WNV infection was more efficient than ZIKV infection (Fig. 4.9).

Expression of cell type-specific markers OCT4 (Fig 4.9), PAX6 (Fig 4.7) and β-Tubulin (Fig 4.8) was confirmed in infected iPSCs, NSCs and neurons, respectively. In each infection experiment, mock infected cells were negative for E protein expression

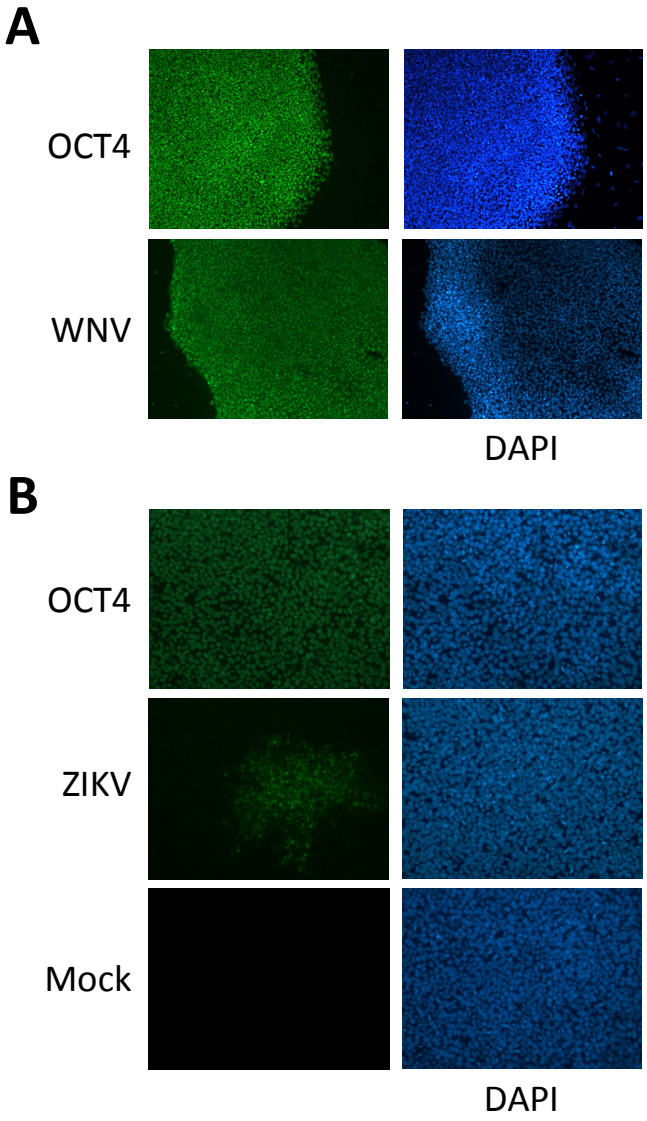

Fig. 4.9: WNV and ZIKV infection of iPSCs. **(A)** WNV infection of iPSCs at MOI 1; IF for flavivirus envelope E protein and the pluripotency marker OCT4 was perfomed at 72 hpi; nuclei stained with DAPI; magnification 10×. **(B)** ZIKV infection of iPSCs at MOI 0.1; IF for flavivirus envelope E protein and OCT4 was perfomed at 96 hpi; nuclei stained with DAPI; magnification 20×.

4.3.2 Replication kinetics of flaviviruses in hiPSCs, NSCs, and neurons

Replication kinetics was evaluated in time-course experiments of infection at different MOIs (0.01, 0.1, and 1) in hiPSCs, NSCs, and undifferentiated neurons. Viral RNA load was measured by qRT-PCR in supernatants of infected cells collected every 24 h until death of most cells. Results are summarized in figure 4.10. ZIKV replication was more efficient in NSCs than in hiPSCs and neurons, as demonstrated by both qRT-PCR and TCID50 assay (Fig. 4.10A-B-C).

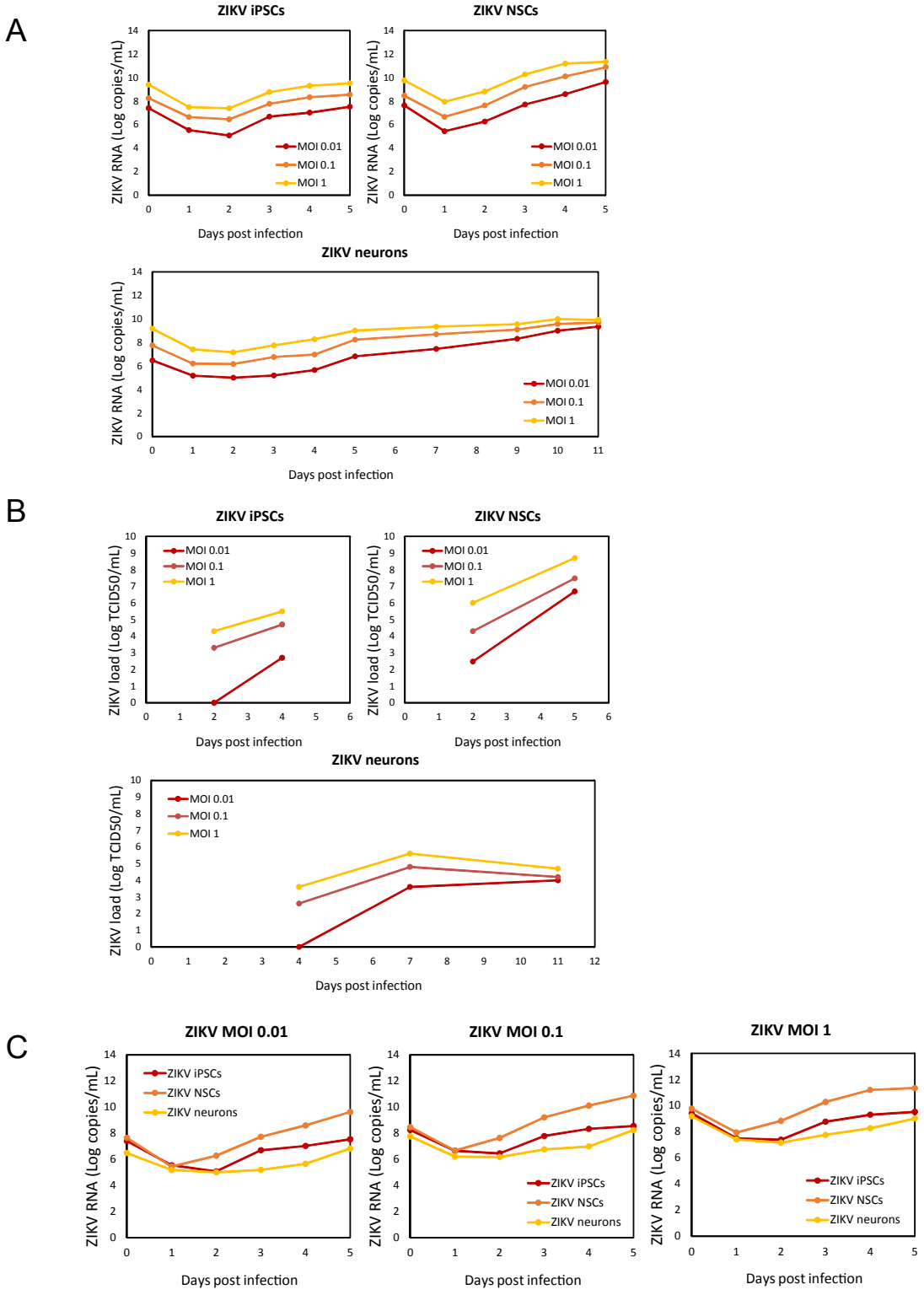

Fig. 4.10: Replication kinetics of ZIKV in hiPSCs, NSCs, and neurons. **(A)** ZIKV RNA load measured by qRT-PCR in cells infected with ZIKV at MOI 0.01, 0.1, and 1. (**B**) ZIKV titer measured by TCID50 assay in hiPSCs, NSCs, neurons infected at MOI 0.01, 0.1, and 1. (**C**) Comparison of ZIKV replication kinetics, measured by qRT-PCR, hiPSCs, NSCs, and neurons.

WNV replicated very efficiently in NSCs and rapidly reached high viral load, while replication was slower in differentiated neurons (Figure 4.11).

Comparison between ZIKV and WNV showed was higher replication efficiency of WNV than ZIKV in all cell types, i.e., hiPSCs, NSCs, and neurons (Figure 4.12). In particular, in neurons, WNV RNA load rapidly increased during the first days post infection, followed by a plateau, while ZIKV RNA load increased slowly and progressively during the time course experiment up to day 11 pi (Figure 4.13).

The kinetics of DENV-2 and USUV replication was also evaluated in NSCs. Both viruses could replicate in NSCs, but DENV-2 replication was shower than that of USUV, characterized by a rapid increase of viral load up to 48 hpi, followed by a plateau.

Comparison of replication kinetics of the different flaviviruses showed that WNV had the highest efficiency, as shown by a more rapid increase in viral titer, followed by ZIKV, while DENV-2 and USUV showed the lowest replication efficiency in NSCs (Fig. 4.15).

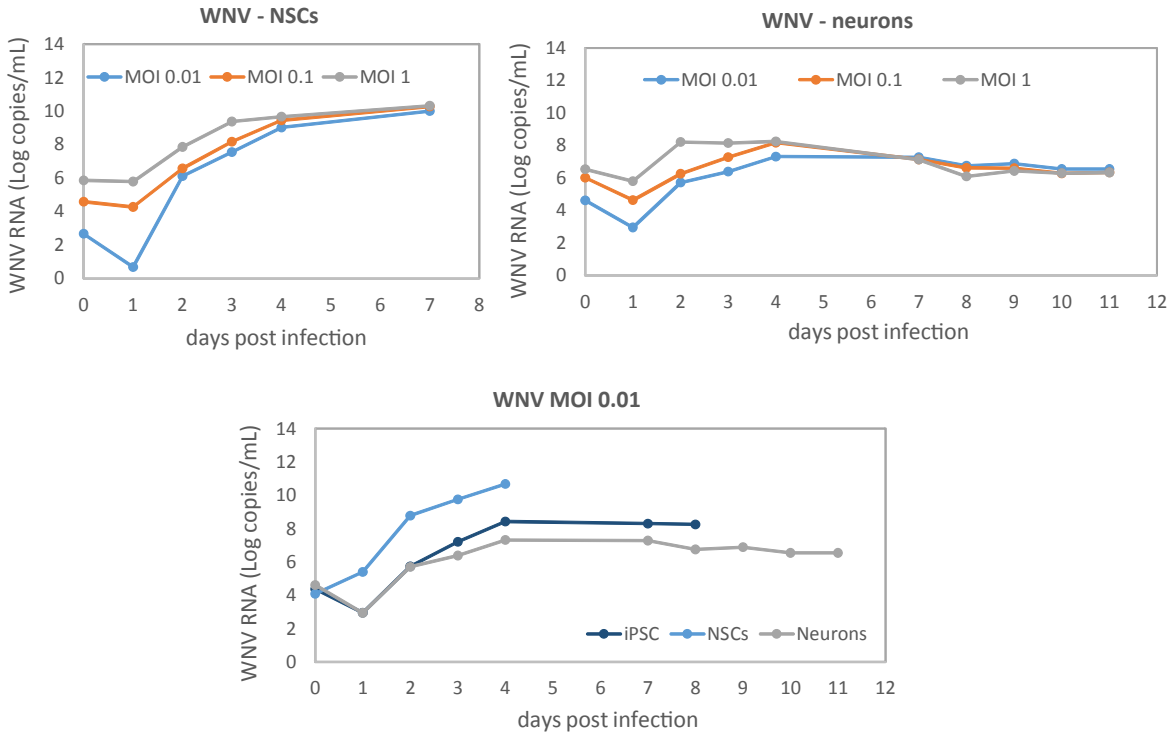

Fig. 4.11: Replication kinetics of WNV in hiPSCs, NSCs, and neurons. **(A)** WNV RNA load measured by qRT-PCR in NSCs infected at different MOI. (**B**) WNV RNA load measured by qRT-PCR in neurons infected at different MOI. (**C**) Comparison of WNV replication efficiency in hiPSCs, NSCs, and neurons after infection at MOI 0.01; WNV RNA load was measured by qRT-PCR.

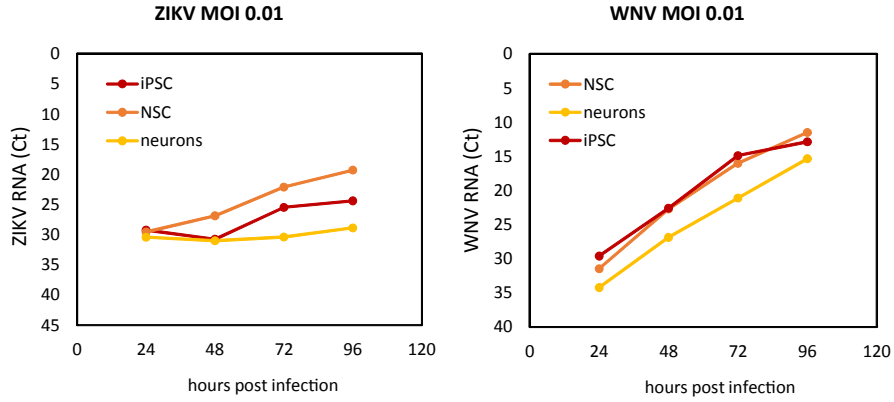

Fig. 4.12: Comparison of replication kinetics of ZIKV and WNV in hiPSCs, NSCs, and neurons after infection with MOI 0.01. Viral RNA load was measured by qRT-PCR and reported as threshold cycle (Ct) value.

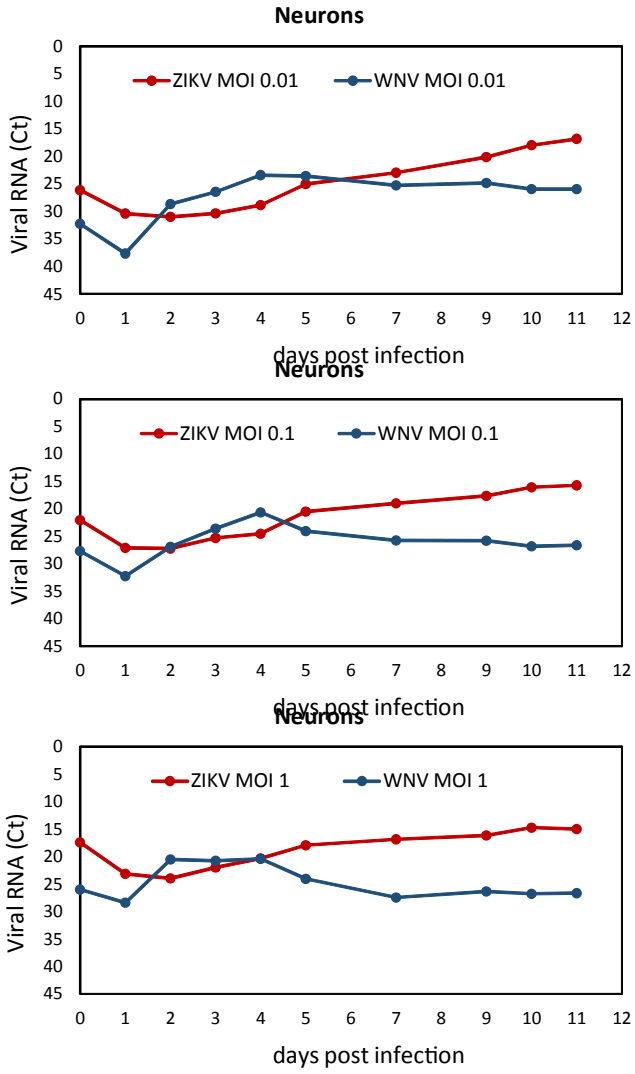

Fig. 4.13: Comparison of replication kinetics of ZIKV and WNV in neurons after infection with MOI 0.01, 0.1, and 1. Viral RNA load was measured by qRT-PCR and reported as threshold cycle (Ct) value.

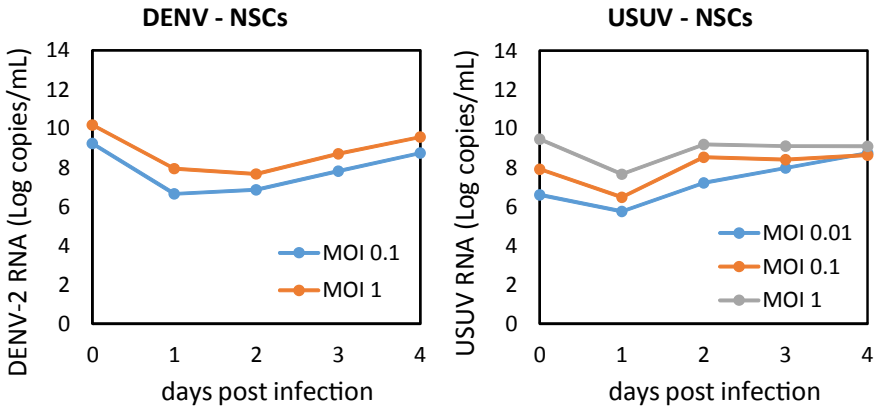

Fig. 4.14: Replication kinetics of DENV-2 and USUV in NSCs. Viral RNA load was measured by qRT-PCR in cells infected with different MOIs.

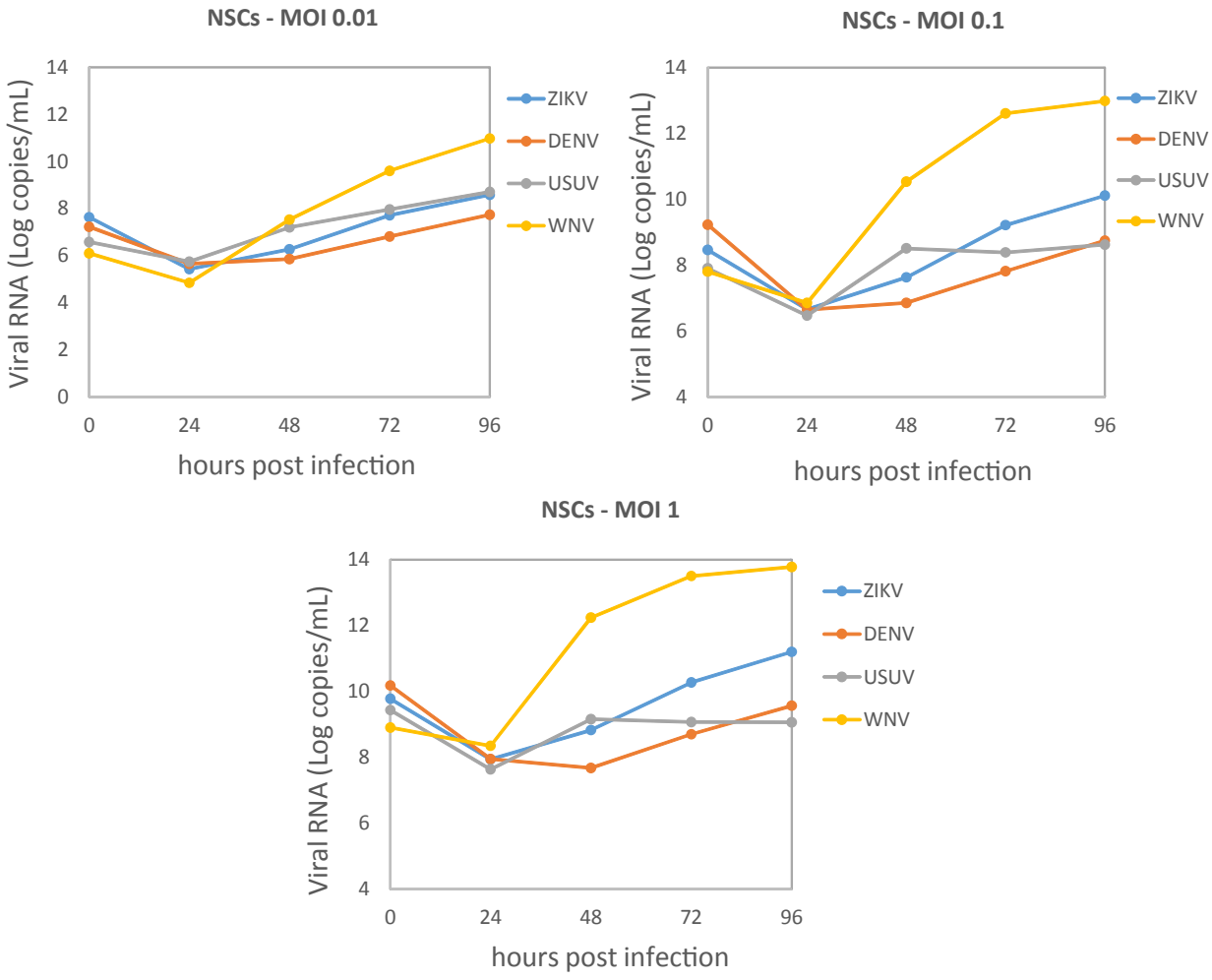

Fig. 4.15: Comparison of replication kinetics of ZIKV, WNV, USUV and DENV-2 in NSCs after infection with different MOIs. Viral RNA load was measured by qRT-PCR.

4.4 Cytopatic effects and cell death by apoptosis in infected cells

ZIKV exerted a cytopatic effect (CPE) not only in NSCs, but also in hiPSCs and neurons infected at different MOI (0.01, 0.1, 1; Fig. 4.16). Microscopic analysis showed in all infected cell types the presence of rounded cells, nuclear and citoplasmatic inclusion bodies and lysis plaques that increased in number with time. At 96 hpi, detachment of cell monolayers from the substrate was observed.

An aggressive CPE was observed also in WNV-infected cells, while no CPE was apparent in DENV-2- and USUV-infected cells at 96 hpi.

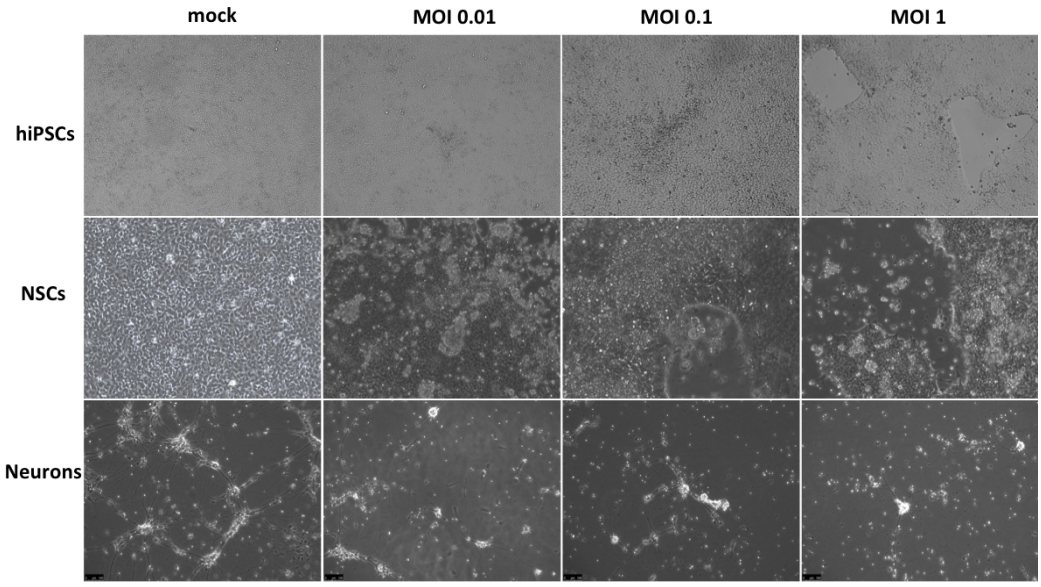

Fig. 4.16: images of ZIKV cytopatic effect (CPE) in hiPSCs, NSCs and neurons at 96h p.i. (MOI 0.01, 0.1, 1).

Cell death by apoptosis was evaluated in NSCs infected with ZIKV, WNV, and DENV-2 (MOI 1) at 72 hpi and 96 hpi. Briefly, collected cells were fixed with PFA 4% solution, permeabilized in 90% methanol and incubated with anti-cleaved Caspase-3 primary antibody prior to flow cytometer measurement. As shown in the graphs (Fig. 4.12), a 3-fold and 6-fold increase of caspase-3 activity was demonstrated in ZIKV- and WNV-infected NSCs, respecetively, compared to mock-infected control NSCs at 96 hpi, while at 72 hpi caspase-3 activity was not significantly higher than in the control. Furthermore, at 96 hpi, no significant changes in cell apoptosis were measured in DENV-2-infected NSCs.

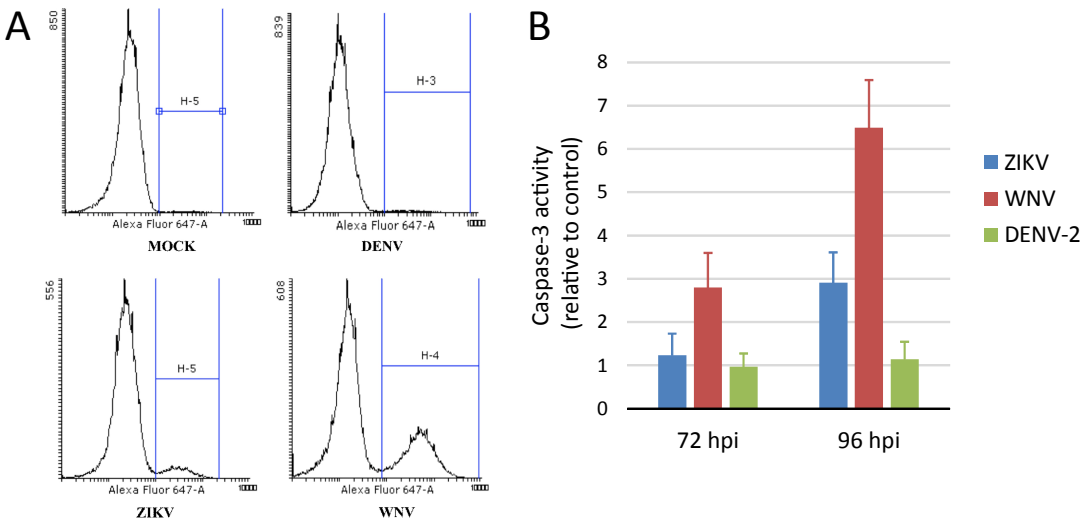

Fig. 4.17: (**A**) Flow cytometry analysis for detection of activated Caspase-3 in NSCs after mock, DENV, ZIKV, and WNV (MOI 1) infection (96 hpi). (**B**) Activity of Caspase-3 in ZIKV-, WNV-, and DENV-2-infected NSCs (MOI 1) at 72 hpi and 96 hpi.

The MTT test was performed to determine NSC viability after ZIKV, WNV, USUV, and DENV-2 infection at MOI 1. Briefly, cells were incubated with a solution of MTT and after 4 hours with a solubilization solution; the next day, the absorbance was read at 620 nm. Figure 4.18 shows the percentage of cell viability at 72 hpi and 96 hpi. At 72 hpi with ZIKV, NSCs were still viable, while at 96h p.i. infection induced a moderate decrease (about 10%) in cell viability. Contrarwise, after WNV infection, only 15% of NSCs were viable at 72 hpi and no viable cells were detected at 96 hpi.

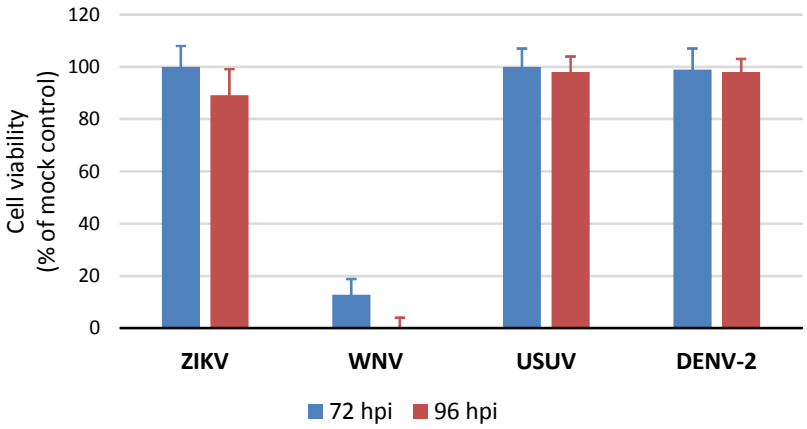

Fig. 4.18: MTT assay attesting viability of ZIKV- and WNV- infected NSCs (MOI 1) at 72 hpi and 96 hpi.

4.5 Innate antiviral immune response gene expression in infected cells

The modulation of genes involved in innate antiviral immune response was analyzed by qRT-PCR on hiPSCs, NSCs and neurons after infection with ZIKV (MOI 1), WNV (MOI 0.01), USUV (MOI 1), and DENV-2 (MOI 1) at 96 hpi. Briefly, infected-cells were detached by Accutase treatment, and RNA was extracted, quantified and reverse-transcribed. cDNA was used to amplify *IFIT1, IFIT2, MDA5, RIG-I, TLR3, IL-β* and *VIPERIN* mRNA; expression fold change was calculated by the ΔΔCt method.

In NSCs, all flaviviruses significantly up-regulated the *PRR IFH1 (MDA5)*, *IFN-induced protein with tetratricopeptide repeats 1 (IFIT1) and 2 (IFIT2)* genes (Fig. 4.19). WNV, although used at lower MOI than the other flaviviruses, induced in NSCs the highest levels of innate immune response gene transcripts with a particularly strong stimulation of IFIT2, a critical mediator involved in antiviral immunity. USUV also strongly induced expression of innate immune response genes, with particularly high levels of IFIT1, IFIT2, MDA5, and RIG-I. DENV-2 and ZIKV infection was associated with lower levels of innate antiviral response gene expression than WNV- and USUV-infected NSCs. In DENV-2-infected NSCs, *MDA5* and *IFIT1* mRNA levels were significantly higher than in ZIKV-infected NSCs. Notably, DENV and ZIKV did not significantly change *TLR3* expression.

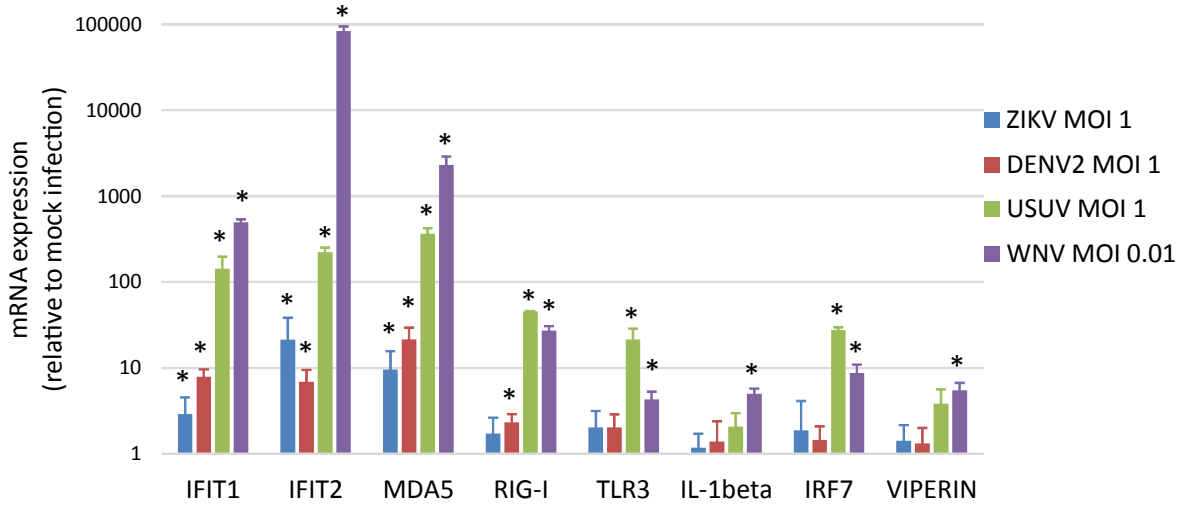

Fig. 4.19: qRT-PCR analysis of innate antiviral immune response gene expression in NSCs infected with ZIKV (MOI 1), WNV (MOI 0.01), USUV (MOI 1), and DENV-2 (MOI 1) at 96 hpi. Data are represented as mean ± SD. * $p < 0.05$.

In neurons, WNV infection, althoug at lower MOI, induced significantly and markedly higher mRNA levels of innate immune response genes than ZIKV, with the exception of *TLR3*, which has

higher mRNA levels in ZIKV-infected neurons than in WNV-infected neurons. Also in neurons, *IFIT1, IFIT2* and *MDA5* showed the highest increase of expression (Fig. 4.15).

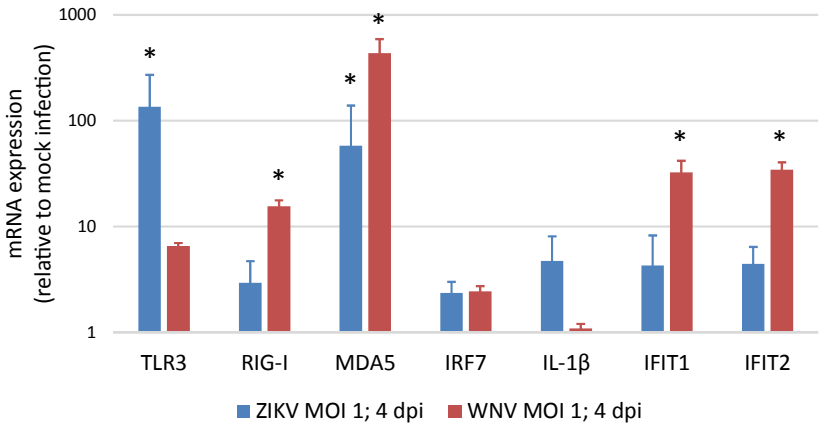

Fig. 4.20: qRT-PCR analysis of innate antiviral immune response gene expression in ZIKV- and WNV-infected neurons at 96 hpi. Data are represented as mean ± SD. * p< 0.05 vs- mock infection.

ZIKV and WNV infection induced expression of innate immune response genes also in hiPSCs, leading to a marked increase of *MDA5, IFIT1, IFIT2*, and *IFN-β*. The *IFIT2* gene exhibited the highest induction and expression level compared to the other examined genes (Fig. 4.16).

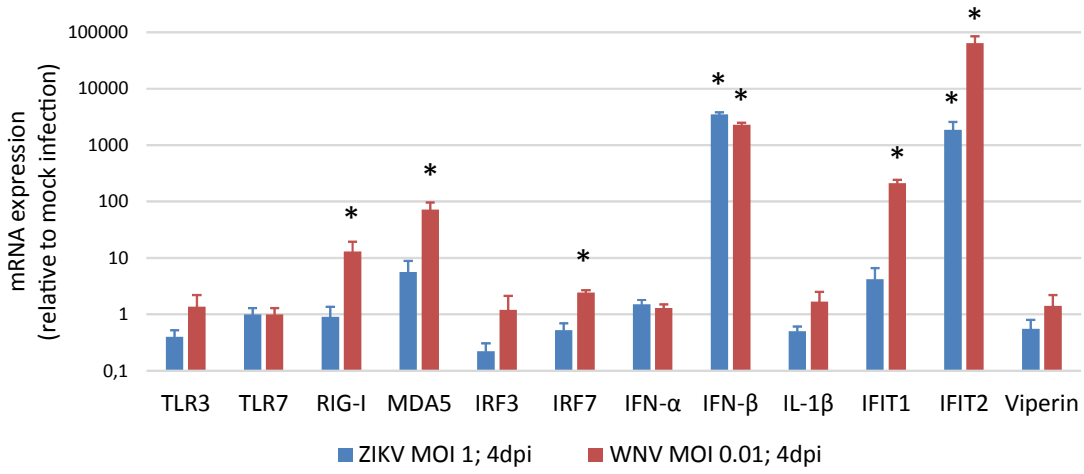

Fig. 4.21: qRT-PCR analysis of the innate antiviral immune response gene expression in ZIKV- and WNV-infected hiPSCs at 96h p.i.. Data represented as mean ± SD. * p< 0.05 vs. mock infection.

4.6 ZIKV infection and replication during neurogenesis

In order to evaluate the impact of ZIKV infection during neurogenesis, hiPSCs and NSCs were infected with ZIKV and then differentiated into NSCs, and neurons, respectively.

4.6.1 ZIKV infection during hiPSC differentiation into NSCs

In order to monitor the differentiation of hiPSCs into NSCs upon infection, about 10^5 hiPSCs/well were plated on Geltrex-coated wells and infected at MOI 0.1 and 1 for 90 min, by the end of which the neural induction process was triggered. Supernatants were harvested every 24 hours until 7 days pi for viral titration by qRT-PCR and TCID50 assay.

As early as day 1 pi, ZIKV titer in cells infected with MOI 1 was 10^2 TCID50/mL, while viral titre was still undetectable for the lower MOI 0.1. From day 2 pi onward, viral titers progressively increased with peaks at 6 and 7 dpi for MOI 1 and 0.1, respectively, when peak titers of about 10^9 TCID50/mL were reached (Fig. 4.22A). In agreement with TCID50 measurements, ZIKV RNA copies/mL increased rapidly from day 1 p.i., in a MOI- and time-dependent fashion, reaching peak titers at 7days p.i. (Fig. 4.22B).

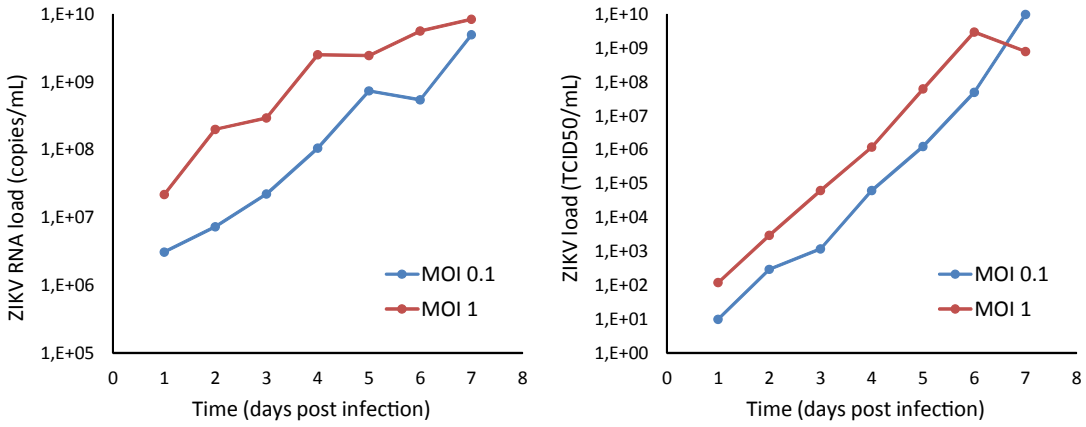

Fig. 4.22: ZIKV replication kinetics in hiPSCs during differentiation into NSCs. Infection at MOI 0.1 and 1; viral titer evaluated from 1 to 7 dpi. ZIKV RNA load was measured in cell supernatant by qRT-PCR **(A)** and TCID50 **(B)**.

ZIKV infection induced massive cell death, starting from 48 hpi, with a CPE characterized by shrinking and detachment of cells that increased with time (Fig. 4.23A).

The presence of ZIKV in infected cells was confirmed by IF assay for the E protein at 7 dpi, when the neural induction was almost completed. As shown in Fig. 4.18B at 7 dpi, most infected cells

were positive for ZIKV E protein. Expression of PAX6, a marker of the early ectoderm, demonstrated that differentiation process was successful. Thus, ZIKV infection did not seem to affect cell differentation process.

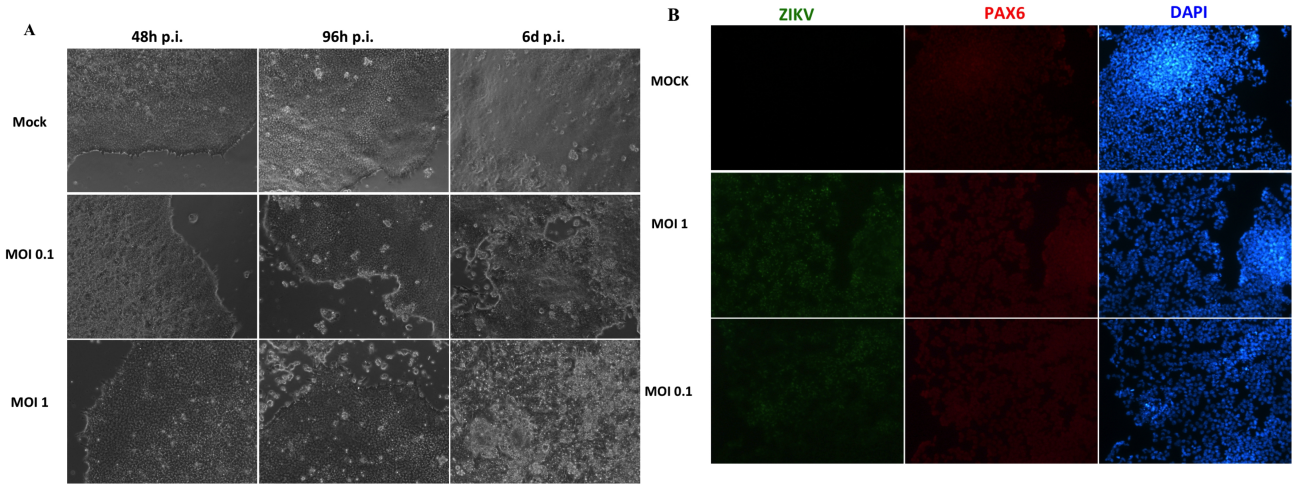

Fig. 4.23: (**A**) CPE of ZIKV-infected differentiating hiPSCs (MOI 0.1 and 1) at 2, 4, and 6dpi. (**B**) IF assay assessing the expression of E protein (green) and Pax6 (red) in ZIKV-infected differentiating hiPSCs (MOI 0.1, and 1) at 7dpi. Nuclei were stained with DAPI. 20× magnification.

4.6.2 ZIKV infection of NSCs during differentiation into neurons

In order to monitor the neurogenesis process upon infection, about 10^5 NSCs/well were plated on poly-L-ornithine- and laminin-coated wells and infected at MOI of 0.1, and 1. The differentiation process started as soon as the virus adsorption ended. At different dpi, cells were harvested for viral titration by qRT-PCR and TCID50 assay.

Supernatants of infected NSCs were collected at days 2, 3, 6, and 8 pi, for viral titration by TCID50. Infectious viral titer in the supernatant of cells infected at MOI 1 reached a peak of 10^9 TCID50/mL at 6 dpi, while peak titer for MOI 0.1 was reached at 8 dpi, with 10^6 TCID50/mL. At 8 dpi, for MOI 1, a decrease of infectious viral titer was observed, due to massive cell death (Fig. 4.24A).

Viral load was also measured by qRT-PCR in supernatants collected every 24 hours until day 8 pi, and at days 11, 14, and 16 pi. Viral RNA copy number increased starting from 2 dpi in a MOI-dependent fashion, reaching the peak titer of 10^{10} copies/mL in supernatant of differentiating NSCs infected at a MOI of 1, at 6 dpi. Viral load was not measured after day 8 pi due to the lack of live cells. For MOI 0.1, peak titer was reached at 11 dpi, with 10^9 copies/mL, trending to a plateau in the following dpi. (Fig. 4.24B).

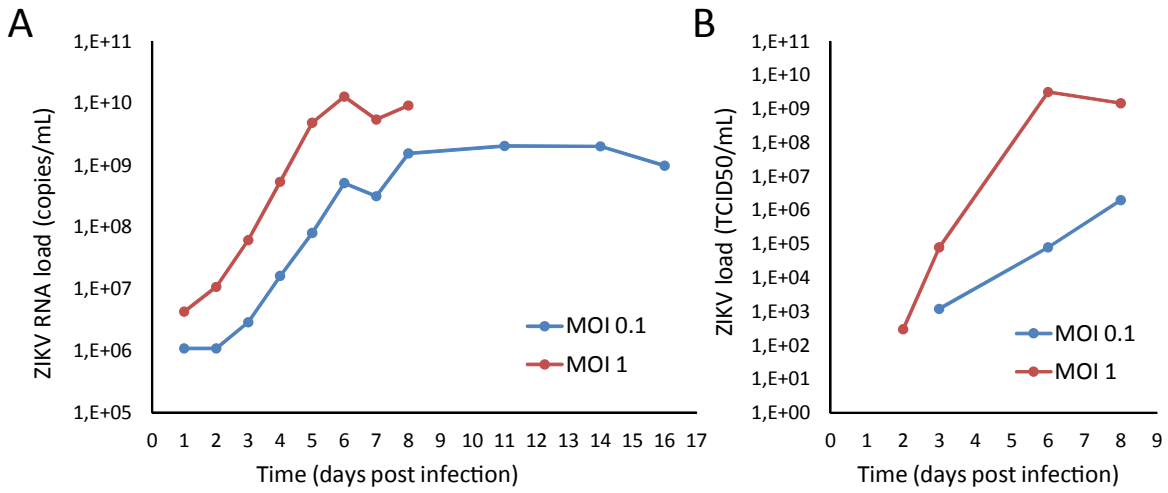

Fig. 4.24: **(A)** ZIKV titer on infected differentiating NSCs (MOI 0.1 and 1) at 2, 3, 6, and 8 dpi. **(B)** ZIKV replication kinetics in infected differentiating NSCs (MOI 0.1, and 1) by qRT-PCR from 1 to 8, and at 11, 14, and 16 dpi.

Expression of E protein was confirmed by IF at days 8 and 20 pi, respectively, i.e. at early and late phases of the neuron induction process (Fig. 4.25). Notably, infection did not block the neural differentation process, since IF assay confirmed the expression of the neuron-specific protein β-Tubulin in infected cells (Fig. 4.25).

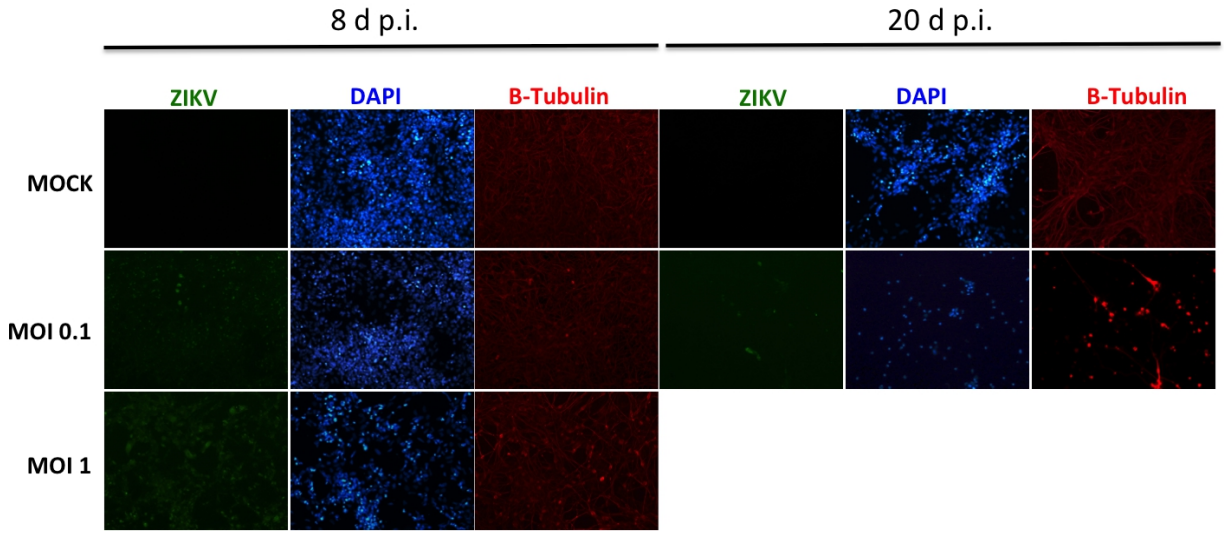

Fig. 4.25: IF assay assessing the presence of E protein in ZIKV-infected differentiating NSCs (MOI 0.1 and 1) at 8 and 20 dpi. Nuclei stained with DAPI. 20× magnification.

ZIKV infection caused as early as day 6 pi the appearance of cell death that increased with time, leading to a complete cell loss before completion of the differentiation process after infection at MOI 1 (Fig. 4.26).

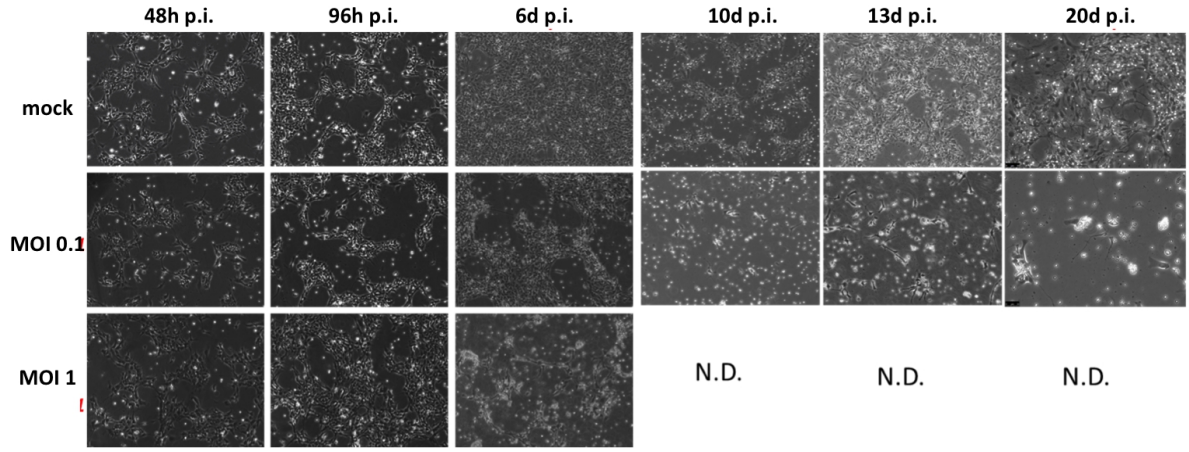

Fig. 4.26: CPE of ZIKV-infected differentiating NSCs (MOI 0.1 and 1) at 2, 4, 6, 10, 13, and 20 days p.i..

4.6.3 ZIKV infection and replication in embryoid bodies

hiPSCs were infected at MOI 1 and, after 2 days, cells were detached by collagenase IV treatment in order to initiate differentiation of embryoid bodies (EBs), i.e., micro-tissue similar to native tissue elements. Briefly, detached infected hiPSC colonies were resuspended in iPSC medium without bFGF supplementation to prevent stemness retention, and grown in suspension for 7 days. At day 7, growing EBs were plated on 0.1% porcine gelatin in order to allow them to grow in adhesion (see paragraph 3.9).

Viral infection was monitored collecting the supernatants of infected cells and analyzing viral RNA copies number by qRT-PCR at different time points pi. Viral RNA load increased with time, reached a peak at 5 dpi and then decreased in parallel with the decrease of the number of live cells (Fig. 4.27).

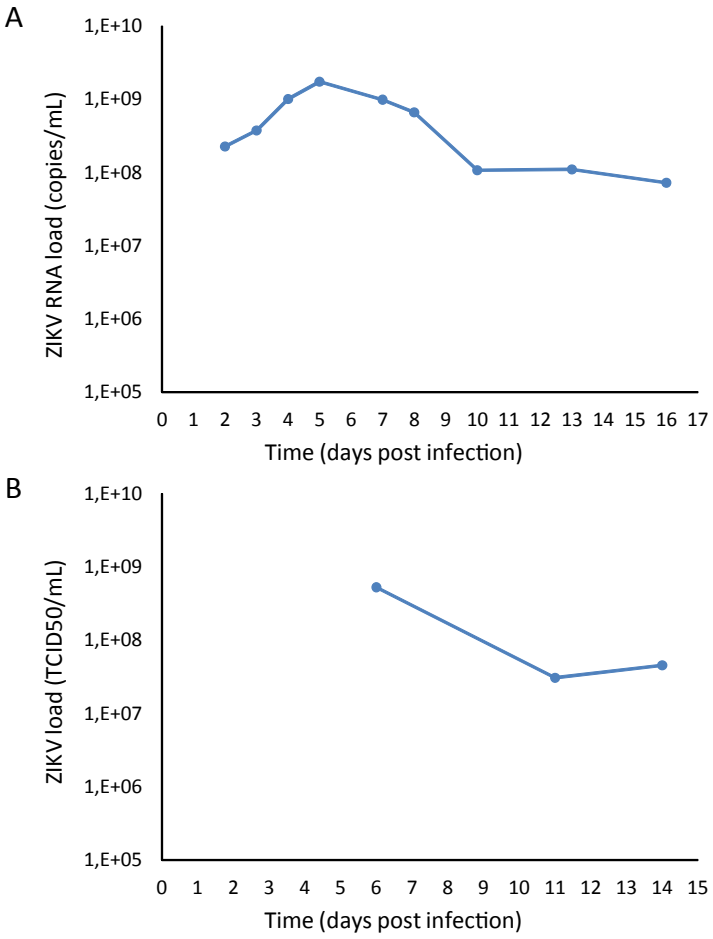

Fig. 4.27: ZIKV replication kinetics in infected EBs (MOI 1) by qRT-PCR from 2 to 16 dpi.

As shown in the Fig. 4.28**,** ZIKV infection of hiPSCs and subsequent random differentiation into EBs growing in suspension, outlined a progressive reduction in the volume and number of the EBs that displayed jagged edges when compared to mock controls. When the adhesion stimuli were added, infected EBs were not able to fully attach to the gelatin-coated plastic. Surviving adherent infected cells started to die with subsequent detachment.

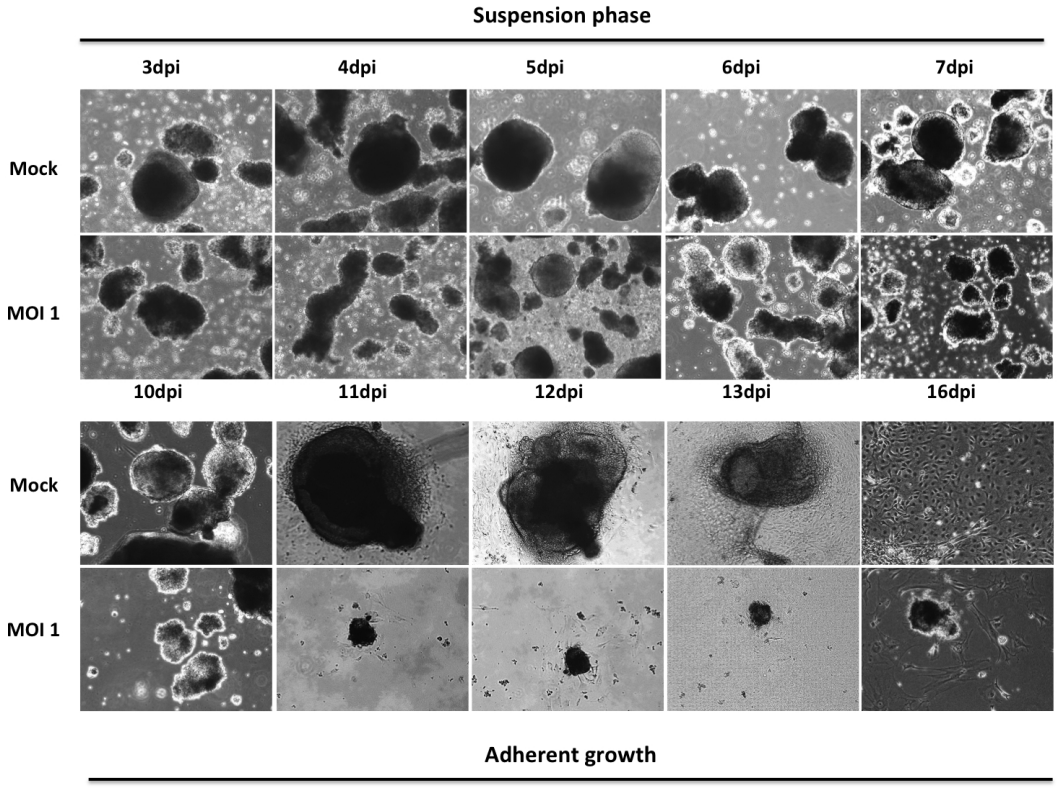

Fig. 4.28: CPE of ZIKV-infected EBs (MOI 1) during differentation process.10x magnification.

4.7 Modelling patient-specific susceptibility to West-Nile neuroinvasive disease

Once validated, the hiPSCs-based infection model was employed to set up patient-specific *in vitro* infection models to investigate the mechanisms of individual susceptibility to severe disease outcome.

4.7.1 Reprogramming and characterization of patient-specific hiPSCs

hiPSCs were obtained by reprogramming from peripheral blood mononuclear cells (PBMCs) of patients who experienced WNV asymptomatic infection and WNV neuroinvasive disease without co-morbidities. PBMCs were expanded and differentiated into erythroblasts for 10 days in EM medium. Then, $2x10^5$ cells were transduced with non-integrating Sendai virus vectors expressing the four Yamanaka factors (Oct4, Sox2, Klf4 and c-Myc) at MOI 10. Approximately 20 days after transduction, colonies exhibiting typical human stem cell morphology appeared. Then, colonies were manually picked, expanded, frozen for back-up purposes and characterized.

In order to test the pluripotency state, clones were seeded onto Geltrex feeder-free substrate, cultured in StemMACS medium and the main pluripotency markers (OCT4, Dnmt3b, NANOG, TERT) were analyzed by RT-PCR. As seen in Figure 4.22A, all hiPS clones expressed the stemness genes, confirming their pluripotency status. Immunostaining also confirmed expression of the pluripotency proteins Oct4, Klf4 and SSEA4 in all hiPS clones (Fig. 4.29B). In this case, cells were cultivated on MEF-coated 24-well plates and analyzed for marker expression by immunofluorescent staining.

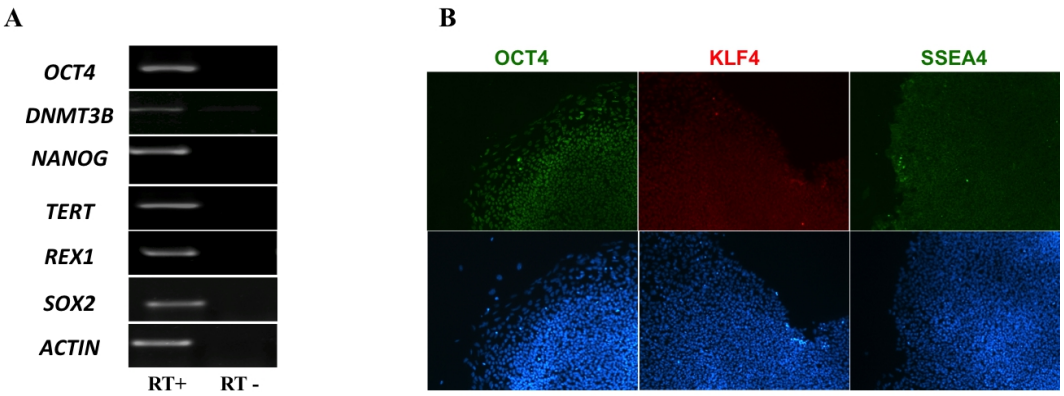

Fig. 4.29: Characterization of patient-specific hiPSCs. (**A**) RT-PCR analysis of pluripotency marker genes expression in hiPSCs. (**B**) Immunofluorescence assay for pluripotency protein expression. Nuclei were stained with DAPI. 20x magnification

To test the differentation potential of patient-specific hiPSCs, EB assay was performed. Cells were cultured in suspension for 7 days in iPS medium without b-FGF to allow their differentiation and for further 7 days in adhesion on 0,1% gelatine layer in DMEM 10% FBS medium. (Fig. 4.30A). The EBs formation test showed that hiPSCs could spontaneously differentiate into cells that highly expressed *TUBB, PAX6* (ectoderm), *FLK1, GATA2, PECAM, CDH5* (mesoderm), *AFP, GATA4* (endoderm) (Fig. 4.30B). These results confirmed that hiPSCs were pluripotent and could differentiate into all three germ layers.

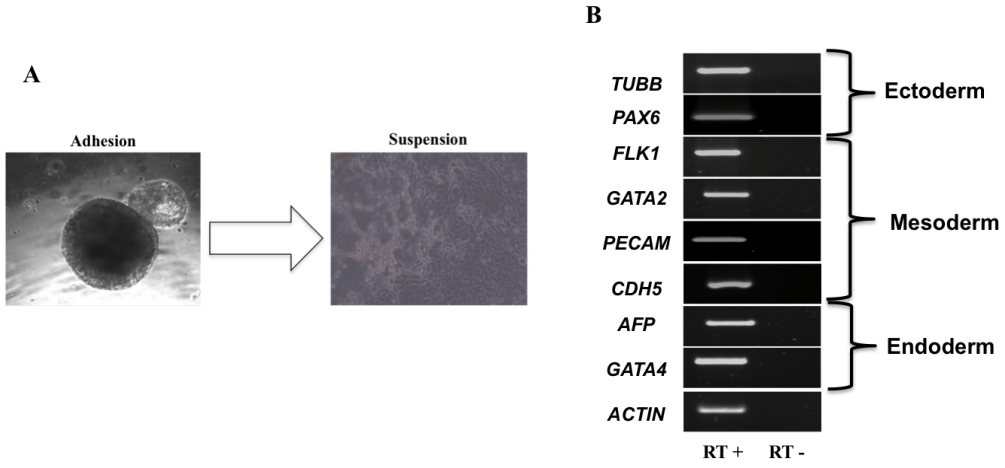

Fig. 4.30: (**A)** iPSCs grown in suspension form EBs that produced all kind of cells coming from embryonic three germ layers when cultured in adhesion. (**B**) RT-PCR products derived from amplification of three germ layers differentiation genes.

4.7.2 Neural differentation of patient-specific hiPSCs

Patient-specific hiPSCs were differentiated into NSCs to generate an *in vitro* human model of infection. hiPSCs seeded on Geltrex in StemMACs medium were cultured using Neural induction medium (see paragraph n. 3.4). After 7 days, NSCs proliferated and generated a monolayer of cells with a typical neural morphology (Fig. 4.31A). NSCs were expanded, frozen for backup purpose and characterized.

RT-PCR results demonstrated expression of NSCs markers *NESTIN, PAX6, SOX1* and *SOX2* in hiPSCs-derived NSCs. As attended, the stem cell gene *OCT4* was not expressed (Fig. 4.31B).

NSCs generated from iPSC differentiation were immunostained for the intermediate filament protein Nestin and the transcription factor PAX6. To prove the loss of the pluripotency, expression of the pluripotency marker OCT4 was examined. An intense fluorescent signal, when observed at a fluorescent microscope, indicated the expression of Nestin and PAX6, while pluripotency protein OCT4 was not detected. (Fig. 4.31C).

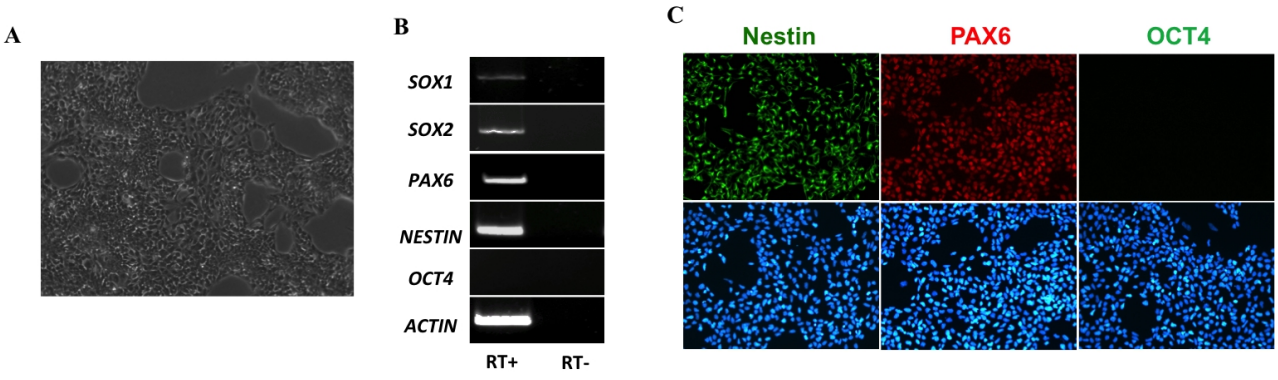

Fig. 4.31: Characterization of patient-specific hiPSCs-derived NSCs. (**A**) Neural stem cells (p1) at the end of the neural induction phase. (**B**) RT-PCR analysis of the neural marker genes expression in NSCs. (**C**) Immunofluorescence assay for the NSCs proteins. Nuclei were stained with DAPI. 20x magnitude.

4.7.3 Susceptibility of patient-specific NSCs to WNV infection

Preliminary studies, exploiting this *in vitro* patient-specific hiPSCs-derived neural model, were performed to investigate the mechanisms of susceptibility to WNV in patients who experienced viral asymptomatic infection and neuroinvasive disease.

Patient-specific NSCs were seeded into 24 well plates ($5x10^4$ /well) in quadruplicate and next day they were infected with WNV at MOI 0.01. Viral replication kinetics was analyzed by quantifying the viral load in a time-point experiment (24 h, 48 h, 72 h, 96 h pi) using qRT-PCR on RNA extracted from supernatants collected from infected cells. A progressive increase of WNV RNA load was demonstrated in both cell lines, but viral titers were higher in the NSCs derived from the patient with neuroinvasive disease than in the NSCs derived from the asymptomatic blood donor (Fig. 4.32).

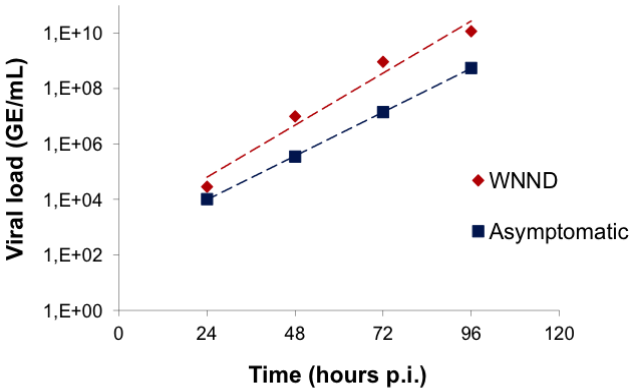

Fig. 4.32: Replication kinetics of WNV (MOI 0.01) in NSCs derived from a patient with a previous neuroinvasive disease (WNND) and from an asymptomatic donor.

The effect of WNV infection on cell viability was analyzed at 96 hpi by MTT test in patient-specific NSCs infected at MOI 1, 0.1 and 0.01. At 96 hpi, higher viability was demonstrated in NSCs derived from the asymptomatic patient than in cells derived from the patient with neuroinvaasive disease (Fig. 4.33A). In fact, at MOI 1, the MTT test detected about 15% viable NSCs from the asymptomatic donor and only 3.5% viable NSCs from the case with neuroinvasive disease. The ability of WNV to induce cell death by apoptosis in NSCs was evaluated at 96h p.i. Flow cytometry analysis detected a four-fold increase of caspase-3 activity in WNV-infected NSCs derived from the patient compared to mock-infected control cells (Fig. 4.33B-C).

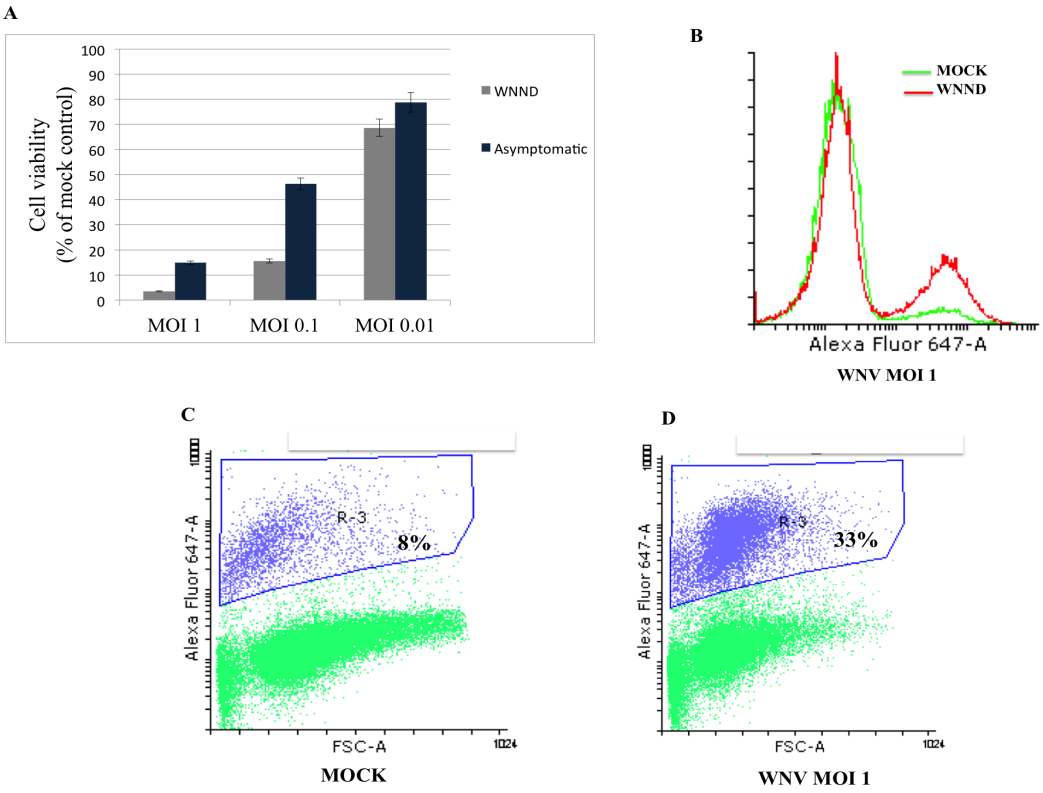

Fig. 4.33: WNV infection induces cell viability and apoptotic cell death in patient-specific NSCs. **(A)** MTT assay attesting cell viability in NSCs derived from asymptomatic and neuroinvasive disease patients at different MOIs at 96 hpi. **(B)** Flow cytometry analysis for detection of activated caspase-3 in neuroinvasive disease patient-specific NSCs after mock and WNV (MOI 1) infection at 96h p.i. **(C-D)** Flow cytometry analysis showing the percentage of NSCs with activated caspase-3 in mock-infected and WNV-infected NSC cultures.

5. DISCUSSION

ZIKV, WNV, and DENV are important human pathogens, members of the *Flavivirus* genus in the *Flaviviridae* family of positive-stranded RNA viruses [412]. Although most human infections are asymptomatic, symptoms may occur, ranging from relatively mild fever to severe hemorrhagic and encephalitic disease [9]. In addition, the emerging mosquito-borne flavivirus Usutu virus (USUV) may cause fatal neuroinvasive disease in different bird species and it has been recently shown to infect humans but its pathogenicity is unknown. These viruses belong to the mosquito-borne group, with ZIKV and DENV transmitted by *Aedes spp*. mosquitoes and amplified in primates, while WNV and USUV are transmitted by *Culex spp*. mosquitoes and birds represent the amplifying hosts.

DENV is the most widespread flavivirus with approximately 500 million infections per year, of these 1 million are clinically severe, including DHF and DSS, while neurological complications have been rarely reported [316,317]. WNV and ZIKV have recently emerged as important human pathogens and associated neurological complications. WNV causes neuroinvasive disease in about 1 out of 150 infected individuals, mostly immunocompromised and elderly patients [413]. ZIKV infection has been recently associated with Guillän Barrè syndrome and fetal microcephaly [414].

Experimental studies have clarified some mechanisms of ZIKV pathogenesis: *in vivo* studies in newborn and pregnant mice showed that the virus is able to infect NSCs and affect brain development [169,179]; neurotropism was also confirmed in knockout mice with defects of interferon signalling, showing how interferon plays a key antiviral innate immune response [176]. An *in vitro* study on hiPSC-derived NPCs demonstrated that these cells are highly susceptible to ZIKV infection, which dysregulated the cell-cycle and induced apoptosis [33]. Many other studies exploited both hiPSC-and fetal brain tissue-derived neural progenitor cells in monolayer, 3D neurosphere cultures and brain organoids [137,138,146] as models of ZIKV infection in the CNS. These studies demonstrated ZIKV neurotropism, targeted cell-types, cytopathic effects, and impairment of neurogenesis.

In the epidemiological context of WNV emergence in Europe and ZIKV epidemics in the Americas, aim of this project was to set up *in vitro* models of viral infection in human NSCs and neurons and to use these models to investigate and compare ZIKV and WNV infection and pathogenesis. In addition, patient-specific iPSCs-derived NSCs and neurons were generated to investigate the mechanisms of individual susceptibility to severe neuroinvasive disease.

Similarly to the accumulating evidences reporting infection of NSCs by ZIKV [33,137,145,146], this study confirmed the permissiveness of hiPSCs-derived NSCs to ZIKV infection by detection of

E protein expression in infected cells and by demonstration of a progressive increase of viral load in cell supernatant during time-course experiments.

Immature neurons and hiPSCs also supported ZIKV replication, although replication efficiency in these cell types was lower than in NSCs. These data are in contrast to a previous study by Tang and colleagues [33] who showed that infection of undifferentiated hiPSCs and immature neurons was inefficient. Different observations were reported in other studies [415] that demonstrated permissiveness of developing immature neurons to ZIKV infection as well as relative resistence of mature neurons in adult human brains.

DENV-2 and WNV also infected NSCs and neurons. DENV-2 infected hNSCs with a similar rate as ZIKV, in agreement with the results described by Garcez and colleagues [137]. At variance, WNV infected and replicated in all cell types with significantly higher efficiency than ZIKV. Notably, WNV was able to infect hiPSCs and immature neurons, contrary to what was reported by Shresta B. and colleagues [416], who showed the resistence of mouse embryonic stem cells (ESCs) and ESC-derived immature neurons to WNV infection, but in agreement with other reports on the permissivenes neurons to WNV infection. In particular, Luca and colleagues described the susceptibility of mouse neuron-enriched cultures to WNV infection, displaying 90% infected cells, cytophatic changes and cell death [417]. USUV could also infect and replicate in NSCs, with a rapid increase in the viral load till 48h p.i., followed by a plateau.

The discrepancy of these results with the literature data on ZIKV infection of stem cells might be due to differences in experimental design, laboratory conditions and cells cultures (hiPSCs grown in clumps *versus* hiPSCs grown in single cells for ZIKV infection; mouse ESCs versus hiPSCs for WNV infection). Different viral strains were also used: in this study, a ZIKV strain belonging to the Asian lineage was used, while Tang and colleagues [33] used African lineage ZIKV MR766 strain; in this study WNV lineage 2 was used, while Shresta B. and colleagues [415] used WNV lineage 1.

Both ZIKV and WNV exerted CPEs in hiPSCs, NSCs and neurons, leading to massive cell death, due in part to apoptosis mediated by activation of caspase-3, in agreement with reports in the literature [33,136]. At variance, DENV-2 infection had milder CPEs on NSCs and did not induce cell apoptosis, confirming results in literature [137]. Also USUV-infected NSCs presented no morphological cytophatic effect and their viability was not affected, as shown by the MTT assay. Cell viability assays demonstrated that WNV induced massive cell death with 100% of cell loss at 96h p.i., while only 10% reduction of NSC viability was observed after ZIKV infection. These findings suggest that ZIKV replication is slower and the virus can persist for a longer time in infected cells.

Regarding the innate antiviral response during ZIKV infection, many studies based on different cell types and viral strains led to different observations. In primary human skin fibroblasts, ZIKV Asian lineage induced the upregulation of three important PRRs known to be activated by viral dsRNA, specifically TLR3, DDX58 (RIG-I), IFIH1 (MDA5) and, also, other factors involved in downstream pathways, such as IFN regulatory factor 7 (IRF7), IFNα, IFNβ and C-C motif chemokine ligand 5 (CCL5) [156]. Frumence and colleagues reported that ZIKV (H/PF/2013) stimulated the production of type-I IFN, ISGs and pro-inflammatory cytokines, in particular IL-1β, in the human lung epithelial cell line A549 [418].

In the CNS, *TLR3* was upregulated in cerebral organoids and human neurospheres after ZIKV MR766 infection, and TLR3 activation was associated with cell apoptosis, organoid shrinkage and dysregulation of neurogenesis induced by ZIKV infection [146]. However, Hanners and colleagues [142] described that ZIKV Asian lineage induced partial CPE and did not stimulate cytokine secretion in human fetal neural progenitors.

Our study showed that ZIKV, WNV, DENV-2 and USUV infection induced the expression of a set of antiviral innate immune response genes in NSCs, neurons and hiPSCs, especially *MDA5* and the IFN-induced protein with tetracopeptide repeats 1 (*IFIT1*) and 2 (*IFIT2*) genes. The highest expression levels of the antiviral genes was observed in cells infected by WNV, flowed by USUV-infected cells, while ZIKV and DENV infections had milder effects on host innate antiviral response.

MDA5 is a cytoplasmic helicase able to detect intracellular viral products such as viral RNA genome to signal IFNα and IFNβ production in infected cells [419]. *IFIT1* and *IFIT2* are important interferon-stimulated genes (ISGs); they belong to the IFIT gene family whose members function to restrict virus infection through alteration of cellular protein synthesis [420].

Previous studies demonstrated an antiviral function of IFIT2 in controlling viral replication in the CNS [420,421] and IFIT2 has been suggested to have antiviral activity against WNV [422]. However, WNV uses the 2' O-mehylation of the 5' guanosine cap as a mechanism to evade the antiviral effects of IFIT1 and IFIT2 [423]. This is consistent with our observations in infected cells, where WNV infection led to a stronger upregulation of *IFIT2* than ZIKV and DENV-2 infection. Also IFIT2 triggers a mitochondrial pathway of apoptosis accompanied by the pro-apoptotic proteins Bax and Bak with the activation of caspase 3 [424]. Accordingly, in our study we could observe overexpression of *IFIT2* in infected NSCs and activation of caspase-3.

The literature reports absent or low levels of innate immune response against viral infection in mESCs [425], hESCs [426] and, also, in hiPSCs [425]. At variance, our data demonstrate that hiPSCs infected by WNV and ZIKV are able to activate an innate antiviral response characterized

by upregulation of *MDA5, IFIT1, IFIT2* and other ISGs. Therefore, innate immunity represents an uncharacterized property of pluripotent stem cells that requires further studies to elucidate the molecular mechanisms.

Neurogenesis is most active during pre-natal development, and this could explain why ZIKV can provoke neurological complications in fetuses, and rarely in adults. Since a normal brain develops from NSCs and differentiated neural cells, microcephaly could be likely associated with the abnormal function of these cells due to ZIKV infection. Recent reports demonstrated that ZIKV directly infects NSCs of the fetus and impairs growth in mice [168]. ZIKV has a negative impact on neurogenesis either by abrogating it completely or by disrupting neural cell organization [137,146].

To further investigate if ZIKV could impair the formation of neural precursors and neurons, the effect of viral infection during the neural differentation process, which is critical for brain development, was analyzed. Our experiments showed that ZIKV infected and replicated in hiPSCs during their differentiation into NSCs, inducing CPE and cell death, but it did not affect the differentation process, as demonstrated by the maintenance of the NSC marker Pax6 at the end of the neural induction phase. Likewise, in NSCs infected prior to their differentation into neurons, ZIKV did not block neuronal development, as confirmed by the expression of the neuron marker β-tubulin during neurogenesis. In these cells, ZIKV induced massive cell death that increased with time leading to a complete disruption of cell monolayer, so the neurogenesis process could not be completed.

Similar findings were reported by Garcez and colleagues [137] who demonstrated that ZIKV infection of human NSCs growing as neurospheres and brain organoids reduced cell viability and growth, abrogating neurogenesis. Inhibition of NSCs dfferentation, as a consequence of ZIKV infection, resulted in cortical thinning and microcephaly in embryonic mouse brain [169]. Similar results were achieved by Cugola *et al.* [138], who demonstrated that ZIKV infects human cortical progenitor cells in organoids, leading to an increase in cell death, a reduction of proliferative zones and disruption of cortical layers.

Since 2D *in vitro* studies on hiPSCs and NSCs do not present organizational features typical of 3D structures, making more difficult to address the link between ZIKV and microcephaly, EBs, i.e. 3D aggregates of pluripotent stem cells, were exploited to investigate the effect of ZIKV infection during embryogenesis. Cells forming EBs exhibit heterogeneous patterns of differentiated cell types from the three germ lineages and are able to respond to similar cues that direct embryonic development [427]. Therefore, this 3D structure enables differentation and morphogenesis yielding micro-tissues similar to native tissue structures. Upon ZIKV infection of hiPSCs, the EB formation process was triggered. ZIKV infected EBs leading to a reduction in their volume and number.

Consequently, the surviving EBs were not able to fully attach to the substrate and died. In the literature, the negative effects of ZIKV on neurodevelopment have been also demonstrated on infected immature human organoids, when the emergence of the neuro-epithelial layer coincides with the transition from EBs to cerebral organoid structure. On these types of structure, a significant decreased size of the neuro-epithelium and overall organoid was observed [146]. In a model of forebrain organoids, ZIKV led to reduced organoid size and tickness, and enlarged lumen, resembling the dilated ventricles observed in microcephalic fetuses [145]. Other studies on 3D structures have been done on neurospheres, i.e., free-floating clusters of NSCs that present the very early characteristics of neurogenesis. ZIKV-infected neurospheres had morphological abnormalities, cell detachment, and apoptosis. These findings suggest that ZIKV abolishes neurogenesis during early human brain development [428].

Recently McGrath and colleagues [429] describes a cell-strain-dependent response of hNSCs to Asian ZIKV infection, suggesting that human fetal brain-derived-NSCs of different individuals vary in neuronal differentation potential following ZIKV infection. This could explain why a higher number of fetal microcephaly cases are reported than the number of Guillän Barrè syndrome cases, why only some fetuses or newborns of infected pregnant women developed neurological abnormalities and why NSCs had a higher susceptibility to ZIKV in the first trimester of the gestation [430] during the neural development.

In summary, this study demonstrated that ZIKV infects and replicates in NSCs, neurons and hiPSCs *in vitro*, leading to CPE and massive cell death and abrogating cell differentation and EBs formation, which can explain the CNS damage tipically observed in fetuses with ZIKV infection. Also, the virus induced an innate antiviral response characterized by the upregulation of *MDA5*, *IFIT1* and *IFIT2* genes. On the other hand, DENV infection had similar effect on NSCs, while WNV replication as well as the effects on neural cell viability and antiviral responses in NSCs, neurons, and hiPSCs were higher than ZIKV and DENV.

In conclusion, these findings highlight high similarities in ZIKV, WNV, and DENV mechanisms of infection of neural cells and induction of cell damage, thus suggesting a role for other virus-specific mechanisms of crossing the blood-placenta barrier by ZIKV. Thi study also validate this *in vitro* infection model, which will be used in future research to analyze and characterize particular molecular aspects of ZIKV and other flavivirus infection: for example, to explain the reasons of the upregulation of IFIT2 gene and to investigate other possible mechanisms of cell death induced by ZIKV infections, such as autophagy and pyroptosis [431,432].

In the second part of this study, this *in vitro* infection model was employed to investigate virus-host interactions in patient-specific hiPSCs-derived NSCs from patients with different clinical

presentation of WNV infection (asymptomatic infection or neuroinvasive disease) in order to highlight individual susceptibility to severe infectious disease.

Flaviviruses, such as the neurotropic WNV, cause severe clinical manifestations only in a small percentage of infected individuals; the reasons are probably numerous and have not completely elucidated, but host-dependent genetic factors might be important. Regarding WNV severe complications, candidate gene studies have associated WNV symptomatic infection with single nucleotide polymorphisms (SNPs) in the 2'-5' oligoadenylate synthetase (*OAS*) gene family [401,433] and in *IRF3* and *MX1* innate immune response and effector genes [434]. Moreover a 32-bp deletion within the monocyte and T lymphocyte chemokine receptor type 5 (CCR5) coding sequence was correlated with an increased susceptibility to WNV infection and death [401,402].

In this study, preliminary data demonstrated that NSCs derived from patients who experienced severe neuroinvasive disease were more susceptible to WNV infection and cell damage than cells derived from blood donors who experienced asymptomatic infection. These results support the hypothesis of individual genetic traits predisposing to neurological complications of WNV infection.

6. ACKNOWLEDGMENTS

I would like to thank Dr. Alessandro Sinigaglia, Dr. Giulia Masi, Dr. Alessandro Berto and Dr. Silvia Riccetti for the technical support, and Prof. Luisa Barzon, Dr. Marta Trevisan and Dr. Monia Pacenti for the supervision.

7. REFERENCES

1. Hubalek, Z., Rudolf, I., Nowotny, N. Arboviruses Pathogenic for Domestic and Wild Animals. *Advances in Virus Research* 2014; 89:201-75.

2. Go, Y.Y., Balasuriya, UBR., Lee, C. Zoonotic encephalitides caused by arboviruses: transmission and epidemiology of alphaviruses and flaviviruses. *Clin Exp Vaccine Res*. 2014. 3(1):58-77.

3. Hernandez, R., Brown, D.T., Paredes, A. Structural differences observed in arboviruses of the alphavirus and flavivirus genera. *Adv Virol*. 2014;2014:259382.

4. Lequime, S., Lambrechts L. Vertical transmission of arboviruses in mosquitoes: A historical perspective. *Infect. Genet. Evol.* 2014, http://dx.doi.org/10.1016/j.meegid.2014.07.025.

5. Huang, Y.J., Higgs, S., Horne, K.M., Vanlandingham, D.L.. Flavivirus-mosquito interactions. *Viruses*. 2014. 6(11):4703-30. doi: 10.3390/v6114703.

6. Holbrook, M.R.. Historical Perspectives on Flavivirus Research. 2017; 30;9(5). pii: E97. doi: 10.3390/v9050097.

7. Petterson, J.H., Fiz-Palacios, O..Dating the origin of the genus *Flavivirus* in the light of Beringian biogeography. *J. Gen. Virol*. 2014. 95, 1969-1982.

8. Cleaton, N., Koopmans, M., Reimerink, J., *et al*. Come fly with me: Review of clinically important arboviruses for global travellers. *Journal of Clinical Virology*. 2012. 55: 191-203.

9. Gould, E.A., Solomon, T. Pathogenic flaviviruses. *Lancet.* 2008. 371:500–9.

10. Ye, J., Zhu, B., Fu, Z.F., *et al*.. Immune evasion strategies of flavivureses. *Vaccine.* 2013. 461-471.

11. Villordo, S.M., Carballeda, J.M., Filomatori, C.V., Gamarnik, A.V.. RNA structure duplications and Flavivirus host adaptation. *Trends Microbiol*. 2016. 24(4): 270–283. doi:10.1016/j.tim.2016.01.002.

12. Beck, C., Jimenez-Clavero, M.A., Leblond, A., *et al*.. Flaviviruses in Europe: complex circulation patterns and their consequences for the diagnosis and control of West Nile disease. *Int. J. Environ. Res. Public Health* 2013, 10, 6049-6083.

13. Yan-Jang, S. Huang. et al.. Flavivirus-mosquito interactions. *Viruses*. 2014 Nov; 6(11): 4703–4730. doi: 10.3390/v6114703.

14. Sirohi, D., *et al*..The 3.8 Å resolution cryo-EM structure of Zika virus. *Science*. 2016. 352 (6284): 467–470.

15. Wang, A., Thurmond, S., Islas, L., Hui, K., Hai, R.. Zika virus genome biology and molecular pathogenesis. *Emerg. Microbes Infect.* 2017. 6(3): e13. doi: 10.1038/emi.2016.141

16. Faye, O., Freire, C., Iamarino, A., et al.. Molecular Evolution of Zika Virus during Its Emergence in the 20th Century. *PLoS Neglected Tropical Diseases*. 2014. 8 (1): e2636.

17. Pierson, T.C., Diamond, M.S.. Degrees of maturity: the complex structure and biology of flaviviruses. *Curr Opin Virol* 2012;2:168–75.

18. Blitvich, B.J., Firth, A.E. Insect-specific flaviviruses: a systematic review of their discovery, host range, mode of transmission, superinfection exclusion potential and genomic organization. *Viruses*. 2015; 7:1927–1959.

19. Yu, L., Nomaguchi, M., Padmanabhan, R., Markoff, L.. Specific requirements for elements of the 5' and 3' terminal regions in flavivirus RNA synthesis and viral replication. *Virology* 374 (1): 170–85.

20. Murray, C.L., Jones, C.T., Rice, C.M.. Architects of assembly: roles of Flaviviridae non- structural proteins in virion morphogenesis. *Nat. Rev. Microbiol*. 2008: 6: 699-708.

21. Mackenzie, J.S., Gubler, D.J.& Petersen L.R.. Emerging flaviviruses: the spread and resurgence of Japanese encephalitis, West Nile and dengue viruses. *Nat. Med*. 2004;10(12 Suppl):S98-109

22. Pierson, T.C., Diamond, M.S. Flaviviruses. In: Knipe DM, Howley PM, editors. Fields Virology. Philadelphia: Lippincott Williams & Wilkins, Wolters Kluwer; 2013. p. 747–94.

23. Martìn-Acebes, M.A, Vàzquez-Calvo, Á., Saiz, J.C.. Lipids and flaviviruses, present and future perspectives for the control of dengue, Zika, and West Nile viruses. Progress in Lipid Research. 2016. 64: 123-137. https://doi.org/10.1016/j.plipres.2016.09.005

24. Perera-Lecoin, M., Meertens, L., Carnec, X., Amara, A. Flavivirus entry receptors: an up- date. *Virus* 2013;6:69–88.\l

25. Amara, A., Mercer, J..Viral apoptotic mimicry. *Nat Rev Microbiol*. 2015. 13:461–9.

26. Cruz-Oliveira, C., Freire, J.M., Conceicao, T.M., Higa, L.M., Castanho, M.A., Da Poian, A.T.. Receptors and routes of dengue virus entry into the host cells. *FEMS Microbiol Rev*.2015. 39:155–70.\l

27. Zhu, Y.Z., Xu, Q.Q., Wu, D.G., Ren, H., Zhao, P., Lao, W.G., et al. Japanese encephalitis virus enters rat neuroblastoma cells via a pH-dependent, dynamin and caveola-mediated endocytosis pathway. *J Virol.* 2012.86:13407–22.\l

28. Kalia, M., Khasa, R., Sharma, M., Nain, M., Vrati, S.. Japanese encephalitis virus infects neuronal cells through a clathrin-independent endocytic mechanism. *J Virol*. 2013.87:148–62.\l

29. Van der Schaar, H.M., Rust, M.J., Chen, C., Van der Ende-Metselaar, H., Wilschut, J., Zhuang, X., et al. Dissecting the cell entry pathway of dengue virus by single-particle tracking in living cells. *PLoS Pathog.* 2008. 4, e1000244.\l

30. MacKenzie, J.M., Westaway, E.G. Assembly and maturation of the flavivirus Kunjin virus appear to occur in the rough endoplasmic reticulum and along the secretory pathway, respectively. *J Virol* .2001. 75:10787–10799. PubMed: 11602720

31. Li, L., Lok, S.M., Yu, I.M., Zhang, Y., Kuhn, R.J., Chen, J., Rossmann, M.G. The flavivirus precursor membrane- envelope protein complex: Structure and maturation. *Science*. 2008. 319:1830–1834. PubMed: 18369147

32. Mukhopadhyay, S., Kuhn, R.J., Rossmann, M.G.. A structural perspective of the flavivirus life cycle. *Nat Rev Microbiol*. 2005. 3:13–22. PubMed: 15608696

33. Tang, H.; Hammack, C.; Ogden, SC.; Wen, Z.; Qian, X.; Li, Y.; et al. Zika virus infects human cortical neural progenitors and attenuates their growth. *Cell Stem Cell* 2016;18:587–90.\l

34. O'Leary, DR.; Kuhn, S.; Kniss, KL.; Hinckley, AF.; Rasmussen, SA.; Pape, WJ., et al. Birth outcomes following West Nile Virus infection of pregnant women in the United States: 2003-2004. *Pediatrics* 2006;117:e537–45.

35. Chaturvedi, UC.; Mathur, A.; Chandra, A.; Das, SK.; Tandon, HO.; Singh, UK. Transplacental infection with Japanese encephalitis virus. *J Infect Dis* 1980;141:712–5.\J

36. Schuler-Faccini, L.; Ribeiro, EM.; Feitosa, IML.; Horovitz, DDG.; Cavalcanti, DP.; Pessoa, A.; et al. Possible association between Zika virus infection and microcephaly - Brazil, 2015. MMWR Morb Mortal Wkly Rep 2016; 5:59–62.\J

37. Oehler, E.; Watrin, L.; Larre, P.; Leparc-Goffart, I.; Lastere, S.; Valour, F.; et al. Zika virus infection complicated by Guillain-Barre syndrome–case report, French Polynesia, December 2013. *Euro Surveill* 2014:19.\J

38. Lazear, HM.; Diamond, MS. Zika virus: new clinical syndromes and its emergence in the Western Hemisphere. *J Virol* 2016;90:4864–75.\J

39. Verma, S.; Kumar, M.; Gurjav, U.;Lum, S.; Nerurkar, VR. Reversal of West Nile virus-induced blood– brain barrier disruption and tight junction proteins degradation by matrix metalloproteinases inhibitor. *Virology.* 2010; 397:130–138.

40. Samuel, MA.; Wang, H.; Siddharthan, V.; Morrey, JD.; Diamond, MS. Axonal transport mediates West Nile virus entry into the central nervous system and induces acute flaccid paralysis. *Proc Natl Acad Sci* USA. 2007; 104:17140–17145.

41. Suen, W.; Prow, N.; Hall, R.; Bielefeldt-Ohmann, H. Mechanism of West Nile virus neuroinvasion: a critical appraisal. *Viruses* 2014;6:2796–825.\J

42. Chan-Tack, KM.; Forrest, G. West Nile virus meningoencephalitis and acute flaccid paralysis after infliximab treatment. *J Rheumatol* 2006;33:191–2.

43. Misra, UK.; Kalita, J. Overview: Japanese encephalitis. *Prog Neurobiol* 2010;91:108–20

44. Carteaux, G.; Maquart, M.; Bedet, A.; Contou, D.; Brugières, P.; Fourati, S. et al. Zika virus associated with meningoencephalitis. *N Engl J Med* 2016;374:1595–6.

45. Schwartz, DA. Viral infection, proliferation, and hyperplasia of Hofbauer cells and absence of inflammation characterize the placental pathology of fetuses with congenital Zika virus infection. *Arch Gynecol Obstet* 2017: 295, 1361-1368.

46. Sheridan, MA.; Yunusov, D.; Balaraman, V.; Alexenko, AP; Yabe, S.; Verjovski- Almeida, S. et al. Vulnerability of primitive human placental trophoblast to Zika virus. *Proc Natl Acad Sci* U S A 2017;114:E1587–96.

47. Gromowski, GD.; Firestone, C-Y.; Whitehead, SS. Genetic determinants of Japanese encephalitis virus vaccine strain SA14-14-2 that govern attenuation of virulence in mice. *J Virol* 2015;89:6328–37.

48. Chambers, TJ.; Diamond, MS. Pathogenesis of flavivirus encephalitis. *Adv Virus Res* 2003;60:273–342.

49. Pokidysheva, E., Zhang, Y.; Battisti, AJ. et al. Cryo-EM reconstruction of dengue virus in complex with the carbohydrate recognition domain of DC-SIGN. Cell. 2006; 124: 485-493 \J

50. Lee, E.; Leang, SK.; Davidson, A. et al. Both E protein glycans adversely affect\J dengue virus infectivity but are beneficial for virion release. *J Virol* 2010; 84: 5171–5180. \J

51. Beasley, DWC.; Whiteman, MC.; Zhang, S. et al. Envelope protein glycosylation status influences mouse neuroinvasion phenotype of genetic lineage 1 West Nile virus strains. *J Virol* 2005; 79: 8339–8347.

52. Haddow, A. D., Schuh, A. J., Yasuda, C. Y., Kasper, M. R., Heang, V., Huy, R., et al.. Genetic characterization of Zika virus

strains: geographic expansion of the Asian lineage. *PLoS Negl. Trop. Dis.* 2012. 6:e1477. doi: 10.1371/journal.pntd. 0001477

53. Kuno, G., Chang, GJ. Full-length sequencing and genomic characterization of Bagaza, Kedougou, and Zika viruses. *Arch Virol*. 2007. 152:687– 696. http://dx.doi.org/10.1007/s00705-006-0903-z.

54. Berthet, N., Nakouné, E., Kamgang, B., Selekon, B., Descorps-Declère, S., Gessain, A., Manuguerra, J.C., Kazanji, M. Molecular characterization of three Zika flaviviruses obtained from sylvatic mosquitoes in the Central African Republic. *Vector Borne Zoonotic Dis.* 2014.14:862– 865. http: //dx.doi.org/10.1089/vbz.2014.1607.

55. Lanciotti, R.S., Kosoy, O.L., Laven, J.J., Velez, J.O., Lambert, A.J., Johnson, A.J., Stanfield, S.M., Duffy, M.R. Genetic and serologic properties of Zika virus associated with an epidemic, Yap State, Micronesia, 2007. *Emerg Infect Dis*. 2008. 14:1232–1239. http://dx.doi.org/10.3201/eid1408.080287.

56. Vandenbogaert, M., Cao-Lormeau, V-M., Diancourt, L., Thiberge, J-M., Sall, A., Kwasiborski, A., Musso, D., Després, P., Manuguerra, J-C., Caro, V.. Full-length genome sequencing and analysis of 3 ZIKV strains on an Ion Torrent PGM sequencer, abstr 22.133. 63rd Am Soc Trop Med Hyg (ASTMH) Meet, New Orleans, LA, 2 to 6 November 2014.

57. Lanciotti, R.S., Lambert, A.J., Holodniy, M., Saavedra, S., del Carmen Castillo Signor, L.. Phylogeny of Zika virus in Western Hemisphere, 2015. *Emerg Infect Dis* http://dx.doi.org/10.3201/eid2205 .160065.

58. Zanluca, Camila., Melo, Vanessa Campos Andrade de., Mosimann, Ana Luiza Pamplona., et al. First report of autochthonous transmission of Zika virus in Brazil. Memórias *do Instituto Oswaldo Cruz.* 2015. 110 (4): 569–572.

59. Li, Y., He, L., He, R. L., and Yau, S. S.Zika and Flaviviruses phylogeny based on the alignment-free natural vector method. *DNA Cell Biol.*2017 36, 109–116. doi: 10.1089/dna.2016.3532

60. Gong, Z., Gao, Y., and Han, G. Z. Zika virus: two or three lineages? *Trends Microbiol.*2016 24, 521–522. doi: 10.1016/j.tim.2016.05.002

61. Vorou, R.. Zika virus, vectors, reservoirs, amplifying hosts, and their potential to spread worldwide: what we know and what we should investigate urgently. *Int. J. Infect. Dis.* 2016. 48, 85–90. doi: 10.1016/j.ijid.2016.05.014

62. Diallo, D., Sall, A. A., Diagne, C. T., Faye, O., Faye, O., Ba, Y., et al.. Zika virus emergence in mosquitoes in southeastern Senegal, 2011. *PLoS ONE.* 2014. 9:e109442. doi: 10.1371/journal.pone.0109442

63. Faye, O., Faye, O., Diallo, D., Diallo, M., Weidmann, M., and Sall, A. A. Quantitative real-time PCR detection of Zika virus and evaluation with field- caught mosquitoes. *Virol. J.* 2013. 10:311. doi: 10.1186/1743-422x-10-311

64. Hayes, E.B. Zika virus outside Africa. *Emerg Infect Dis*. 2009.15:1347–50. http://dx.doi.org/10.3201/eid1509.090442

65. Grard, G., Caron, M., Mombo, I.M., Nkoghe, D., Mboui, Ondo S.,Jiolle, D., et al. Zika virus in Gabon (Central Africa)—2007: a new threat from *Aedes albopictus? PLoS Negl Trop Dis*. 2014. 8:e2681. http://dx.doi.org/10.1371/journal.pntd.0002681

66. McCrae, A.W.,Kirya, B.G..YellowfeverandZikavirusepizooticsand enzootics in Uganda. *Trans R Soc Trop Med Hyg*. 1982. 76:552–562. http://dx .doi.org/10.1016/0035-9203(82)90161-4.

67. Dick, G.W., Kitchen, S.F., Haddow, A.J..Zika virus. I. Isolations and serological specificity. *Trans R Soc Trop Med Hyg.* 1952. 46:509 –520.

68. Marchette, N.J., Garcia, R., Rudnick, A.. Isolation of Zika virus from *Aedes aegypti* mosquitoes in Malaysia. *Am J Trop Med Hyg* . 1969. 18:411– 415

69. Duffy, M. R., Chen, T. H., Hancock, W. T., Powers, A. M., Kool, J. L., Lanciotti, R. S., et al..Zika virus outbreak on yap island, federated states of micronesia. *N. Engl. J. Med*. 2009. 360, 2536–2543. doi: 10.1056/NEJMoa0805715

70. Ledermann, J. P., Guillaumot, L., Yug, L., Saweyog, S. C., Tided, M., Machieng, P., et al. *Aedes hensilli* as a potential vector of Chikungunya and Zika viruses. *PLoS Negl. Trop. Dis.* 2014. 8:e3188. doi: 10.1371/journal.pntd.00 03188

71. Richard, V., Paoaafaite, T., and Cao-Lormeau, V. M.. Vector competence of French polynesian *Aedes aegypti* and *Aedes polynesiensis* for Zika Virus. *PLoS Negl. Trop. Dis. 2016.* 10:e0005024. doi: 10.1371/journal.pntd.0005024

72. Gardner, L.M., Chen, N., Sarkar, S..Global risk of Zika virus depends critically on vector status of *Aedes albopictus*. *Lancet Infect*. 2016 16: 00176-6.

73. Ferreira-de-Brito, A., Ribeiro, I. P., Miranda, R. M., Fernandes, R. S., Campos, S. S., Silva, K. A., et al. First detection of natural infection of *Aedes aegypti* with Zika virus in Brazil and throughout South America. *Mem. Inst. Oswaldo Cruz*. 2016. 111, 655–658. doi: 10.1590/0074-02760160332

74. Chan, Jasper F.W., Choi, Garnet K.Y., Yip, Cyril C.Y., et al.. Zika fever and congenital Zika syndrome: An unexpected emerging arboviral disease. *Journal of Infection*. 2016. 72 (5): 507.

75. Hills, SL., Russell, K, Hennessey, M, et al.. Transmission of Zika Virus Through Sexual Contact with Travelers to Areas of Ongoing Transmission — Continental United States, 2016. *MMWR. Morbidity and Mortality Weekly Report,* 2016. 65 (8).

76. Moreira, J., Peixoto, T. M., Siqueira, A. M., and Lamas, C. C..Sexually acquired Zika virus: a systematic review. *Clin. Microbiol. Infect.* 2017. 23, 296–305. doi: 10.1016/j.cmi.2016.12.027

77. Musso, D., Roche, C., Robin, E., Nhan, T., Teissier, A., and Cao-Lormeau, V. M..Potential sexual transmission of Zika virus. *Emerg. Infect. Dis.*2015. 21, 359–361. doi: 10.3201/eid2102.141363

78. Matheron, S., d'Ortenzio, E., Leparc-Goffart, I., Hubert, B., de Lamballerie, X., and Yazdanpanah, Y.. Long-lasting persistence of Zika virus in semen. *Clin. Infect. Dis.* 2016 63:1264. doi: 10.1093/cid/ciw509

79. Barzon, L., Pacenti, M., Franchin, E., Lavezzo, E., Trevisan, M., Sgarabotto, D., Palù, G. Infection dynamics in a traveller with persistent shedding of Zika virus RNA in semen for six months after returning from Haiti to Italy, January 2016.*Euro Surveill*. 2016. 21(32). doi: 10.2807/1560-7917.ES.2016.21.32.30316

80. Nicastri E, Castilletti C, Liuzzi G et al. Persistent detection of Zika virus RNA in semen for six months after symptom onset in a traveller returning from Haiti to Italy, February 2016. *Euro Surveill* 2016; 21: 30314.

81. Prisant, N., Bujan, L., Benichou, H., Hayot, P. H., Pavili, L., Lurel, S., et al.. Zika virus in the female genital tract. *Lancet Infect. Dis.* 2016. 16, 1000–1001. doi: 10.1016/s1473-3099(16)30193-1

82. Prisant, N., Breurec, S., Moriniere, C., Bujan, L., and Joguet, G. Zika virus genital tract shedding in infected women of childbearing age. *Clin. Infect. Dis.* 2017. 64, 107–109. doi: 10.1093/cid/ciw669

83. Murray, K. O., Gorchakov, R., Carlson, A. R., Berry, R., Lai, L., Natrajan, M., et al. Prolonged detection of Zika virus in vaginal secretions and whole blood. *Emerg. Infect. Dis.*2017. 23, 99–101. doi: 10.3201/eid2301.161394

84. Gourinat, A.C., O'Connor, O., Calvez, E., Goarant, C., Dupont-Rouzeyrol, M. Detection of Zika virus in urine. *Emerg Infect Dis*. 2015. 21:84 – 86. http://dx.doi.org/10.3201/eid2101.140894.

85. Musso, D., Roche, C., Nhan, T.X., Robin, E., Teissier, A., Cao-Lormeau, V.M.. Detection of Zika virus in saliva. *J Clin Virol.* 2015. 68:53–55. http://dx .doi.org/10.1016/j.jcv.2015.04.021.

86. Barzon, L., Pacenti, M., Berto, A., Sinigaglia, A., Franchin, E., Lavezzo, E., Brugnaro, P., Palù, G.. Isolation of infectious Zika virus from saliva and prolonged viral RNA shedding in a traveller returning from the Dominican Republic to Italy, January 2016. *Euro Surveill*. 2016;21(10):30159. doi: 10.2807/1560-7917.ES.2016.21.10.30159

87. Bonaldo, M.C., et al.. Isolation of Infective Zika Virus from Urine and Saliva of Patients in Brazil. *PLoS Negl Trop Dis.* 2016. 10(6):e0004816. doi: 10.1371/journal.pntd.0004816. eCollection 2016 Jun.

88. Brasil, P., Pereira, J.P., Raja Gabaglia, C., et al.Zika Virus Infection in Pregnant Women in Rio de Janeiro – Preliminary Report. *New England Journal of Medicine* 2016

89. Mlakar, J., Korva, M., Tul, N., Popovic , M., Poljsak-Prijatelj, M., Mraz, J., Kolenc, M., Resman Rus, K., Vesnaver Vipotnik, T., Fabjan Vodusek, V., et al. Zika virus associated with microcephaly. N. Engl. J. Med. 2016. 374, 951–958.

90. Naing, Z.W., Scott, G.M., Shand, A., Hamilton, S.T., van Zuylen, W.J., Basha, J., Hall, B., Craig, M.E., Rawlinson, W.D..Congenital cytomegalovirus infection in pregnancy: a review of prevalence, clinical features, diagnosis and prevention. *Aust N Z J Obstet Gynaecol* . 2016. 56:9 –18. http://dx.doi.org /10.1111/ajo.12408.

91. Banatvala, J.E., Brown, D.W..Rubella. *Lancet.* 2004. 363:1127–1137. http: //dx.doi.org/10.1016/S0140-6736(04)15897-2.

92. Basurko, C., Carles, G., Youssef, M., Guindi, W.E..Maternal and foetal consequences of dengue fever during pregnancy. *Eur J Obstet Gynecol Reprod Biol*. 2009. 147:29 –32. http://dx.doi.org/10.1016/j.ejogrb.2009.06.028

93. Tan, P.C., Rajasingam, G., Devi, S., Omar, S.Z..Dengue infection in pregnancy: prevalence, vertical transmission, and pregnancy outcome. *Obstet Gynecol*. 2008. 111:1111–1117. http://dx.doi.org/10.1097/AOG.0b013e31816a49fc.

94. Stewart, R.D., Bryant, S.N., Sheffield, J.S..West Nile virus infection in pregnancy. *Case Rep Infect Dis* . 2013. 2013:351872

95. Paisley, J.E., Hinckley, A.F., O'Leary, D.R., Kramer, W.C., Lanciotti, R.S., Campbell, G.L., Hayes, E.B.. West Nile virus infection among pregnant women in a northern Colorado community, 2003 to 2004. *Pediatrics*. 2006. 117:814 – 820. http://dx.doi.org/10.1542/peds.2005-1187.

96. Besnard, M., Lastere, S., Teissier, A. et al.Evidence of perinatal transmission of Zika virus, French Polynesia, December 2013 and February 2014. *Euro Surveill.* 2014. 19 (13): 20751

97. Dupont-Rouzeyrol, M., Biron, A., O'Connor, O., Huguon, E., and Descloux, E. Infectious Zika viral particles in breastmilk. *Lancet.* 2016. 387, 1051. doi: 10.1016/s0140-6736(16)00624-3

98. Centers for Disease Control and Prevention. Possible West Nile virus transmission to an infant through breast-feeding—Michigan, 2002. *MMWR Morb Mortal Wkly Rep.* 2002. 51:877– 878.

99. Barthel, A., Gourinat, A.C., Cazorla, C., Joubert, C., Dupont-Rouzeyrol, M., Descloux, E. Breast milk as a possible route of vertical transmission of dengue virus? *Clin Infect Dis*. 2013. 57:415– 417. http://dx.doi.org/10.1093 /cid/cit227.

100. Franchini, M.; Velati, C. Blood safety and zoonotic emerging pathogens: now it's the turn of Zika virus!. *Blood Transfusion.*

2016. (14): 93–94.

101. Guillaume, Theiry. Zika virus-associated Guillain–Barré syndrome: a warning for critical care physicians. *Intensive Care Medicine*. 2016. 1–2.

102. Barjas-Castro, M.L., Angerami, R., Cunha, M., *et al*.Probable transfusion-transmitted Zika virus in Brazil. *Transfusion.* 2016

103. Vasquez, Amber M., Sapiano, Mathew R.P.. Basavaraju, Sridhar V.. et al. Survey of Blood Collection Centers and Implementation of Guidance for Prevention of Transfusion-Transmitted Zika Virus Infection — Puerto Rico, 2016. *MMWR. Morbidity and Mortality Weekly Report.* 2016. 65 (14): 375–378.

104. MacNamara, F.N. Zika virus: A report on three cases of human infection during an epidemic of jaundice in Nigeria. *Transactions of the Royal Society of Tropical Medicine and Hygiene.* 1954. 48 (2): 139–145.

105. Simpson, D.I.H. Zika virus infection in man. *Transactions of the Royal Society of Tropical Medicine and Hygiene.* 1964. 58 (4): 339–348.

106. Olson, J. G., Ksiazek, T. G. Zika virus, a cause of fever in Central Java, Indonesia. *Transactions of the Royal Society of Tropical Medicine and Hygiene.* 1981. 75(3): 389–393.

107. Baden, Lindsey R., Petersen, Lyle R., Jamieson, Denise J., Powers, Ann M., Honein, Margaret A. Zika Virus. *New England Journal of Medicine*. 2016. 374 (16): 1552–1563.

108. Musso, D.,Nilles, E.J., Cao-Lormeau, V.-M.Rapid spread of emerging Zika virus in the Pacific area. *Clinical Microbiology and Infection.* 2014. 20 (10): 595–6.

109. Roth, A., Mercier, A., Lepers, C., Hoy, D., Duituturaga, S., Benyon, E., Guillaumot, L., Souarès, Y. Concurrent outbreaks of dengue, chikungunya and Zika virus infections – an unprecedented epidemic wave of mosquito-borne viruses in the Pacific 2012 -2014. *Eurosurveillance.* 2014. 19 (41): 20929

110. Besnard, M., Eyrolle-Guignot, D., Guillemette-Artur, P., *et al.*. Congenital cerebral malformations and dysfunction in fetuses and newborns following the 2013 to 2014 Zika virus epidemic in French Polynesia. *Euro Surveill.* 2016. 21(13).

111. Gatherer, D., Kohl, A. Zika virus: a previously slow pandemic spreads rapidly through the Americas. *Journal of General Virology.* 2015. 97(2): 269–273.

112. Calvet, G.A., Filippis, A.M., Mendonca, M.C., *et al*. First detection of autochthonous Zika virus transmission in a HIV-infected patient in Rio de Janeiro, Brazil. *J Clin Virol.* 2015. 74: 1-3

113. Zammarchi, L, Stella, G., Mantella, A., et al. Zika virus infections imported to Italy: Clinical, immunological and virological findings, and public health implications. *Journal of Clinical Virology.* 2015 63: 32–35.

114. Sarmiento-Ospina, A., Vásquez-Serna, H., Jimenez-Canizales, C.E., *et al*. Zika virus associated deaths in Colombia. *Lancet Infect Dis.* 2016. 16: 30006-8

115. Enfissi, A., Codrington, J., Roosblad, J., *et al*. Zika virus genome from the Americas. *Lancet.* 2016. 387: 227-8

116. Venturi, G., Zammarchi, L., Fortuna, C., *et al.* An autochthonous case of Zika due to possible sexual transmission, Florence, Italy, 2014. *Euro Surveill.* 2016. 21 (8).

117. Sikka, V., Chattu, V.K., Popli, R.K., et al.The emergence of zika virus as a global health security threat: A review and a consensus statement of the INDUSEM Joint Working Group (JWG). *Journal of Global Infectious Diseases*. 2016. 8 (1): 3–15.

118. Rosen, Meghan. Rapid spread of Zika virus in the Americas raises alarm. *Science News* (Society for Science and the Public). 2016. 189 (4): 16.

119. Heang, Vireak., Yasuda, Chadwick Y., Sovann, Ly., et al. Zika Virus Infection, Cambodia, 2010. *Emerging Infectious Diseases*. 2012. 18 (2): 349–351

120. Ahmad, S. S., Amin, T. N., and Ustianowski, A. Zika virus: management of infection and risk. *BMJ*. 2016. 352:i1062. doi: 10.1136/bmj.i1062

121. Aubry, M., Teissier, A., Huart, M., Merceron, S., Vanhomwegen, J., Roche, C., et al. Zika virus seroprevalence, French Polynesia, 2014-2015. *Emerg. Infect. Dis.* 2017. 23, 669–672. doi: 10.3201/eid2304.161549

122. Chen, Lin H., Hamer, Davidson H.Zika Virus: Rapid Spread in the Western Hemisphere. *Annals of Internal Medicine*.2016

123. Paploski, I. A., Prates, A. P., Cardoso, C. W., Kikuti, M., Silva, M. M., Waller, L. A., et al. Time lags between exanthematous illness attributed to Zika virus, Guillain-Barre syndrome, and microcephaly, Salvador, Brazil. *Emerg. Infect. Dis.* 2016. 22, 1438–1444. doi: 10.3201/eid2208.160496

124. Leis, A. A., and Stokic, D. S. Neuromuscular manifestations of west nile virus infection. *Front. Neurol.* 2012. 3:37. doi: 10.3389/fneur.2012.00037

125. Verma, R., Sahu, R., and Holla, V..Neurological manifestations of dengue infection: a review. *J. Neurol. Sci.* 2014. 346, 26–34. doi: 10.1016/j.jns.2014. 08.044

126. Ravi, V., Taly, A. B., Shankar, S. K., Shenoy, P. K., Desai, A., Nagaraja, D., et al. Association of Japanese encephalitis virus infection with Guillain-Barre syndrome in endemic areas of south India. *Acta Neurol. Scand.* 1994. 90, 67–72. doi: 10.1111/j.1600-0404.1994.tb02681.x

127. Cao-Lormeau, V.M., Blake, A., Mons, S. *et al.*Guillain-Barré syndrome outbreak associated with Zika virus infection in French Polynesia: a case-control study. *Lancet*. 2016. pii: S0140-6736(16): 00562-6.

128. Mécharles, S., Herrmann, C., Poullain, P., et al. Acute myelitis due to Zika virus infection. *Lancet*. 2016. pii: S0140-6736(16): 00644-9.

129. Cauchemez, S., Besnard, M., Bompard, P., et al. Association between Zika virus and microcephaly in French Polynesia, 2013-15: a retrospective study. *Lancet.*2016. pii: S0140-6736(16): 00651-6.

130. Driggers, R.W., Ho, C.Y., Korhonen, E.M., et al. Zika virus infection with prolonged maternal viremia and fetal brain abnormalities. *N Engl J Med*. 2016.

131. Oliveira, Melo AS, Malinger, G., Ximenes, R., et al. Zika virus intrauterine infection causes fetal brain abnormality and microcephaly: tip of the iceberg? *Ultrasound Obstet Gynecol.* 2016 47: 6-7.

132. de Paula Freitas, B., de Oliveira, Dias J., Prazeres, J., et al. Ocular findings in infants with microcephaly associated with presumed zika virus congenital infection in salvador, brazil. *JAMA Ophthalmology*. 2016

133. Sarno, Manoel., et al.Zika Virus Infection and Stillbirths: A Case of Hydrops Fetalis, Hydranencephaly and Fetal Demise.

PLOS Negl Trop Dis. 2016. 10 (2): e0004517.

134. Dick, G. W. Zika virus. II. Pathogenicity and physical properties. *Trans. R. Soc. Trop. Med. Hyg.* 1952. 46, 521–534. doi: 10.1016/0035-9203(52)90043-6

135. Bell, T. M., Field, E. J., and Narang, H. K.. Zika virus infection of the central nervous system of mice. *Arch. Gesamte Virusforsch.* 1971. 35, 183–193. doi: 10.1007/BF01249709

136. Souza, B. S., Sampaio, G. L., Pereira, C. S., Campos, G. S., Sardi, S. I., Freitas, L. A., et al.. Zika virus infection induces mitosis abnormalities and apoptotic cell death of human neural progenitor cells. *Sci. Rep.* 2016. 6:39775. doi: 10.1038/srep39775

137. Garcez, P. P., Loiola, E. C., Madeiro da Costa, R., Higa, L. M., Trindade, P., Delvecchio, R., et al.. Zika virus impairs growth in human neurospheres and brain organoids. *Science.* 2016. 352, 816–818. doi: 10.1126/science.aaf6116

138. Cugola, F. R., Fernandes, I. R., Russo, F. B., Freitas, B. C., Dias, J. L., Guimaraes, K. P., et al. The Brazilian Zika virus strain causes birth defects in experimental models. *Nature.* 2016. 534, 267–271. doi: 10.1038/nature18296

139. Retallack, H., Di Lullo, E., Arias, C., Knopp, K. A., Laurie, M. T., Sandoval- Espinosa, C., et al.. Zika virus cell tropism in the developing human brain and inhibition by azithromycin. *Proc. Natl. Acad. Sci. U.S.A.* 2016. 113, 14408–14413. doi: 10.1073/pnas.1618029113

140. Onorati, M., Li, Z., Liu, F., Sousa, A. M., Nakagawa, N., Li, M., et al. Zika virus disrupts phospho-TBK1 localization and mitosis in human neuroepithelial stem cells and radial glia. *Cell Rep.* 2016. 16, 2576–2592. doi: 10.1016/ j.celrep.2016.08.038

141. Liang, Q., Luo, Z., Zeng, J., Chen, W., Foo, S. S., Lee, S. A., et al. Zika Virus NS4A and NS4B proteins deregulate Akt-mTOR signaling in human fetal neural stem cells to inhibit neurogenesis and induce autophagy. *Cell Stem Cell.* 2016. 19, 663–671. doi: 10.1016/j.stem.2016.07.019

142. Hanners, N. W., Eitson, J. L., Usui, N., Richardson, R. B., Wexler, E. M., Konopka, G., et al.. Western Zika virus in human fetal neural progenitors persists long term with partial cytopathic and limited immunogenic e ects. *Cell Rep.* 2016. 15, 2315–2322. doi: 10.1016/j.celrep.2016.05.075

143. Gabriel, E., Ramani, A., Karow, U., Gottardo, M., Natarajan, K., Gooi, L. M., et al.. Recent Zika Virus isolates induce premature di erentiation of neural progenitors in human brain organoids. *Cell Stem Cell.* 2017. 20, 397–406.e5. doi: 10.1016/j.stem.2016.12.005

144. Wells, M. F., Salick, M. R., Wiskow, O., Ho, D. J., Worringer, K. A., Ihry, R. J., et al. Genetic ablation of AXL does not protect human neural progenitor cells and cerebral organoids from Zika virus infection. *Cell Stem Cell.* 2016. 19, 703–708. doi: 10.1016/j.stem.2016.11.011

145. Qian, X., Nguyen, H. N., Song, M. M., Hadiono, C., Ogden, S. C., Hammack, C., et al. Brain-region-specific organoids using mini-bioreactors for modeling ZIKV exposure. *Cell.* 2016. 165, 1238–1254. doi: 10.1016/j.cell.2016.04.032

146. Dang, J., Tiwari, S. K., Lichinchi, G., Qin, Y., Patil, V. S., Eroshkin, A. M., et al. Zika virus depletes neural progenitors in human cerebral organoids through activation of the innate immune receptor TLR3. *Cell Stem Cell*. 2016. 19, 258–265. doi: 10.1016/j.stem.2016.04.014

147. Kadoshima, T., Sakaguchi, H., Nakano, T., Soen, M., Ando, S., Eiraku, M., and Sasai, Y.. Self-organization of axial polarity, inside-out layer pattern, and species-specific progenitor dynamics in human ES cell-derived neocortex. *Proc. Natl. Acad. Sci.*

USA. 2013 110, 20284–20289.

148. Lancaster, M.A., Renner, M., Martin, C.A., Wenzel, D., Bicknell, L.S., Hurles, M.E., Homfray, T., Penninger, J.M., Jackson, A.P., and Knoblich, J.A.. Cerebral organoids model human brain development and microcephaly. *Nature.* 2013. 501, 373–379.

149. Mariani, J., Coppola, G., Zhang, P., Abyzov, A., Provini, L., Tomasini, L., Amen- duni, M., Szekely, A., Palejev, D., Wilson, M., et al.. FOXG1-dependent dysregulation of GABA/glutamate neuron differentiation in autism spectrum disorders. *Cell.* 2015. 162, 375–390.

150. Pasca, A.M., Sloan, S.A., Clarke, L.E., Tian, Y., Makinson, C.D., Huber, N., Kim, C.H., Park, J.Y., O'Rourke, N.A., Nguyen, K.D., et al. Functional cortical neurons and astrocytes from human pluripotent stem cells in 3D culture. *Nat. Methods.* 2015. 12, 671–678.

151. Rasmussen, S.A., Jamieson, D.J., Honein, M.A., and Petersen, L.R.. Zika virus and birth defects—reviewing the evidence for causality. *N. Engl. J. Med*. 2016. *374*, 1981–1987.

152. Zhang, F., Hammack, C., Ogden, S.C., Cheng, Y., Lee, E.M., Wen, Z., Qian, X., Nguyen, H.N., Li, Y., Yao, B., et al.. Molecular signatures associated with ZIKV exposure in human cortical neural progenitors. *Nucleic Acids Res*. 2016a 44, 8610–8620.

153. Barrows, N.J., Campos, R.K., Powell, S.T., Prasanth, K.R., Schott-Lerner, G., Soto-Acosta, R., Galarza-Mun˜ oz, G., McGrath, E.L., Urrabaz-Garza, R., Gao, J., et al.. A screen of FDA-approved drugs for inhibitors of Zika virus infection. *Cell Host Microbe*. 2016. *20*, 259–270

154. Xu, M., Lee, E.M., Wen, Z., Cheng, Y., Huang, W.K., Qian, X., Tcw, J., Kouznet- sova, J., Ogden, S.C., Hammack, C., et al.. Identification of small-molecule inhibitors of Zika virus infection and induced neural cell death via a drug repurposing screen. *Nat. Med*. 2016.*22*, 1101–1107.

155. Hamel, R., Ferraris, P., Wichit, S., Diop, F., Talignani, L., Pompon, J., et al.. African and Asian Zika virus strains di erentially induce early antiviral responses in primary human astrocytes. *Infect. Genet. Evol*. 2017. 49, 134–137. doi: 10.1016/j.meegid.2017.01.015

156. Hamel, R., Dejarnac, O., Wichit, S., Ekchariyawat, P., Neyret, A., Luplertlop, N., et al. Biology of Zika virus infection in human skin cells. *J. Virol*. 2015. 89, 8880–8896. doi: 10.1128/jvi.00354-15

157. Nowakowski, T.J., Pollen, A.A., Di Lullo, E., Sandoval-Espinosa, C., Bershteyn, M., and Kriegstein, A.R.. Expression analysis highlights AXL as a candi- date Zika virus entry receptor in neural stem cells. *Cell Stem Cell*. 2016. 18, 591–596.

158. Meertens, L., Labeau, A., Dejarnac, O., Cipriani, S., Sinigaglia, L., Bonnet- Madin, L., et al. Axl mediates ZIKA virus entry in human glial cells and modulates innate immune responses. *Cell Rep.* 2017. 18, 324–333. doi: 10.1016/j. celrep.2016.12.045

159. Liu, S., DeLalio, L. J., Isakson, B. E., and Wang, T. T.. AXL-mediated productive infection of human endothelial cells by Zika virus. *Circ. Res*. 2016. 119, 1183–1189. doi: 10.1161/circresaha.116.309866

160. Tabata, T., Petitt, M., Puerta-Guardo, H., Michlmayr, D., Wang, C., Fang-Hoo- ver, J., Harris, E., and Pereira, L.. Zika virus targets different primary human placental cells, suggesting two routes for vertical transmission. *Cell Host Microbe*. 2016. 20, 155–166.

161. Meertens, L., Carnec, X., Lecoin, M.P., Ramdasi, R., Guivel-Benhassine, F., Lew, E., Lemke, G., Schwartz, O., and Amara, A.. The TIM and TAM Families of Phosphatidylserine Receptors Mediate Dengue Virus Entry. *Cell Host Microbe.* 2012. 12, 544–557.

162. Bhattacharyya, S., Zago´ rska, A., Lew, E.D., Shres- tha, B., Rothlin, C.V., Naughton, J., Diamond, M.S., Lemke, G., and Young, J.A. Enveloped Viruses Disable Innate Immune Responses in Dendritic Cells by Direct Activation of TAM Receptors. *Cell Host Microbe.* 2013. 14, 136–147.

163. Miner, J.J., Daniels, B.P., Shrestha, B., Proenca- Modena, J.L., Lew, E.D., Lazear, H.M., Gorman, M.J., Lemke, G., Klein, R.S., and Diamond, M.S. The TAM receptor Mertk protects against neuroinvasive viral infection by maintaining blood-brain barrier integrity. *Nat. Med*.2015. 21, 1464–1472.

164. Lum, F. M., Low, D. K., Fan, Y., Tan, J. J., Lee, B., Chan, J. K., et al.. Zika virus infects human fetal brain microglia and induces inflammation. *Clin. Infect. Dis*. 2017. 64, 914–920. doi: 10.1093/cid/ciw878

165. Frumence, E., Roche, M., Krejbich-Trotot, P., El-Kalamouni, C., Nativel, B., Rondeau, P., et al.. The south pacific epidemic strain of Zika virus replicates e ciently in human epithelial A549 cells leading to IFN-beta production and apoptosis induction. *Virology.* 2016. 493, 217–226. doi: 10.1016/j.virol. 2016.03.006

166. Tiwari, S. K., Dang, J., Qin, Y., Lichinchi, G., Bansal, V., and Rana, T. M.. Zika virus infection reprograms global transcription of host cells to allow sustained infection. *Emerg. Microbes Infect.*2017. 6, e24. doi: 10.1038/emi.2017.9

167. Yockey, L.J., Varela, L., Rakib, T., Khoury-Hanold, W., Fink, S.L., Stutz, B., Szi- geti-Buck, K., Van den Pol, A., Lindenbach, B.D., Horvath, T.L., and Iwasaki, A.Vaginal exposure to Zika virus during pregnancy leads to fetal brain infection. *Cell*. 2016. 166, 1247–1256.e4.

168. Wu, K.Y., Zuo, G.L., Li, X.F., Ye, Q., Deng, Y.Q., Huang, X.Y., Cao, W.C., Qin, C.F., and Luo, Z.G.. Vertical transmission of Zika virus targeting the radial glial cells affects cortex development of offspring mice. *Cell Res*.2016. *26*, 645–654.

169. Li, C., Xu, D., Ye, Q., Hong, S., Jiang, Y., Liu, X., Zhang, N., Shi, L., Qin, C.F., and Xu, Z.. Zika virus disrupts neural progenitor development and leads to microcephaly in mice. *Cell Stem Cell*. 2016 a.19, 120–126.

170. Ghouzzi, V.E., Bianchi, F.T., Molineris, I., Mounce, B.C., Berto, G.E., Rak, M., Lebon, S., Aubry, L., Tocco, C., Gai, M., et al. ZIKA virus elicits P53 acti- vation and genotoxic stress in human neural progenitors similar to mutations involved in severe forms of genetic microcephaly and p53. *Cell Death Dis*. 2016. *7*, e2440

171. Grant, A., Ponia, S.S., Tripathi, S., Balasubramaniam, V., Miorin, L., Souris- seau, M., Schwarz, M.C., Sa´ nchez-Seco, M.P., Evans, M.J., Best, S.M., and Garcı´a-Sastre, A. Zika virus targets human STAT2 to inhibit type I inter- feron signaling. *Cell Host Microbe*. 2016. 19, 882–890.

172. Aliota, M. T., Caine, E. A., Walker, E. C., Larkin, K. E., Camacho, E., and Osorio, J. E.. Characterization of lethal zika virus infection in AG129 Mice. *PLoS Negl. Trop. Dis.* 2016. 10:e0004682. doi: 10.1371/journal.pntd. 0004682

173. Zmurko, J., Marques, R. E., Schols, D., Verbeken, E., Kaptein, S. J., and Neyts, J. The viral polymerase inhibitor 7-Deaza-2'-C-methyladenosine is a potent inhibitor of in vitro Zika virus replication and delays disease progression in a robust mouse infection model. *PLoS Negl. Trop. Dis.* 2016. 10:e0004695. doi: 10.1371/journal.pntd.0004695

174. Julander, J. G., Siddharthan, V., Evans, J., Taylor, R., Tolbert, K., Apuli, C., et al. Efficacy of the broad-spectrum antiviral compound BCX4430 against Zika virus in cell culture and in a mouse model. *Antiviral Res.* 2017.137, 14–22. doi: 10.1016/j.antiviral.2016.11.003

175. Rossi, S. L., Tesh, R. B., Azar, S. R., Muruato, A. E., Hanley, K. A., Auguste, A. J., et al.. Characterization of a novel murine model to study Zika virus. *Am. J. Trop. Med. Hyg.* 2016. 94, 1362–1369. doi: 10.4269/ajtmh.16-0111

176. Lazear, H. M., Govero, J., Smith, A. M., Platt, D. J., Fernandez, E., Miner, J. J., et al.. A mouse model of Zika virus pathogenesis. *Cell Host Microbe*. 2016. 19, 720–730. doi: 10.1016/j.chom.2016.03.010

177. Li, H., Saucedo-Cuevas, L., Regla-Nava, J. A., Chai, G., Sheets, N., Tang, W., et al.. Zika virus infects neural progenitors in the adult mouse brain and alters proliferation. *Cell Stem Cell.* 2016. 19, 593–598. doi: 10.1016/j.stem.2016. 08.005

178. Dowall, S. D., Graham, V. A., Rayner, E., Atkinson, B., Hall, G., Watson, R. J., et al. A susceptible mouse model for Zika virus infection. *PLoS Negl. Trop. Dis.* 2016. 10:e0004658. doi: 10.1371/journal.pntd.0004658

179. Fernandes, N. C., Nogueira, J. S., Ressio, R. A., Cirqueira, C. S., Kimura, L. M., Fernandes, K. R., et al.. Experimental Zika virus infection induces spinal cord injury and encephalitis in newborn Swiss mice. *Exp. Toxicol. Pathol.* 2017. 69, 63–71. doi: 10.1016/j.etp.2016.11.004

180. Huang, W. C., Abraham, R., Shim, B. S., Choe, H., and Page, D. T. Zika virus infection during the period of maximal brain growth causes microcephaly and corticospinal neuron apoptosis in wild type mice. *Sci. Rep*. 2016.6:34793. doi: 10.1038/srep34793

181. Shao, Q., Herrlinger, S., Yang, S. L., Lai, F., Moore, J. M., Brindley, M. A., et al.. Zika virus infection disrupts neurovascular development and results in postnatal microcephaly with brain damage. *Development*. 2016. 143, 4127–4136. doi: 10.1242/dev.143768

182. Miner, J. J., Cao, B., Govero, J., Smith, A. M., Fernandez, E., Cabrera, O. H., et al.. Zika virus infection during pregnancy in mice causes placental damage and fetal demise. *Cell.* 2016. 165, 1081–1091. doi: 10.1016/j.cell.2016.05.008

183. Ma, W., Li, S., Ma, S., Jia, L., Zhang, F., Zhang, Y., et al.. Zika virus causes testis damage and leads to male infertility in mice. *Cell.* 2016. 167, 1511.e10–1524.e10. doi: 10.1016/j.cell.2016.11.016

184. Beasley, DW.. Recent advances in the molecular biology of west nile virus. *Curr Mol Med*. 2005. 5:835-850.

185. Bondre VP., Jadi Rs., Mishra C., et al.. West Nile virus isolates from India: evidence for a distinct genetic lineage. *J Gen Virol* 2007; 88:875-884.\l

186. Donadieu E., Bahuon C., Lowenski S., et al. Differential virulence and pathogenesis of West Nile viruses. *Viruses*. 2013, 5(11): 2856-2880

187. May FJ., Davis CT., Tesh RB., et al.. Phylogeography of West Nile virus: from the cradle of evolution in Africa to Eurasia, Australia, and the Americas. *J Virol*,2011. 85:2964-2974.

188. Papa A., Bakonyi T., Xanthopoulou K., et al.. Genetic characterization of West Nile virus lineage 2, Greece, 2010. *Emerg Infect Dis*. 2011.1:920-2.

189. Di Sabatino D., Bruno R., Sauro R., et al. Epidemiology of West Nile Disease in Europe and in the Mediterranean Basin from 2009 to 2013. *BioMed Research International* .2014. Vol. 2014, Article ID 907852, 10 pages.

190. Marka A., Diamantidis A., Papa A., et al.. West Nile virus state of the art report of MALWEST project. *Int J Environ Res Health*. 2013. 10, 6534-6610.

191. Vazquez A., Sanchez-Seco MP., Ruiz S., et al. *Putative new Lineage of West Nile virus, Spain. Emerg Infect Dis.* 2010. 16, 549-552.

192. Lanciotti RS., Roehrig JT., Deubel V., et al. Origin of the West Nile virus responsible for an outbreak of encephalitis in the northeastern United States. *Science.* 1999. 286, 233-2337

193. Lanciotti RS., Ebel GD., Deubel V., et al.. Complete genome sequences and phylogenetic analysis of West Nile virus strains isolated from the United States, Europe, and the Middle East. *Virology*. 2002.298: 96-105.

194. Bakonyi T., Ivanics E., Erdelyi K., et al. Lineage 1 and 2 strains of encephalic West Nile virus, central Europe. *Emerg Infect Dis*.2006. 12:618-623.

195. Bakonyi T., Hubalek Z., Rudolf I., et al. Novel flavivirus or new lineage of West Nile virus, central Europe. *Emerg Infect Dis.* 2005. 11:225-31.

196. Bagnarelli P., Marinelli K., Trotta D., et al. Human case of autochthonous West Nile virus lineage 2 infection in Italy, September 2011. *Euro Surveill* .2011. 43:1-4.

197. Magurano F., Remoli ME., Baggieri M., et al. Circulation of West Nile virus lineage 1 and 2 during an outbreak in Italy. *Clin Microbiol Infect.* 2012. 18(12):E545-E547.

198. Barzon L., Pacenti M., Franchin E., et al.. The complex epidemiological scenario of West Nile virus in Italy. *Int J Environ Res Public Health*. 2013a.10: 4669- 4689.

199. Gray TJ., Webb CE. A review of the epidemiological and clinical aspects of West Nile virus. *International Journal of General Medicine*, 2014. 7, 193-203.

200. Smithburn K.C., Hughes T.P., et al. A neurotropic virus isolated from the blood of a native of Uganda. *Am J Trop Med Hyg*. 1940. 20:471-92.

201. Hubalek Z., Halouzka J. West nile fever – A reemerging mosquito-borne viral disease in Europe. *Emerging Infect. Dis*. 1999. 5, 643-650.

202. Bernkopf H., Levine S., Nerson R. Isolation of West Nile virus in Israel. *J Infect Dis*.1953. 93 (3):207-218.

203. Melnick JL., Paul JR., Riordan JT., et al. Isolation from human sera in Egypt of a virus apparently identical to West Nile virus. *Proc Soc Exp Biol Med*.1951. 77:661-665

204. Hayes CG. West Nile virus: Uganda, 1937, to New York city, 1999. *Ann N Y Acad Sci*.2001.951:25-37.

205. Jupp, P. G. The ecology of West Nile virus in South Africa and the occurrence of outbreaks in humans. *Ann. N. Y. Acad. Sci*. 1951:143–152.

206. Platonov AE.West Nile encephalitis in Russia 1999–2001. Were we ready? Are we ready? In: White DJ., Morse DL., editors. West Nile virus detection, surveillance, and control. V ol. 951. New Y ork: New Y ork Academy of Sciences. 2001. pp. 102–116.

207. Nash D., Mostashari F., Fine A., et al. The outbreak of West Nile virus infection in the New York City area in 1999. *N Engl J Med*. 2001. 344:1807-1814

208. Marfin AA., Gubler DJ.West Nile encephalitis: an emerging disease in the United States. *Clin Infect Dis*. 2001. 33:1713-1719.

209. Giladi M., Metzkor-Cotter E., Martin DA., et al.West Nile encephalitis in Israel, 1999: the New York connection. *Emerg Infect Dis* 2001. 7:659–661.

210. De Filette M., Ulbert S., Diamond M. Recent progress in West Nile virus diagnosis and vaccination. *Veterinary Research*. 2012. 43:16.

211. Campbell GL., Ceianu CS., Savage HM., et al. Epidemic West Nile encephalitis in Romania: Waiting for history to repeat itself. *Ann N Y Acad Sci.*2001, 951: 94-101

212. Triki H., Murri S., Le Guenno B., et al.West Nile viral meningo- encephalitis in Tunisia. *Med Trop (Mars.)* 2001. 61: 487-490.

213. Brown A., Bolisetty S., Whelan P., et al. Reappearance of human cases due to Murray Valley encephalitis virus and Kunjin virus in central Australia after an absence of 26 years. *Commun Dis Intell.* 2002. 26: 39-44.

214. Calistri P., Giovannini A., Hubalek Z., et al. Epidemiology of west nile in europe and in the mediterranean basin. *Open Virol J*. 2010. 4: 29-37.

215. Bakonyi T., Ferenczi E., Erdelyi K., et al. Explosive spread of neuroinvasive lineage 2 West Nile virus in Central Europe, 2008/2009. *Vet Microbiol.* 2013, 165: 61-70.

216. Rizzo C., Salcuni P., Nikoletti L., et al. Epidemiological surveillance of West Nile neuroinvasive diseases in Italy, 2008 to 2011. *Eur Surveill.* 2012. 17.

217. CDC 2013. West Nile virus disease cases reported to CDC by State and year, 1999- 2012. Available online: http://www.cdc.gov/westnile/resources/pdfs/cummulative/99_2012_cummulativeHu manCases.pdf. (accessed on 30 October 2013).

218. Pauvolid-Correa A., Morales MA., Levis S., et al. Neutralising antibodies for West Nile virus in horses from Brazilian Pantanal. *Mem Inst Oswaldo Cruz*. 2011; 106(4):467-474.

219. Autorino GL., Battisti A., Deubel V., et al.West Nile virus epidemic in horses, Tuscany region, Italy. *Emerg Infect Dis*. 2002, 8: 1372-1378.

220. Rossini G., Cavrini F., Pierro A., et al. First human case of West Nile virus neuroinvasive infection in Italy, September 2008 – case report. *Euro Surveill* .2008.13, 13

221. Barzon, L.; Squarzon L., Cattai M., et al. West Nile virus infection in Veneto region, Italy, 2008-2009. *Euro Surveill* 2009, 14.

222. Macini P., Squintani G., Finarelli AC., et al. Detection of West Nile virus infection in horses, Italy, September 2008. *Euro Surveill*.2008. 13.

223. Rossini G., Carletti F., Bordi L., et al. Phylogenetic analysis of West Nile virus isolates, Italy, 2008-2009. *Emerg Infect Dis*. 2011, 17: 903-906.

224. Capobianchi MR., Sambri V., Castilletti C., et al.Retrospective screening of solid organ donors in Italy, 2009, reveals unpredicted circulation of West Nile virus. *Euro Surveill* .2010.15.

225. Calzolari M., Gaibani P., Bellini R., et al. Mosquito, birds and human surveillance of West Nile virus and Usutu viruses in

Emilia-Romagna Region (Italy) in 2010. *PLoS One*. 2012, 7

226. Barzon L., Pacenti M., Franchin E., et al. Clinical and virological findings in the ongoing outbreaks of West Nile virus Livenza strain in northern Italy, July to September 2012. *Euro Surveill* .2012, 17.

227. Barzon L., Pacenti M., Franchin E., et al. Whole genome sequencing and phylogenetic analysis of West Nile virus lineage 1 and lineage 2 from human cases of infection, Italy, August 2013. *Euro Surveill*. 2013, 18.

228. Hayes EB., Komar N., Nasci RS., et al. Epidemiology and transmission dynamics of West Nile virus disease. *Emerging Infect Dis*. 2005, 11, 1167-1173.

229. Rossi SL., Ross TM., Evans JD. West Nile virus. *Clin Lab Med*. 2010 March; 30(1):47-65.

230. Colpitts TM., Conway MJ., Montgomery RR., et al. West Nile virus: Biology, transmission, and human infection. *Clin. Microbiol. Rev.* 2012. 25(4):635. Doi:10.1128/CMR.00045-12.\l

231. Martin-Acebes MA. And Saiz JC. West Nile virus: a re-emerging pathogen revisited. *World J Virol*.2012 April 12;1(2):51-70.

232. Brault AC. Changing patterns of West Nile virus transmission: altered vector competence and host susceptibility. *Vet Res* 2009; 40:43

233. Zeller HG. And Schuffenecker I.West Nile virus: an overview of its spread in Europe and the Mediterranean basin in contrast to its spread in the Americas. *Eur J Clin Microbial Infect Dis*. 2004. 23: 147-156.

234. Francis RO., Strauss D., Williams JD., et al.West Nile virus infection in blood donors in the New York area during the 2010 seasonal epidemic. *Transfusion*. 2012, 52:174-182.

235. Iwamoto M., Jernigan DB., Guasch A., et al. Transmission of West Nile virus from an organ donor to four transplant recipients. *N Engl J Med.* 2003; 348: 2196-2203.\l

236. CDC. 2002. Intrauterine West Nile virus infection_New York 2002. MMWR 2002, 51:1135-1136.

237. Hinckley AF., O'Leary DR., Hayes EB. Transmission of West Nile virus through breast milk seems to be rare. *Pediatrics* 2007, 119, 666-671.\l

238. Hayes EB., O'Leary DR.West Nile virus infection: a pediatric perspective. 2004; 113: 1375-1381.

239. Kelley, RE., Berger, JR., Kelley, BP. West Nile virus meningo-encephalitis: possible sexual transmission. J La State Med Soc. 2016. 168 (1): 21-2. Epub 2016 Feb 15.

240. Samuel MA. and Diamond MS. Pathogenesis of West Nile virus infection: a balance between virulence, innate and adaptive immunity, and viral evasion. *J Virol*. 2006, 80: 9349-9360.

241. Lim PY, Behr MJ, Chadwick CM, et al. Keratinocytes are cell targets of West Nile virus in vivo. *J. Virol*. 2011. 85:5197–5201.

242. Johnston LJ., Halliday GM., King NJ. Langerhans cells migrate to local lymph nodes following cutaneous infection with an arbovirus. *J Invest Dermatol*. 2000. 114: 560-568.

243. Bai, F. et al. A paradoxical role for neutrophils in the pathogenesis of West Nile virus. *J. Infect. Dis*. 2010, 202: 1804–1812.

244. Samuel, M. A. et al.PKR and RNase L contribute to protection against lethal West Nile Virus infection by controlling early viral spread in the periphery and replication in neurons. *J. Virol.*. 2006, 80: 7009–7019.

245. Sejvar JJ. Clinical manifestation and outcomes of West Nile virus infection. *Viruses*. 2014, 6: 606-623.

246. Emig, M.; Apple, D.J. Severe West Nile virus disease in healthy adults. *Clin. Infect. Dis*. 2004, 38, 289–292.

247. Watson, J.T.; Pertel, P.E.; Jones, R.C.; et al. Clinical characteristics and functional outcomes of West Nile Fever. *Ann. Intern. Med*. 2004, 141, 360–365.

248. Campbell GL., Marfin AA., Lanciotti RS., et al. West Nile virus. *Lancet Infect Dis*. 2002 Sep; 2(9):519-29.

249. O'Leary DR., Marfin AA., Montgomery Sp., et al. The epidemic of West Nile virus in the United States, 2002. *Vector Borne Zoonotic Dis.* 2004, 4: 61-70.

250. Pardridge, W.M. Brain metabolism: A perspective from the blood-brain barrier. *Physiol. Rev*. 1983. 63, 1481–1535.

251. Johnston RT., Mims CA.Pathogenesis of viral infections of the nervous system. *New Engl J Med*. 1968, 278:23-30.\l

252. Diamond, M. S., Shrestha, B., Mehlhop, E., et al. Innate and adaptive immune responses determine protection against disseminated infection by West Nile encephalitis virus. *Viral Immunol*. 2003, 16, 259–278.

253. Wang, T. et al.Toll-like receptor 3 mediates West Nile virus entry into the brain causing lethal encephalitis. *Nature Med.* 2004. 10, 1366–1373.

254. Wang, P. et al.Matrix metalloproteinase 9 facilitates West Nile virus entry into the brain. *J. Virol*. 2008, 82, 8978–8985

255. Garcia-Tapia, D.; Loiacono, C.M.; Kleiboeker, S.B. Replication of West Nile virus in equine peripheral blood mononuclear cells. *Vet. Immunol. Immunopathol*. 2006, 110, 229–244\l

256. Suthar MS., Diamond SM., Gale M. Jr. West Nile virus infection and immunity. *Nat Rev Microbiol*. 2013 Feb; 11(2):115-28.

257. Lim JK., Louie CY., Glaser C., et al. Genetic deficienty of chemokine receptor CCR5 is a strong risk factor for symptomatic West Nile virus infection: a meta-analysis of 4 cohorts in the US epidemic. *JID*. 2008, 197: 262-265.\l

258. Sips GJ., Wilschut J., Smit JM. Neuroinvasive flavivirus infections. *Rev Med Virol*. 2012, 22: 69-87.

259. Cho H., Diamond MS. Immune responses to West Nile virus infection in the Central Nervous System. *Viruses* 2012, 4, 3812-3830

260. Hunsperger, E.A.; Roehrig, J.T. Temporal analyses of the neuropathogenesis of a West Nile virus infection in mice. *J. Neurovirol*. 2006, 12, 129–139.

261. Kramer-Hämmerle, S.; Rothenaigner, I.; Wolff, H.; et al. Cells of the central nervous system as targets and reservoirs of the human immunodeficiency virus. *Virus Res*. 2005, 111, 194–213.

262. Verma, S.; Lo, Y.; Chapagain, M.; Lum, S.; et al.West Nile virus infection modulates human brain microvascular endothelial cells tight junction proteins and cell adhesion molecules: Transmigration across the in vitro blood-brain barrier. *Virology*. 2009, 385, 425–433.

263. Diamond, M. S., Mehlhop E., Oliphant T., et al.The host immunologic response to West Nile encephalitis virus. *Frontiers in*

Bioscience 2009, 14: 3024- 3040.

264. Wu SJ., et al. Human skin Langerhans cells are targets of dengue virus infection. *Nat Med.* 2000 6:816-820.

265. Lim PY., Louie KL., Styer LM., et al. Viral pathogenesis in mice is similar for West Nile virus derived from mosquito and mammalian cells. *Virology* .2010.400: 93- 103

266. Fredericksen BL.The neuroimmune response to West Nile virus. *J Neurovirol*. 2014, 20(2):113-121.\l

267. Lim MS., Koraka P., Osterhaus A., et al. West Nile virus: Immunity and Pathogenesis. *Viruses.* 2011, 3, 811-828.

268. Lopes H., Redig P., Glaser A., et al. Clinical findings, lesions, and viral antigen distribution in great gray owls (Strix nebulosa) and barred owls (Strix varia) with spontaneous West Nile virus infection. *Avian Dis*. 2007.51:140–145

269. Van Marle G., Antony J., Ostermann H., et al.West Nile virus-induced neuroinflammation: glial infection and capsid protein-mediated neurovirulence. *J Virol.2008.* 81:10933–10949\l

270. Hussmann KL., Samuel MA., Kim KS., et al. Differential replication of pathogenic and nonpathogenic strains of West Nile virus within astrocytes. *J Virol*. 2013. 87:2814–2822\l

271. Cheeran MC., Hu S., Sheng WS., et al. Differential responses of human brain cells to West Nile virus infection. *J Neurovirol.* 2005. 11:512–524\l

272. Suthar, M. S. *et al.* IPS-1 is essential for the control of West Nile virus infection and immunity. *PLoS Pathog.2010.* 6, e1000757

273. Jensen S., Thomsen R. Sensing of RNA viruses: a reviwe of innate immune receptors involved in recognizing RNA virus invasion. *Journal of Virology*. 2012, 2900-2010.

274. Kato H, et al. Cell type-specific involvement of RIG-I in antiviral response. I*mmunity*. 2005. 23:19–28\l

275. Quicke KM., Suthar MS. The innate immune playbook for restricting West Nile virus infection. *Virus*es. 2013, 5: 2643-2658

276. Fredericksen, B. L., Keller, B. C., Fornek, J., Katze, M. G. & Gale, M. Jr. Establishment and maintenance of the innate antiviral response to West Nile virus involves both RIG-I and MDA5 signaling through IPS-1. *J. Virol.* 2008. 82, 609–616.

277. Takeuchi O. and Akira S. Innate immunity to virus infection. *Immunological reviews*.2009. 227: 75-86.

278. Yamamoto, M. et al. Role of adaptor TRIF in the MyD88-independent Toll-like receptor signaling pathway. *Science.* 2003. 301, 640–643

279. Daffis S., Samuel MA., Suthar MS., et al. Toll-like receptor 3 has a protective role against West Nile virus infection. *J. Virol*. 2008, 82, 10349–10358.

280. Szretter KJ., Daffis S., Patel J., et al. The innate immune adaptor molecule MyD88 restricts West Nile virus replication and spread in neurons of the central nervous system. *J. Virol.* 2010. 84, 12125–12138.\l

281. Ramos, H. J. et al. IL-1β signaling promotes CNS- intrinsic immune control of West Nile virus infection. *PLoS Pathog.*2012. 8, e1003039

282. Sato M., et al. Distinct and essential roles of transcription factors IRF-3 and IRF-7 in response to viruses for IFN-α/β gene induction. *Immunity.*2000. 13, 539–548.

283. Honda K., et al.IRF-7 is the master regulator of type-I interferon-dependent immune responses. *Nature*. 2005. 434, 772–777 (2005).

284. Zanotto, P.M., Gould, E.A., Gao, G.F., Harvey, P.H. & Holmes, E.C. Population dynamics of flaviviruses revealed by molecular phylogenetics. *Proc. Natl. Acad. Sci. USA.* 1996. 93, 548–553.

285. Rico-Hesse, R. Microevolution and virulence of dengue viruses. *Adv Virus Res*. 2003. 59, 315-341

286. Holmes EC. Molecular epidemiology and evolution of emerging infectious diseases. *Brit Mel Bull*. 1998. 54:533e543.

287. Rico-Hesse, R. Molecular evolution and distribution of dengue viruses type 1 and 2 in nature. *Virology*. 1999. 174(2), 479-493.

288. Mustafa, M.S., Rasotagi, V., Jain, S., Gupta, V. Discovery of fifth serotype of dengue virus (DENV-5): A new public health dilemma in dengue control. *Armed Forces Medical Services (AFMS).* 2015. 71, 67-70

289. Normile, D. Surprising new dengue virus throws a spanner in disease control efforts. *Science*. 2013. 342:415.

290. Hammon, W.M. et al. New hemorrhagic fevers of children in the Philippines and Thailand. *Trans. Assoc. Am. Physicians.* 1960. 73, 140–155

291. World Health Organization WHO. Dengue and severe dengue. 2015. http://www. who.int/mediacentre/factsheets/fs117/en/. Accessed 11 Jun 2015.

292. Kutsuna, S., Kato, Y., Moi, M.L., Kotaki, A., Ota, M., Shinohara, K., et al. Autochthonous dengue fever, Tokyo, Japan, 2014. *Emerg Infect Dis*. 2015. 21:517–20.

293. Bhatt, S., Gething, PW., Brady, O.J., Messina, JP., Farlow, AW., Moyes, CL., et al. The global distribution and burden of dengue. *Nature*. 2013. 496:504–7.

294. Rush, B. An account of the bilious remitting fever. As it appeared in philadelphia, in the summer and autumn of the year 1780. *The American Journal of Medicine*. 1951.11(5), 546-550

295. Halstead. Dengue : Overview and History. In S. Halstead (Ed.), Dengue. London: Imperial College Press.2008

296. Sabin, A. B. Research on dengue during World War II. *Am J Trop Med Hyg*. 1952. 1(1), 30-50.

297. Guzman, A., & Isturiz, R. E. Update on the global spread of dengue. *Int J Antimicrob Agents*. 2010. 36 Suppl 1, S40-42. doi: 10.1016/j.ijantimicag.2010.06.018

298. Sim, S. and Hibberd, ML. Genomic approaches for understanding dengue: insights from the virus, vector, and host. *Genome Biology*. 2016. 17:38 DOI 10.1186/s13059-016-0907-2

299. Higa, Y. Dengue Vectors and their spatial distribution. *Tropical Medicine and Health*. 2011 39(4), 17-27

300. Scott, T. W., & Takken, W.Feeding strategies of anthropophilic mosquitoes result in increased risk of pathogen transmission. *Trends Parasitol*. 2012,28(3), 114-121. doi: 10.1016/j.pt.2012.01.001

301. Powell , J. a. T., WJ. History of domestication and spread of Aedes aegypti - A Review. *Mem Inst Oswaldo Cruz*. 2013. 108, 11-17. doi: 10.1590/0074-0276130395

302. WHO. Comprehensive Guideline for Prevention and Control of Dengue and Dengue Haemorrhagic Fever. New delhi: World

Health Organization, Regional Office for South-East Asia.2011

303. Gratz, N. G. Critical review of the vector status of Aedes albopictus. *Med Vet Entomol*. 2004.18(3), 215-227. doi: 10.1111/j.0269-283X.2004.00513.x

304. Carvalho, R. G., Lourenco-de-Oliveira, R., & Braga, I. A. Updating the geographical distribution and frequency of Aedes albopictus in Brazil with remarks regarding its range in the Americas. *Mem Inst Oswaldo Cruz*. 2014. 109(6), 787-796.

305. Roche, B., Léger, L., L'Ambert, G., Lacour, G., Foussadier, R., Besnard, G., Fontenille, D.The Spread of Aedes albopictus in Metropolitan France: Contribution of Environmental Drivers and Human Activities and Predictions for a Near Future. *PLoS One*. 2015. 10(5), e0125600. doi: 10.1371/journal.pone.0125600

306. Kraemer, M. U., Sinka, M. E., Duda, K. A., Mylne, A. Q., Shearer, F. M., Barker, C. M., Hay, S. I.The global distribution of the arbovirus vectors Aedes aegypti and Ae. albopictus .*Elite* 2015.(Vol. 4). doi: 10.7554/eLife.08347

307. Paupy, C., Delatte, H., Bagny, L., Corbel, V., & Fontenille, D. Aedes albopictus, an arbovirus vector: from the darkness to the light. Microbes Infect. 2004. 11(14-15), 1177-1185. doi: 10.1016/j.micinf.2009.05.005

308. Li, Y., Kamara, F., Zhou, G., Puthiyakunnon, S., Li, C., Liu, Y., Chen, X.G. Urbanization Increases <italic>Aedes albopictus</italic> Larval Habitats and Accelerates Mosquito Development and Survivorship. *PLoS Negl Trop Dis*. 2014. 8(11), e3301. doi: 10.1371/journal.pntd.0003301

309. Schaffner, F., Vazeille, M., Kaufmann, C., Failloux, A-B, Mathis, A. Vector competence of *Aedes japonicus* for chikungunya and dengue viruses. *Eur Mosq Bull.*2011.29:141–2.

310. Moore, P.R., Johnson, P.H., Smith, G.A., Ritchie, S.A., Van Den Hurk, A.F. Infection and dissemination of dengue virus type 2 in *Aedes aegypti*, *Aedes albopictus*, and *Aedes scutellaris* from the Torres Strait, Australia. *J Am Mosq Control Assoc.* 2007. 23:383–8. doi:10.2987/5598.1

311. Rosen, L., Rozeboom, L.E., Sweet, B.H., Sabin, A.B.. The transmission of dengue by *Aedes polynesiensis* marks. *Am J Trop Med Hyg.* 1954. 3:878–82.

312. Yacoub, S., Mongkolsapaya, J., & Screaton, G. The pathogenesis of dengue. *Curr Opin Infect Dis*. 2013. 26(3), 284-289. doi:10.1097/QCO.0b013e32835fb938\l

313. Kurane, I. & Ennis, F.A. Immunopathogenesis of dengue virus infections, in *Dengue and Dengue Hemorrhagic Fever* (eds. Gubler, D.J. & Kuno, G.) 273–290 (CAB International, London, 1997) \l

314. Gubler, D.J. Dengue and dengue hemorrhagic fever. *Clin. Microbiol. Rev.*1998. 11, 480–496. \l

315. Murthy,JM. Neurological complication of dengue infection. *Neurology India*. 2010; 58: 581–584. DOI: 10.4103/0028-3886.68654

316. Varatharaj, A. Encephalitis in the clinical spectrum of dengue infection. *Neurology India*.2010; 58: 585–591. DOI: 10.4103/0028-3886.68655

317. Gulati, S., Maheshwari, A. Atypical manifestations of dengue. *Tropical Medicine & International Health.* 2007; 12: 1087–1095. DOI: 10.1111/j.1365-3156.2007.01891. \l

318. Yauch, L.E., Shresta, S. Mouse models of dengue virus infection and disease. *Antiviral Research*. 2008; 80: 87–93. DOI:

10.1016/j. antiviral.2008.06.010

319. Chaturvedi, U.C., Dhawan, R., Khanna, M., et al. Breakdown of the blood–brain barrier during dengue virus infection of mice. *Journal of General Virology.* 1991.72(Pt 4): 859–866.

320. Miagostovich. M.P., Ramos, R.G., Nicol, A.F., et al. Retrospective study on dengue fatal cases. *Clinical Neuropathology*.1997.16: 204–208.\l

321. Jan, J.T., Chen, B.H., Ma, S.H., et al. Potential dengue virus-triggered apoptotic pathway in human neuroblastoma cells: arachido- nic acid, superoxide anion, and NF- kappaB are sequentially involved. *Journal of Virology*. 2000; 74: 8680–8691.

322. Sanchez-Burgos, G., Hernandez-Pando, R., Campbell, IL., et al. Cytokine production in brain of mice experimentally infected with dengue virus. *Neuroreport*. 2004; 15: 37–42.

323. An, J., Zhou, D.S., Kawasaki, K., et al. The pathogenesis of spinal cord involvement in dengue virus infection. *Virchows Archiv*.2003.442: 472–481. DOI: 10.1007/s00428- 003-0785-3

324. Kurane, I., Innis, B. L., Nimmannitya, S., Nisalak, A., Meager, A. & Ennis, F. A.High levels of interferon alpha in the sera of children with dengue virus infection. *Am J Trop Med Hyg*. 1993. 48, 222-9.

325. Diamond, M. S., Roberts, T. G., Edgil, D., Lu, B., Ernst, J. & Harris, E. Modulation of Dengue Virus Infection in Human Cells by Alpha, Beta, and Gamma Interferons. *Journal of Virology*. 2000. 74, 4957-4966.\l

326. Espada-murao, L. A. & Morita, K. 2011. Dengue and soluble mediators of the innate immune system. Trop Med Health, 39, 53-62.\l

327. Kurane, I., Innis, B. L., Nisalak, A., Hoke, C., Nimmannitya, S., Meager, A. & Ennis, F. A. Human T cell responses to dengue virus antigens. Proliferative responses and interferon gamma production. *J Clin Invest*. 1989. 83, 506-13.

328. Surasombatpattana, P., Hamel, R., Patramool, S., Luplertlop, N., Thomas, F., Despres, P., Briant, L., Yssel, H. & Misse, D. Dengue virus replication in infected human keratinocytes leads to activation of antiviral innate immune responses. *Infect Genet Evol*. 2011.11, 1664- 73.

329. Dalrymple, N. A. & Mackow, E. R. Endothelial cells elicit immune- enhancing responses to dengue virus infection. *J Virol*. 2012.86, 6408-15.

330. Noisakran, S., Onlamoon, N., Songprakhon, P., Hsiao, HM., Chokephaibulkit, K., Perng, GC. Cells in Dengue Virus Infection In Vivo. *Advances in virology*. 2010. Volume 2010. doi:10.1155/2010/164878

331. Limon-Flores, A.Y., Perez-Tapia, M., Estrada-Garcia, I. et al. Dengue virus inoculation to human skin explants: an effective approach to assess in situ the early infection and the effects on cutaneous dendritic cells. *International Journal of Experimental Pathology*. 2005. vol. 86, no. 5, pp. 323–334.

332. Tassaneetrithep, B., Burgess, T.H., Granelli-Piperno, A. et al. DC-SIGN (CD209) mediates dengue virus infection of human dendritic cells. *Journal of Experimental Medicine*.2003. vol. 197, no. 7, pp. 823–829.

333. Wang, J.P., Liu, P., Latz, E.,Golenbock, D.T.,Finberg, R.W.\l and Libraty, D.H.Flavivirus activation of plasmacytoid dendritic cells delineates key elements of TLR7 signaling beyond

endosomal recognition. *Journal of Immunology*. 2006. vol. 177, no. 10, pp. 7114–7121.\l

334. P. Sun, P., Fernandez, S., Marovich, M.A. et al. Functional characterization of ex vivo blood myeloid and plasmacytoid dendritic cells after infection with dengue virus. *Virology*. 2009. vol. 383, no. 2, pp. 207–215.

335. Miller, J.L., DeWet, B.J.M., Martinez-Pomares, L. et al..The mannose receptor mediates dengue virus infection of macrophages. *PLoS Pathogens*. 2008. vol. 4, article e17

336. Nightingale, Z.D., Patkar, C. and Rothman, A.L.Viral replication and paracrine effects result in distinct, functional responses of dendritic cells following infection with dengue 2 virus. *Journal of Leukocyte Biology*. 2008. vol. 84, no. 4, pp. 1028– 1038.

337. Marovich, M., Grouard-Vogel, G., Louder, M. et al. Human dendritic cells as targets of dengue virus infection. *Journal of Investigative Dermatology Symposium Proceedings*. 2001. vol. 6, no. 3, pp. 219–224.

338. Kyle, J.K., Beatty, P.R., and Harris, E. Dengue virus infects macrophages and dendritic cells in a mouse model of infection,. *Journal of Infectious Diseases*. 2007. vol. 195, no. 12, pp. 1808–1817.

339. Blackley S et al. Primary human splenic macrophages, but not T or B cells, are the principal target cells for dengue virus infection in vitro. *J Virol*. 2007.81(24):13325–34.

340. King, A.D. et al. B cells are the principal circulating mononuclear cells infected by dengue virus. Southeast Asian. *J Trop Med Public Health*. 1999. 30(4):718–28.

341. Huerre, M.R. et al. Liver histopathology and biological correlates in five cases of fatal dengue fever in Vietnamese children. *Virchows Arch*. 2001. 438(2):107–15.

342. Balsitis, S.J. et al. Tropism of dengue virus in mice and humans defined by viral nonstructural protein 3-specific immunostaining. *Am J Trop Med Hyg*. 2009.80(3):416–24.

343. Zellweger, R.M., Prestwood, T.R., Shresta, S. Enhanced infection of liver sinusoidal endothelial cells in a mouse model of antibody-induced severe dengue disease. *Cell Host Microbe*. 2010.7(2):128–39.

344. Sabin, A.B., et al. Production of immunity to dengue with virus modified by propagation in mice. *Science*.1945.101:640–642. [PubMed: 17844088]

345. Sabin, A.B. Recent advances in our knowledge of dengue and sandfly fever. *Am J Trop Med Hyg*. 1955.4:198–207. [PubMed: 14361897]

346. Huang, K.J., et al. Manifestation of thrombocytopenia in dengue-2-virus-infected mice. *J Gen Virol*. 2000. 81 (Pt 9):2177–2182. [PubMed: 10950974]

347. Johnson, A.J., et al. New mouse model for dengue virus vaccine testing. *J Virol*.1999.73:783–786. [PubMed: 9847388]

348. Koraka, P., Benton, S., Amerongen, G.V., Stittelaar, K.J. and Osterhaus, A.D.M.E."Characterization of humoral and cellular immune responses in cynomolgus macaques upon primary and subsequent heterologous infections with dengue viruses. *Microbes and Infection*. 2007.vol. 9, no. 8, pp. 940–946.

349. Guy, B., Barban, V., Mantel, N., et al. Evaluation of interferences between dengue vaccine serotypes in a monkey model. *The American Journal of Tropical Medicine & Hygiene*. 2009.vol. 80, no. 2, pp. 302–311.

350. Onlamoon, N., Noisakran, S., Hsiao, H.-M. et al. Dengue virus—induced hemorrhage in a nonhuman primate model. *Blood* 2010. vol. 115, no. 9, pp. 1823–1834.

351. Ashraf, U.,Ye, J., Ruan, X.,Wan, S., Zhu, B., Cao, S.. Usutu virus: An emerging flavivirus in Europe. *Viruses*. 2015. 219–238. doi:10.3390/v7010219

352. Gaibani, P., Rossini, G.. An overview of Usutu virus. *Microbes Infect.* 2017. 19, 382–387. doi:10.1016/j.micinf.2017.05.003. \l

353. Chvala, S., Kolodziejek, J., Nowotny, N.,Weissenböck, H..Pathology and viral distribution in fatal Usutu virus infections of birds from the 2001 and 2002 outbreaks in Austria. *J. Comp. Pathol*. 2004. 131,176–185. doi:10.1016/j.jcpa.2004.03.004. \l

354. Seitz, R.. Usutu Virus. *Transfus. Med. Hemotherapy*. 2014. 41, 73–82. doi:10.1159/000357106.

355. Weissenback, H., Bakonyi, T., Rossi, G., Mani, P., Nowotny, N.. Usutu virus, Italy, 1996. *Emerg. Infect. Dis*. 2013. 19, 274–277. doi:10.3201/eid1902.121191.

356. D. Cadar, D., et al.. Widespread activity of multiple lineages of Usutu virus, Western Europe, 2016. *Eurosurveillance*. 2017. 22,1–7. doi:10.2807/1560-7917.ES.2017.22.4.30452.

357. Nikolay,B.. A review of West Nile and Usutu virus co-circulation in Europe: How much do transmission cycles overlap?. *Trans. R. Soc. Trop. Med. Hyg.* 2015. 109,609–618. doi:10.1093/trstmh/trv066

358. Nikolay, B., Diallo, M., Boye, C.S.B., Sall, A.A.. Usutu Virus in Africa. *Vector- Borne Zoonotic Dis.* 2011. 11,1417–1423. doi:10.1089/vbz.2011.0631

359. Bakonyi, T., et al..Usutu virus infections among blood donors , Austria , July and August 2017. *Raising awareness for diagnostic challenges*.2017,1–6. doi:10.2807/1560-7917.ES.2017.22.41.17-00644.

360. Gaibani, P., Cavrini, F., Gould, E.A.,Rossini, G., Pierro, A., Landini, M.P., Sambri, S.. Comparative Genomic and Phylogenetic Analysis of the First Usutu Virus Isolate from a Human Patient Presenting with Neurological Symptoms. *PLoS One*. 2013.8,1–10. doi:10.1371/journal.pone.0064761.

361. Scagnolari, C., Caputo, B., Trombetti, S., Cacciotti, G., Soldà, A., Spano, L.,Villari, P., della Torre, A., Nowotny, N., Antonelli, G..Usutu virus growth in human cell lines: Induction of and sensitivity to type I and III interferons. *J. Gen. Virol.* 2013. 94.789–795. doi:10.1099/vir.0.046433-0.

362. Cacciotti, G., Caputo, B., Selvaggi, C., la Sala, A.,Vitiello, L., Diallo, D., Ceianu, C., Antonelli, G., Nowotny, N., Scagnolari,C.. Variation in interferon sensitivity and induction between Usutu and West Nile (lineages 1 and 2) viruses. *Virology*. 2015. 415.189–198. doi:10.1016/j.virol.2015.07.015.

363. Barr, K.L., Anderson, B.D.,Prakoso, D.,Long, M.T.. Working with Zika and Usutu Viruses *in vitro*. *PLoS Negl. Trop. Dis*. 2016. 10.1–13. doi:10.1371/journal.pntd.0004931.

364. Weissenböck, H., Bakonyi, T., Chvala, S., Nowotny, N.. Experimental Usutu virus infection of suckling mice causes neuronal and glial cell apoptosis and demyelination. *Acta Neuropathol*. 2004. 108.453–460. doi:10.1007/s00401-004- 0916-1.

365. Blázquez, A.B., Escribano-Romero, E., Martín-Acebes, M.A.,Petrovic, T., Saiz, J.C.. Limited susceptibility of mice to Usutu virus (USUV) infection and induction of flavivirus cross-protective immunity.*Virology*. 2015. 482.67–71. doi:10.1016/j.virol.2015.03.020.

366. Martín-Acebes, M.A., Blázquez, A.B., Cañas-Arranz, R., Vázquez-Calvo, Á., Merino-Ramos, T., Escribano-Romero, E., Sobrino, F., Saiz, J.C.. A recombinant DNA vaccine protects mice deficient in the alpha/beta interferon receptor against lethal challenge with Usutu virus. *Vaccine*. 2016. 34.2066–2073. doi:10.1016/j.vaccine.2016.03.015.

367. Salinas, S., Constant, O., Desmetz, C., Barthelemy, J., Lemaitre, J.M., Milhavet, O., Nagot, N., Foulongne, V., Perrin,F.E., Saiz, J.C., Lecollinet, S., Van de Perre, P., Simonin, Y.. Deleterious effect of Usutu virus on human neural cells. *PLoS Negl. Trop. Dis.* 2017 e0005913. doi:10.1371/journal.pntd.0005913.

368. Yu, J., Vodyanik, MA., Smuga-Otto, K., Antosiewicz-Bourget, J., Frane, JL., Tian, S., Nie, J., Jonsdottir, GA., Ruotti, V., Stewart, R., Slukvin, II., Thomson, JA. Induced pluripotent stem cell lines derived from human somatic cells. *Science*. 2007. 318(5858):1917-20. \l

369. Takahashi, K., Yamanaka, S. Induction of pluripotent stem cells from mouse embryonic and adult fibroblast cultures by defined from mouse embryonic and adult fibroblast cultures by defined factors. *Cell.* 2006. 126 (4): 663

370. Thomson, JA., Itskovitz-Eldor, J., Shapiro, SS., Waknitz, MA., Swiergiel, JJ., Marshall, VS., Jones, JM. Embryonic stem cell lines derived from human blastocysts. *Science*. 1998, 282(5391):1145–1147. \l

371. Looijenga, LH., Stoop, H., de Leeuw, HP., de Gouveia Brazao, CA., Gillis, AJ., van Roozendaal, KE., van Zoelen, EJ., Weber, RF., Wolffenbuttel, KP., van Dekken, H., Honecker, F., Bokemeyer, C., Perlman, EJ., Schneider, DT., Kononen, J., Sauter, G., Oosterhuis, JW. POU5F1 (OCT3/4) identifies cells with pluripotent potential in human germ cell tumors. *Cancer Research.* 2003. 63 (9): 2244–50.

372. Zaehres, H., Lensch, MW., Daheron, L., Stewart, SA., Itskovitz-Eldor, J., Daley, GQ.High-efficiency RNA interference in human embryonic stem cells. *Stem Cells.* 2005. 23 (3): 299–305.

373. Chambers, I., Tomlinson, SR. The transcriptional foundation of pluripotency. *Development.* 2009. 136 (14): 2311–22.

374. El-Karim; et al. Krüppel-like factor 4 regulates genetic stability in mouse embryonic fibroblasts. *Molecular Cancer*. 2013

375. Maherali, N., Ahfeldt T., Rigamonti, A., Utikal, T., Cowan, C., Hochedlinger, K. A high-efficiency system for the generation and study of human induced pluripotent stem cells. *Cell Stem Cell*. 2008. 3, pp. 340– 345 \l

376. Hockemeyer, D., Soldner, F.,Cook, E.K., Gao, Q., Mitalipova,M., Jaenisch, R. A drug-inducible system for direct reprogramming of human somatic cells to pluripotency. *Cell Stem Cell*. 2008, 3, pp. 346–353 \l

377. Stadtfeld, M., Nagaya, M.,Utikal, J.,Weir, G., Hochedlinger, K.Induced Pluripotent Stem Cells Generated Without Viral Integration. *Science*.2008.322, pp. 945–949 \l

378. Kustikova O, Fehse B. , Modlich, U.,Yang, B., Dullmann, J., Kamino, K.,von Neuhoff, N., Schlegelberger, B., Li, Z., Baum, C. Clonal dominance of hematopoietic stem cells triggered by retroviral gene marking. *Science*.2005. 308, pp. 1171–1174 \l

379. Nakagawa M, Koyanagi, M., Tanabe, K.,Takahashi, T., Ichisaka, T., Aoi, T., Okita, K., Mochiduki, Y., Takizawa, N., Yamanak, S. Generation of induced pluripotent stem cells without Myc from mouse and human fibroblasts. *Nat. Biotechnol*. 2008. 26 pp. 101–106 \l

380. Nakanishi M, Otsu M: Development of Sendai virus vectors and their potential applications in gene therapy and regenerative medicine. *Curr Gene Ther.* 2012, 12(5):410-6. \l

381. Yu J, Hu K., Smuga-Otto K., Tian, S., Stewart, R., Slukvin, II., Thomson, JA. Human induced pluripotent stem cells free of vector and transgene sequences. *Science.* 2009. 8;324(5928):797-801. \l

382. Okita K, Nakagawa, M., Hyenjong, H., Ichisaka, T.,Yamanaka, S. Generation of Mouse Induced Pluripotent Stem Cells Without Viral Vectors. *Science* 2008. 322, pp. 949–953 \l

383. Zhou, H.,Wu, S.,Joo, JY.,Zhu, S.,Han, DW.,Lin, T.,Trauger, S.,Bien, G.,Yao, S., Zhu, Y., Siuzdak, G., Schöler, HR., Duan, L., Ding, S. Generation of induced pluripotent stem cells using recombinant proteins. *Cell Stem Cell*. 2009. 8;4(5):381-4. \l

384. Kim, D., Kim, CH., Moon, JI., Chung, YG., Chang, MY., Han, BS., Ko, S., Yang, E., Cha, KY., Lanza, R., Kim, KS. Generation of human induced pluripotent stem cells by direct delivery of reprogramming proteins. *Cell Stem Cell*. 2009. 5;4(6):472-6. \l

385. Warren, L., et al. Highly efficient reprogramming to pluripotency and directed differentiation of human cells with synthetic modified mRNA. *Cell Stem Cell.* 2010.7(5):618-30.

386. Sterneckert, J.L.; Reinhardt, P.; Schöler, H.R. Investigating human disease using stem cell models. *Nat. Rev. Genet.* 2009. 15: 625–639.

387. Imamura, T.; Cui, L.; Teng, R.; Johkura, K.; Okouchi, Y.; Asanuma, K.; Ogiwara, N.; Sasaki, K. Embryonic stem cell-derived embryoid bodies in three-dimensional culture system form hepatocyte-like cells in vitro and in vivo. *Tissue Eng*. 2004. 10: 1716–1724.

388. Nakano, T.; Kodama, H.; Honjo, T.Generation of lymphohematopoietic cells from embryonic stem cells in culture. *Science.* 1994. 265: 1098–1101.

389. Carpenter, L.; Carr, C.; Yang, C.T.; Stuckey, D.J.; Clarke, K.; Watt, S.M.Efficient differentiation of human induced pluripotent stem cells generates cardiac cells that provide protection following myocardial infarction in the rat. *Stem Cells Dev.* 2012. 21: 977–986

390. Tiscornia, G.; Vivas, E.L.; Izpisúa Belmonte, J.C. Diseases in a dish: Modeling human genetic disorders using induced pluripotent cells". *Nat. Med.*2011. 17: 1570–1576.

391. Ding, Q.; Lee, Y.K.; Schaefer, E.A.; Peters, D.T.; Veres, A.; Kim, K.; Kuperwasser, N.; Motola, D.L.; Meissner, T.B.; Hendriks, W.T.; et al. A TALEN genome-editing system for generating human stem cell- based disease models". *Cell Stem Cell.* 2013. 12: 238–251.

392. Trevisan M., Sinigaglia A., Desole G., Berto A., Pacenti M., Palù G., Barzon L. Modeling Viral Infectious Diseases and Development of Antiviral Therapies Using Human Induced Pluripotent Stem Cell-Derived Systems. *Viruses*. 2015. 7:3835–3856.

393. Schwartz R.E., Trehan K., Andrus L., Sheahan T.P., Ploss A., Duncan S.A., Rice C.M., Bhatia S.N. Modeling hepatitis C virus infection using human induced pluripotent stem cells. *Proc. Natl. Acad. Sci*. USA. 2012.109: 2544–2548.

394. Pijlman, GP.; et al. A highly structured, nuclease-resistant, noncoding RNA produced by flaviviruses is required for pathogenicity. *Cell Host Microbe*. 2008; 4:579–591.

395. Beasley, DW.; Davis, CT.; Whiteman, M.; Granwehr, B.; Kinney, RM.; Barrett, AD. Molecular determinants of virulence of West Nile virus in North America. *Arch Virol Suppl.* 2004; 35–41.

396. Heinz, FX.; Stiasny, K., Allison, SL. The entry machinery of flaviviruses. *Arch Virol Suppl.* 2004; 133–137.

397. Murray, K.; et al. Risk factors for encephalitis and death from West Nile virus infection. *Epidemiol Infect*. 2006; 134:1325–1332.

398. Gubler, DJ. The continuing spread of West Nile virus in North America. *Clin Infect Dis* 2007;45:1039–1046. \l

399. Samuel, CE. Host genetic variability and West Nile virus susceptibility. *Proc Natl Acad Sci* USA. 2002; 99:11555–11557. [PubMed: 12192094]

400. Mashimo, T. et al. A nonsense mutation in the gene encoding 2 -5 - oligoadenylate synthetase/L1 isoform is associated with West Nile virus susceptibility in laboratory mice. *Proc Natl Acad Sci* USA 2002;99:11311–11316. \l

401. Lim, JK.et al. Genetic variation in OAS1 is a risk factor for initial infection with West Nile virus in man. *PLoS Pathog*. 2009; 5:e1000321. [PubMed: 19247438]

402. Glass, WG. et al. CCR5 deficiency increases risk of symptomatic West Nile virus infection. *J Exp Med*. 2006; 203:35–40.

403. Lim, JK. et al. CCR5 deficiency is a risk factor for early clinical manifestations of West Nile virus infection but not for viral transmission. *J Infect Dis*. 2010; 201:178–185.

404. Kong, KF. et al. Dysregulation of TLR3 Impairs the Innate Immune Response to West Nile Virus in the Elderly. *J Virol*. 2008; 82:7613–7623

405. Bigham, A.W.; et al. Host genetic risk factors for West Nile Virus infection and disease progression. *PLoS ONE* 2011, *6*, e24745

406. Yang, W., Mills, J.A., Sullivan, S., Liu, Y., French, D.L., Gadue, P. iPSC Reprogramming from Human Peripheral Blood Using Sendai Virus Mediated Gene Transfer. StemBook [Internet]; 2012 Jun 10. \l

407. Livak, K.J., Scmittgen, T.D. Analysis of relative gene expression data using real-time quantitative PCR and 2(-Delta Delta C(T)) Method. *Methods*. 25, 402-408 (2001).

408. Barzon, L. *et al.* Isolation of infectious Zika virus from saliva and prolonged viral RNA shedding in a traveller returning from the Dominican Republic to Italy. *Euro Surveill*. 21 (10): 30159 (January 2016).

409. Linke, S. *et al*. Detection of West Nile virus lineages 1 and 2 by real-time PCR. *J Virol Methods*. 146 (1-2), 355-8 (2007).

410. Santiago, GA. *et al.* Analytical and Clinical Performance of the CDC Real Time RT-PCR Assay for Detection and Typing of Dengue Virus. *PLoS Negl Trop Dis* 7 (7): e2311. doi:10.1371/journal.pntd.0002311 (2013)

411. Cavrini, F., Della Pepa, M.E., Gaibani, P., Pierro, A.M., Rossini, G., Landini, M.P., Sambri, V.. A rapid and specific real-time RT-PCR assay to identify Usutu virus in human plasma, serum, and cerebrospinal fluid. *J. Clin. Virol*. 2011.50,221– 223. doi:10.1016/j.jcv.2010.11.008.

412. Lindenbach, B.D.; Thiel, H.J.; and Rice, C.M. Flaviviridae: the viruses and their replication. *In Fields Virology*, D.M. Knipe and P.M. Howley, eds. (Lip- pincott Williams and Wilkins),(2007). pp. 1101–1152.

413. Montgomery, RR. Age-related alterations in immune response to West Nile virus infection. *Clin Exp Immunol*. 2017.187(1):26-34. doi: 10.1111/cei.12863.

414. Watrin, L.; Ghawche, F.; Larre, P.; Neau, J.P.; Mathis, S.; and Four-nier, E. Guillain-Barré syndrome (42 cases) occurring during a Zika virus outbreak in French Polynesia. *Medicine (Baltimore)* 2016*;* 95, e3257.

415. Hughes, B.W.; Addanki, KC.; Sriskanda, A.N; McLean, E.; Bagasra, O. Infectivity of immature neurons to Zika Virus: a link to congenital Zika syndrome. *EBiomedicine* 10 (2016) 65-70

416. Shresta, B.; Gottlieb, D. and Diamond MS. Infection and injury of neurons by West Nile Encephalitis Virus. *Journal of Virology* 2003; p 13203-13213

417. Lucas, M.; et al. Infection of mouse neurons by West Nile is modulated by the interferon-inducible 2'-5' oligoadenylate synthetase 1b protein.2013; Immun. Cell Biol. 81, 230-236

418. Frumence, E., et al. The South Pacific epidemic strain of Zika virus replicates efficiently in human epithelial A549 cells leading to IFN-β production and apoptosis induction. *Virology* 2016; 493, 217–226.

419. Yoneyama, M., and T. Fujita. Function of RIG-I-like receptors in antiviral innate immunity. J. Biol. Chem. 2007, 282:15315–15318

420. Fensterl, V.; Sen, GC. Interferon-induced Ifit proteins: their role in viral pathogenesis. *J Virol* 2015; 89:2462–2468. doi:10.1128/JVI.02744-14.

421. Terenzi, F., et al. Tissue-specific and inducer-specific differential induction of ISG56 and ISG54 in mice. *J. Virol*. 2007;81:8656 – 8665.

422. Cho, H. et al. A role for Ifit2 in Restricting West Nile virus infection in the brain. *Journal of virology* 2013; p. 8363-8371

423. Daffis, S.; et al. 2′-O methylation of the viral mRNA cap evades host restriction by IFIT family members. *Nature*. 2010 November 18; 468(7322): 452–456. doi:10.1038/nature09489.

424. Stawowczyk, M.; et al. The interferon Stimulated Gene 54 promotes apoptosis. Journal of biological chemistry 2011; vol.286, no9, pp 7257-7266

425. Wang R, Wang J, Paul AM, et al. Mouse embryonic stem cells are deficient in type I interferon expression in response to viral infections and double-stranded RNA. J Biol Chem. 2013; 288:15926–15936. [PubMed: 23580653]

426. Chen, LL.; Yang, L.; Carmichael, GG. Molecular basis for an attenuated cytoplasmic dsRNA response in human embryonic stem cells. *Cell Cycle.* 2010; 9:3552–3564. [PubMed: 20814227]

427. Murry, C. E. and Keller, G. Differentiation of Embryonic Stem Cells to Clinically Relevant Populations: Lessons from Embryonic Development. *Cell* 2008; 132 (4): 661–680.

428. Garcez, PP. *et al*. Zika virus impairs growth in human neurospheres and brain organoids. *Science* 2016;16:522-3

429. McGrath, E.L.; et al. Differential response of human fetal brain neural stem cells to Zika virus infection. *Stem Cell Reports* 2017; Vol.8; 715-727; DOI:10.1016/j.stemcr.2017.01.008

430. Petersen, L.R. et al. Zika Virus. *N Engl J Med* 2017; 374:1552-1563April 21, 2016DOI: 10.1056/NEJMra1602113

431. Ghosh Roy S et al. Regulation of cell survival and death during Flavivirus infections. *World J Biol Chem* 2014; 5(2): 93-105 DOI: 10.4331/wjbc.v5.i2.93

432. Chiramel, A.I. et al. Role of autophagy in Zika virus infection and pathogenesis. *Virus Research* 2017; http://dx.doi.org/10.1016/j.virusres.2017.09.006

433. Yakub, I.; Lillibridge, KM.; Moran, A.; Gonzalez, OY.; Belmont, J.; Gibbs, RA., et al. Single nucleotide polymorphisms in genes for 2′-5′-oligoadenylate synthetase and RNase L inpatients hospitalized with West Nile virus infection. *J INFECT DIS*. 2005; 192:1741–1748. [PubMed: 16235172]

434. Bigham, A.W.; Buckingham, K.J.; Husain, S.; Emond, M.J.; Bofferding, K.M.; Gildersleeve, H.; Rutherford, A.; Astakhova, N.M.; Perelygin, A.A.; Busch, M.P.; *et al*. Host genetic risk factors for West Nile Virus infection and disease progression. *PLoS ONE* 2011, *6*, e24745. \l